An Investigation of the Primary Sources of the Cape Town Brown Haze

A dissertation
presented to
the Academic Faculty

by

Stephen John Weber

In partial fulfillment
of the requirements for the degree

Master of Science in Environmental Geochemistry
Department of Geological Sciences

University of Cape Town

[April, 2004]

Abstract

The term atmospheric haze is a condition of reduced visibility, caused by the presence of fine particulate matter in the atmosphere, which can originate from natural or anthropogenic sources. The "Brown Haze" is a phenomenon that is associated with Cape Town and can be described as brown coloured smog. It occurs over the winter months, mainly May to September, due to the strong temperature inversions and windless conditions that can occur during these months. These conditions lead to the build-up of pollutants emitted into the atmosphere.

The Cape Town Brown Haze Phase Two study was used to obtain a detailed analysis of the atmosphere in a programme of lateral and vertical profiles through the Brown Haze. The field campaign took place from the 29th July 2003 to the 26th August 2003 around the Cape Town metropolitan region.

The aim of Phase Two is to examine and verify the validity of the conclusions of the first Brown Haze study (Wicking-Baird *et al.*, 1997), namely that vehicle emissions are the primary source of the observed pollutant clouds, with respect to the sources that emit pollutants directly into the atmosphere, and to further characterise the nature and properties of the brown cloud, with respect to particle size distributions, vertical and horizontal extent and evolution with time. Utilising *in situ* airborne sampling with the aid of the South African Weather Services (SAWS) Aerocommander 690A, as well as Powersonde model aircraft, an assessment and characterisation of the Brown Haze is performed. Chemical and physical properties of the haze are measured through a series of horizontal and vertical flights across the affected areas of the Western Cape, on haze and non-haze days, supported by concurrent ground-based meteorological measurements and ground based trace gas and particle sampling.

The data acquired consisted of meteorological data (wind speed, wind direction and potential temperature), particulate matter data (vertical concentration profiles and size distribution) and chemical composition data. When amalgamating the various data sets obtained, it was clear that the Brown Haze constituents were either being accumulated through the night or emitted into the atmosphere during the early morning.

The various data observations also allowed for a characterisation of the Brown Haze to be performed. The results found that the composition of the haze was predominantly NO_x (especially NO_2) and particulate matter. The fine particulate matter within the haze was

comprised of various salt, soil and composite organic particles. The composite particles showed signs of industrial activities, agricultural activities and vehicle emissions.

The lateral extent of the haze, which extended several kilometres out to sea, was governed by the landscape of the surrounding region and the wind conditions. The vertical extent never exceeded 1 400 m and was concentrated at low altitudes during the morning.

Chemical composition and particle analysis indicated that the major contributors to the Brown Haze were combustion sources, predominantly vehicle emissions as well as domestic burning, hence, the Brown Haze One study was indeed correct in their findings.

Dedication

To my parents, Kelvin and Gwen Weber,
and my beloved, Sarah Cathro

Acknowledgements

The author would like to thank his supervisor, Prof. Harold Annegarn of the Atmospheric and Energy Research Group (AERG), School of Geosciences, University of the Witwatersrand and Honorary Lecturer, Department of Geological Sciences, University of Cape Town. The author would like to thank also the following people for their valuable guidance and assistance through the duration of this project:

- Dr. Stuart Piketh, Climatology Research Group (CRG), University of the Witwatersrand, Principal Investigator of the Brown Haze Two study;
- Dr Luanne Otter, Climatology Research Group (CRG), University of the Witwatersrand, Co-principal Investigator of the Brown Haze Two study;
- Dr Martin van Nierop, Facilitating Innovative Research Environments (FIRE), for contractual and financial management of the Brown Haze Two project;
- Dr. A.N. Roychoudhary, Department of Geological Sciences, University of Cape Town;
- Fellow students of the Wits Climatology Research Group who participated in the Brown Haze Two project and who assisted in data acquisition and processing;
- Mr Grant Ravenscroft, Scientific Services Department, and Mr Hans Linde, Air Pollution Control, City of Cape Town.

The author would like to acknowledge the following organisations for financial or logistical support:

- South African Petroleum Industries Association (SAPIA), for partially funding the Cape Town Brown Haze Two study;
- Eskom TSI supported this work financially through the Remote Sensing Project grant to HJ Annegarn;
- The Department of Trade and Industry for matching funding through the Tertiary Human Resources in Industry Programme (THRIP);
- The Cape Town City Council, specifically the Scientific Services Department; and
- The South African Weather Service (SAWS) for supporting the airborne sampling programme and making available the Aerocommander 690A aircraft.

This research formed part of the sustainability programme of the Wits School for the Environment, supported by the BMW Group endowment for the BMW Chair in Sustainability.

This project used air sampling equipment acquired through the Southern Africa Regional Science Initiative, SAFARI 2000, financed in part by the Department of Science and Technology, the US National Science Foundation and NASA Goddard Space Flight Centre, and operated by the CRG, University of the Witwatersrand.

Table of Contents

List of Tables

List of Figures

List of Acronyms and Abbreviations

ABS	Airborne streaker sampler
ATSDR	Agency for Toxic Substances and Disease Registry
BN	Boron nitride
BS	Backscatter
BSE	Backscattering electron
CCN	Countinuous flow condensation nuclei Counter
CL	Cathodoluminescence
CMB	Chemical Mass Balance
CMC	Cape Metropolitan Council
CRM	Certified reference material
DEAT	Department of Environmental Affairs and Tourism
EC	Elemental carbon
ECA	Environmental Conservation Act
EPA	Environmental Protection Agency of the U.S.
FTIR	Fourier Transform Infra-Red spectroscopy
GFC	Gas Filter Correlation
GNP	Gross Net Profit
NAAQS	National Ambient Air Quality Standards
NAMS	National Air Monitoring Stations
NGOs	National Government Organisation's
NIST	National Institute of Standards and Technology
PCASP	Passive cavity aerosol spectrometer probe
PIXE	Particle-Induced x-ray emission
PM	Suspended Particulate Matter
PM_{10}	Suspended Particulate Matter with aerodynamic diameters less than 10 μm
$PM_{2.5}$	Suspended Particulate Matter with aerodynamic diameters less than 2.5 μm
PMT	Photomultiplier tube
ppb	Parts per billion
ppm	Parts per million
RH	Relative Humidity
SAPIA	South African Petroleum Industries Association
SAWS	South African Weather Services

SE	Secondary electron
SEM	Scanning electron microscope
SRM	Standard Reference Material
THRIP	Tertiary Human Resources in Industry Programme
TSP	Total Suspended Particles
UTC	Universal Time Clock
VOC	Volatile organic carbons
WHO	World Health Organisation

Chapter 1 – Introduction

This thesis investigates an air pollution phenomenon known as "Cape Town Brown Haze", that occurs intermittently during the winter and early spring over the Cape Metropolitan and surrounding areas of the Western Cape (Figures 1 and 2). The thesis forms part of the Brown Haze Phase Two project, which took place during July and August 2003. The aim of Phase Two is to examine and verify the validity of the conclusions of the first Brown Haze study (Wicking-Baird *et al.*, 1997), namely that vehicle emissions are the primary source of the observed pollutant clouds, and to further characterise the nature and properties of the brown cloud, with respect to particle size distributions, vertical and horizontal extent and evolution with time. Utilising *in situ* airborne sampling, an assessment and characterisation of the Brown Haze is performed. Chemical and physical properties of the haze are measured through a series of horizontal and vertical flights across the affected areas of the Western Cape, on haze and non-haze days, supported by concurrent ground-based meteorological measurements and ground based trace gas and particle sampling.

Figure 1: South Africa, showing location of study area.

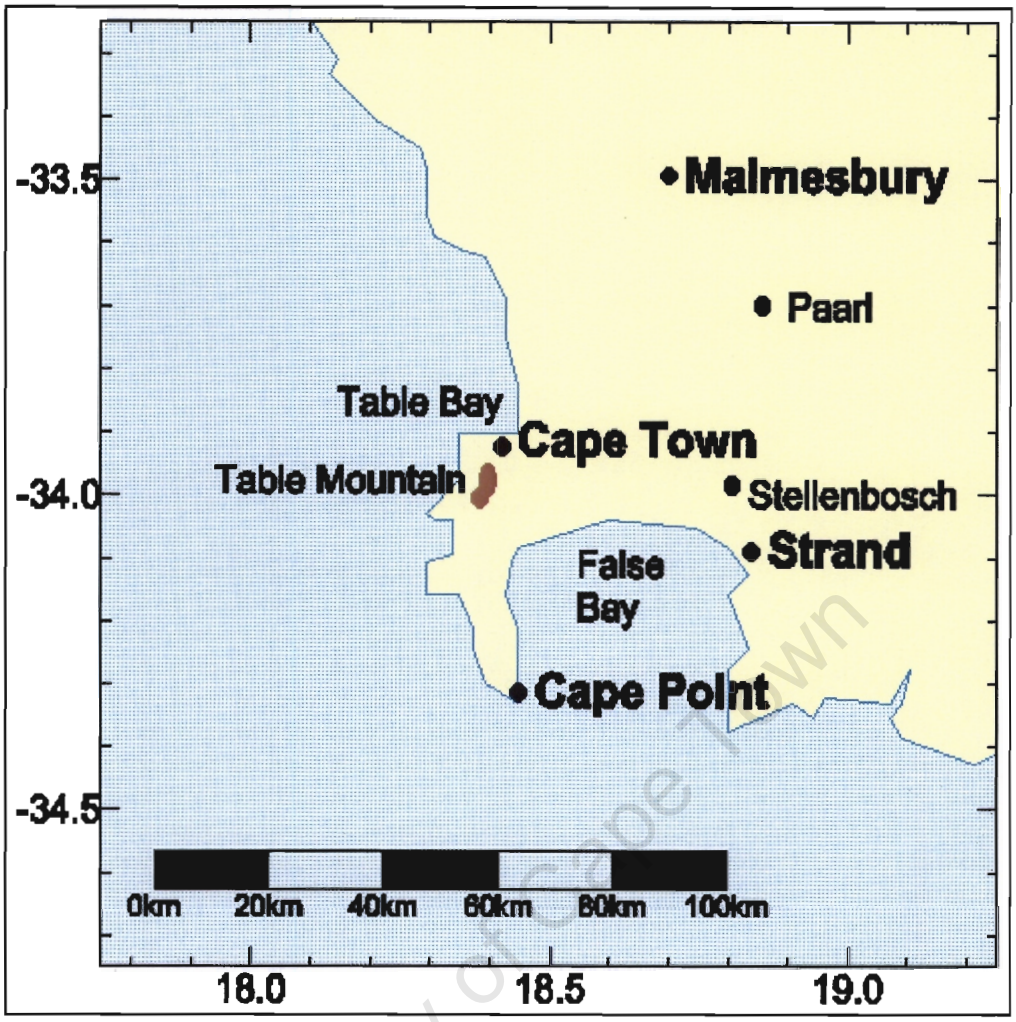

Figure 2: Cape Town and surroundings, showing key sites used in the Brown Haze Two study.

Oxygen in the air is vital for sustaining life. However, if the concentration and constituents of the air change, due to air pollution, we inhale unwanted substances, which can be detrimental to our health. Humans are therefore dependent on the air resource and hence require an environment that supports human health. The Brown Haze phenomenon is an early warning that the quality of the atmosphere over Cape Town is deteriorating. If left unchecked, the situation could evolve until poor air becomes a serious threat that could prevent the citizens of Cape Town from leading a healthy lifestyle. Two previous investigations, discussed in this report, have highlighted some of the problematic areas concerning the Brown Haze. From the previous study of the Cape Town Brown Haze (Wicking-Baird *et al.*, 1997) and the current phase, which is dealt with in this thesis, knowledge can be acquired in order to manage and ultimately eliminate the Brown Haze phenomenon.

The first Cape Town Brown Haze study was based on the Chemical Mass Balance (CMB) methodology, involving source and ambient chemical sampling, primarily of airborne particulate matter. The current Brown Haze study incorporated both ground based and airborne sampling. An Aerocommander 690A aircraft, suitably equipped, was used to obtain the detailed analysis of the atmosphere in a programme of lateral and vertical profiles through the Brown Haze. Atmospheric conditions are best represented by capturing pollution data whilst suspended in the air. The aim of the second phase is to remove any ambiguities in the Chemical Mass Balance (CMB) source apportionment study, performed in Phase One, and to answer the questions left from that same study. Some of these questions include:

- How do the particulate properties change over the course of the day?
- How do the same properties vary between haze days and non-haze days?
- What fraction of the pollution are due to diesel and internal combustion emissions?
- How much does informal tyre burning contribute to the Brown Haze levels?
- What is the contribution of secondary sulphate particles to the haze?

The final report of the Brown Haze Phase Two study will address the above questions. This report focuses on aerosols, more specifically on primary particulate matter. Aerosols can be described as a mixture of any small solid or liquid particles suspended in gas. They are present in many forms such as dust particles (pollen, fly ash or road dust), fog (clouds), spray (insecticide spray), and smoke from combustion (soot, cigarette) or as urban photo-chemical smog activated by sunlight. Insufficient information is known about size distributions, morphology, chemical compositions and number concentration of particles contributing to the Brown Haze phenomenon, or the relationships between the particles and gases. These unknowns will be investigated.

1.1 Aims of the Study

A) To characterise airborne particulate shape, size and composition during Brown Haze episodes in order to understand the nature and origin of the Brown Haze.

OBJECTIVES:

- Determine vertical profiles of the Brown Haze particulate cloud at various times of the day;
- Compare lateral and vertical profiles of particle concentration on haze and non-haze days;

- Determine size distributions of the particles at different stages of evolution of the Brown Haze;
- Determine haze particle composition, size and morphology by electron microscope analysis.

B) To investigate whether the Brown Haze Phase One study was indeed correct in stating that the major source of the Cape Town Brown Haze is vehicle related emissions.

OBJECTIVES:

- Determine gaseous pollutant vertical profiles at key points during the day;
- Compare gaseous pollutant vertical profiles to particle concentration vertical profiles during haze events;
- Determine the particulate haze particle composition and morphology by electron microscope analysis.

1.2 Background

1.2.1 Study area

The study area falls within the province of the Western Cape in South Africa. The dominant city, Cape Town, is a maritime city located in the south west of South Africa (figure 1). The major cities that are also affected by the same pollution phenomenon, but fall outside Cape Town are Stellenbosch, Strand, Paarl, Simonstown and Somerset West.

The Cape Town metropolitan area has an approximate population of 2.68 million and has a total area of 2 150 square kilometres. Cape Town's location along the coast, as well as the region's rich farmland, has led to growth in the food processing industry. Other strong industries within this region include textiles, clothing, furniture products, chemicals, plastics, machinery and technology-based industries.

1.2.2 Main sources of air pollution in South Africa

Air pollution is a global concern, as clean air is a non-renewable resource. This volume is in constant mixing, which means that there is an escalating pressure placed on the South African government by international countries, the general public and NGOs. South Africa is amongst the top ten countries contributing to the global greenhouse effect, making up 1.2 percent of the total contribution in 1990. It also accounts for 15 percent of

the greenhouse gas emissions for the African continent (Scholes and van der Merwe, 1996). South Africa forms part of the global community and has a responsibility to ensure that our standard of air falls within the required limits to sustain life.

South Africa is classified, in global terms, as a "developing country" which needs to mature. This development is in conflict with the environment, as the pollution produced from the expansion is an ever-increasing issue. South Africa has a wide variety of point and non-point sources of air pollution. The cause for these, range from within the main populated urban areas of South Africa to the migration of pollutants from countries in the nearby vicinity.

Before describing these problematic sources in greater detail, the term air pollution will be examined. Air pollution as stated by the new South African "Air Quality Bill", is the modification of the natural composition of air by means of a change in the solid particles, namely smoke, soot, dust and cinders, as well as a change in gases, fumes, aerosols, steam, odorous substances and radioactive substances (Department of Environmental Affairs and Tourism, 2003). The main contributors to air pollution in South Africa are the mining sector, the energy sector, the transportation sector, the agricultural sector, private industry and domestic fuel burning.

Wind blown dust originating from abandoned or poorly managed mine dumps is a serious concern to communities surrounding the mines. This problem is especially prevalent in the gold mining areas of Johannesburg. Electrical generation and petroleum production are the two main divisions within the energy sector that contribute towards the air pollution quantities. The burning of the coal in the power plants, as well as the gas extraction mechanisms are the two major sources of the pollutants. These two sources emit nitrogen oxides, sulphur dioxide and carbon dioxide into the atmosphere. Coal combustion can also contribute to high levels of particulate matter in the air, as well as lead to acid rain. The energy sector constitutes the single largest source of carbon dioxide (CO_2) and sulphur dioxide (SO_2) in South Africa (Scholes and van der Merwe, 1996).

Motor vehicles emit nitrogen oxides, carbon dioxide, carbon monoxide and hydrocarbons from their exhaust systems. It is therefore not surprising that vehicle emissions are considered one of the major contributors to the increasing pollution levels in the urban areas of South Africa. The agricultural sector plays a part in the high levels of carbon monoxide, methane and hydrocarbons found in our atmosphere. The sources for these levels are not solely produced by South Africa. Within South Africa, biomass burning of

the sugar cane fields causes high levels of particulate matter to diffuse into the air. This practice of crop or veldt burning is also a very widely used tool in our neighbouring countries. Fields are burnt in order to prepare the land for its new crop season. This burning allows massive air pollution plumes to migrate in a southerly direction over South Africa and pollute our environment (discovered during the SAFARI 2000 Southern African Regional Science Initiative, Swap *et al.*, 2002).

Various processes used in the industrial activities within South Africa, emit numerous toxic elements into the atmosphere, including: fluorides, aldehydes, lead and cadmium.

The final and by no means the least significant source of air pollution is domestic fuel burning. In many poorer homes, firewood or coal burning is the only economical solution to cooking or heating. On some occasions general waste is used in this process, as the communities find themselves in difficult financial positions. This burning emits carbon monoxide, dioxins, and high particulate emissions. The high particulate emissions have been identified as the major cause of poor air quality in many urban areas of South Africa (Annegarn *et al.*, 1996).

1.2.3 Impacts of air pollution

A wide range of sources are responsible for air pollution. Each of these sources contributes varying concentrations to pollutants. The duration and dilution of the emissions, ultimately determine the effects of the pollution. The pollutants emitted into the atmosphere affect every being that is within the realm of the contaminants. These affects may fluctuate, depending on the host, by short or long-term ill health. Decomposition of building structures due to corrosion or rusting, destruction of vegetation and crops, paint discolouring, domestic irritations and health impacts are some of the physical and aesthetic effects that could occur due to the pollution. All of these effects are an economic burden. The World Bank has estimated this burden from air pollution at a half to two and a half percent of the world gross net product (GNP), some 150 to 750 billion dollars per year.

Health Impacts

Health impacts have the most detrimental effect to humans. This is why many regulatory bodies are involved in solving the air pollution problem. The World Health Organisation (WHO) and the World Bank together have published a large quantity of papers relating to this specific topic (World Health Organisation, 2003). The WHO, in an air pollution fact sheet, stated that indoor exposure to suspended particulate matter increases the risk of

acute respiratory infections, one of the leading causes of infant and child mortality in developing countries. The World Bank has also stated that indoor air pollution causes an estimated two million excess deaths per year, or five percent of the global burden of disease.

Both statements point to the fact that air pollution is a huge contributor to respiratory illnesses. Within the same WHO fact sheet, it stated that air pollution causes an estimated four to five million new cases of chronic bronchitis. Many regulatory bodies have found this air pollution and respiratory relationship. But pollutants such as oxides of nitrogen, sulphur dioxide, volatile organic compounds, ozone and particulate matter have also been correlated with changes in mortality, cardiovascular illnesses, as well as carcinogenicity (Kinney, 1999; Wicking-Baird *et al.*, 1997).

Health effects of pollutants are determined by means of epidemiological studies, as well as laboratory experiments done on both humans and animals. The experiments performed determine the threshold effects of the various pollutants, while epidemiological studies attempt to link changes in ambient pollutant levels with health effects in communities. (Wicking-Baird *et al.*, 1997) The following pollutants are known to be a cause of human illness and are discussed with respect to their threshold values in greater detail below.

Nitrogen dioxide

Out of all the nitrogen compounds present in the atmosphere, nitrogen dioxide (NO_2) possesses to be the biggest concern with respect to health effects. NO_2 is produced in the atmosphere from NO, which undergoes a photochemical reaction. Motor vehicles and fossil fuel-burning power stations are the primary sources of NO emissions to the atmosphere.

Nitrogen oxides are mainly responsible for respiratory problems (WHO, 2001), as they are associated with deep lung penetration as scrubbing of the gas in the nasal passages is not efficient. It has been found from animal experiments that NO_2 can cause an alteration in lung metabolism, structure and function, and an increase in the susceptibility to pulmonary infections. Studies on humans have shown that, with asthmatics in particular, NO_2 has a bronco-constricting effect. With long term exposure, children exhibit increased respiratory symptoms and show a decrease in lung function. These respiratory effects occur at an annual average of NO_2 concentrations in the range of 50-75 $\mu g/m^3$ or higher.

Sulphur dioxide

Sulphur dioxide (SO_2) is mainly formed from the combustion of fossil fuels. Sulphur dioxide is a colourless gas that is soluble in water. It can react with water to produce sulphurous and sulphuric acid, which form aerosol pollutants. This reaction is catalysed by high humidity levels as well as sunlight (McGrath and Barnes, 1982).

High occupational exposures (more than 10 000 $\mu g/m^3$) to the gas give rise to severe broncho-constriction, chemical bronchitis and tracheitis. It has been documented that levels of SO_2 and SO_4 exceeding three times the normal standard for long periods of time, namely one to two weeks, may have serious effects culminating in death. This is mostly in the elderly and those suffering from heart or lung diseases (McGrath and Barnes, 1982). Lower concentrations (500-2 700 $\mu g/m^3$) cause bronchospasm in asthmatics. Typical ambient levels are much lower than the levels mentioned above and generally do not pose a great hazard to our health.

Volatile organic compounds

Volatile organic compounds (VOCs) are defined by the United Nations Economic Commission for Europe as "all organic compounds of anthropogenic nature other than methane that are capable of producing photochemical oxidants by reactions with oxides of nitrogen in the presence of sunlight" (Hoskins, 1995).

Not all VOCs are at a high enough concentration to pose as a health risk to humans. Benzene, aldehydes, 1,3-butadiene, n-hexane, and some chlorinated hydrocarbons are some VOCs that can affect the health of many. The sources of these VOCs are mainly from vehicle emissions and industries that use solvents such as the paint and plasticiser industries (Wicking-Baird *et al.*, 1997).

Health effects of VOCs differ from compound to compound, but in general they have one of the following effects: carcinogenicity, neurobehavioural or nephrotoxic symptoms. Benzene is a well-known carcinogen and is rated in the top ten known carcinogens by the World Health Organisation. Inhaling benzene in small amounts can lead to headaches, dizziness, drowsiness or nausea. In more serious exposure, benzene can lead to sleepiness, irregular heart beats and even death (ATSDR, 2003). Continuous exposures to benzene, as well as 1,3-butadiene, have been linked to higher incidences of leukaemia. Aldehydes, such as formaldehyde, have been linked with irritation of the eyes, nose, throat and upper respiratory tract. n-Hexane affects the respiratory and cardiovascular function, as well as the neurobehavioural properties of a human.

Ozone

Ozone forms from the interaction of either nitrogen oxides or hydrocarbons in the presence of sunlight. In experimental work done, it was found that ozone increased airway reactivity in both animals and man, to aerosols, for example, histamine and carbachol (McGrath and Barnes, 1982).

In general, ozone exposure causes irritation to the airways and structural alterations in the lung (increased permeability in lung tissue). Short-term ozone exposure effects include pulmonary function changes (destruction of pulmonary macrophages), increased airway responsiveness and airway inflammation. Large or intermittent chronic exposures can cause thickening of airways and alveolar membranes with eventual loss of function. High ambient ozone concentrations have been associated with restricted activity, asthma symptoms, and respiratory related admissions to hospitals (Kinney, 1999).

Particulates

Other than gaseous compounds, air pollution also contains a wide variety of particles. They range from 0.01 to 100 µm and consist of metallic, mineral particles or aqueous solution droplets and organic particulate matter. They can take up many forms, they can be homogeneous, heterogeneous or a composition of gaseous and particulate matter.

Many countries have adopted a health standard for particles of aerodynamic diameter less than 10 µm, referred to as PM_{10}. Particles less than 10 µm have the greatest potential to penetrate the upper airways of the respiratory system. Further investigation has put forward that particles regulated by this standard should be divided into a further two categories, coarse and fine. The fine fraction ($PM_{2.5}$) relates to the particles less than 2.5 µm and the coarse fraction to the particles between 2.5 and 10 µm.

The $PM_{2.5}$ has a higher correlation to health effects than PM_{10}. This could be due to the fact that the $PM_{2.5}$ penetrates deeper into the lungs (The World Bank, 2003). It is also stated that exposure to $PM_{2.5}$ is far greater than PM_{10}, this is due to the fact that $PM_{2.5}$ readily penetrates buildings. We are therefore exposed to $PM_{2.5}$ for a longer duration than PM_{10} (Wicking-Baird *et al.*, 1997).

The health impacts that will be mentioned are applicable only to the size range of PM_{10} and $PM_{2.5}$. Very little is known about other particulate matter metrics such as the ultra fine particles. There is also no information on how the health impacts vary with different particulate surfaces. Particulate air pollution contributes mainly to a spectrum of respiratory difficulties and can affect other parts of the body by physically moving out of

the airways and into the blood stream (The World Bank, 2003). It also affects human health by means of toxicity from heavy metals; carcinogenesis from surface organics; direct damage of pulmonary tissue by deposition of granular material; and reduced disease resistance (McGrath and Barnes, 1982). Researchers have shown that particulates are linked to increased mortality and an increase in the hospital admissions for respiratory and cardio-vascular illnesses (Kinney, 1999). The primary metal sulphates attributed to mortality are; copper, zinc, aluminium and magnesium (McGrath and Barnes, 1982).

1.2.4 South African environmental legislation

The sources, the effects and air pollution itself are all concerns and are doing damage to the human race. In order to change this environmental problem, strict legislation and enforcement must be implemented. South Africa as a country has started to execute new air regulations into its legislation to start modifying the trend that our environment is maintaining.

At present the country is transforming from the old and out dated legislation of the Atmospheric Pollution Prevention Act, 45 of 1965 and the Environmental Conservation Act, 73 of 1989 (ECA) to the new draft Air Quality Bill (Department of Environmental Affairs and Tourism, 2003) and the National Environmental Management Act, 107 of 1998 (NEMA). This section will focus on NEMA and the Air Quality Bill to see how this legislation favours the protection of the environment.

In NEMA the concept of sustainable development is brought forward a number of times. This concept examines the fact that we all need to live in harmony with our surroundings. NEMA states that in order to achieve sustainable development in relation to the air we breathe, the following facts must be considered at all times. The pollution and degradation of the environment must be avoided, or where they cannot be altogether avoided, are minimized and remedied. It further states that in management, risk-averse and cautious approaches must be applied. This takes into account the limits of current knowledge about the consequences of decisions and actions. If these facts above are not achieved or obtained, they will cause negative impacts on the environment and on people's environmental rights. This needs to be anticipated and prevented, and where they cannot be altogether prevented, are minimized and remedied.

NEMA stipulates that the environment is held in public trust for the people; the beneficial use of environmental resources must serve the public interest. The environment must,

therefore be protected as the people's common heritage. Environmental justice must be pursued so that adverse environmental impacts shall not be distributed, in such a manner as to unfairly discriminate against any person, particularly vulnerable and disadvantaged persons.

If environmental damage does occur due to pollution, NEMA declares that the costs of remedying the pollution, environmental degradation and consequent adverse health effects and of preventing, controlling or minimizing further pollution, environmental damage or adverse health effects must be paid for by those responsible for harming the environment. The Act goes further than just present actions, it also considers retrospective events, as it has a statement that asserts that "every person who causes, has caused or may cause significant pollution or degradation of the environment must take reasonable measures to prevent such pollution or degradation from occurring, continuing or recurring …".

NEMA has considerations for the anticipation and prevention of environmental damage. Hence, it contains an environmental implementation plan and an environmental management plan. The objective of these plans is to prevent unreasonable action from taking place, as well as monitoring the achievement and protection of a sustainable environment.

The second legal document, the Air Quality Bill, will now be discussed. This Act is said to form part of NEMA and should be read in conjunction with NEMA. The draft bill states that the South African Government's general duty in implementing the Act must be to endeavour to protect, restore and enhance the quality of air in the Republic by taking into account sustainable development. The State also feels that it must achieve these goals by considering the progressive realisation of the rights of all people living in South Africa.

In order to achieve these duties set by the State, the Air Quality Bill describes how various norms and standards are to be implemented nationally to contaminants within a polluted source of air. The standards may differ depending on the specific regulation category or under which authority the norms are set (local and provincial governments may enforce stricter standards if necessary). Ambient air quality and emissions from point or non-point sources are the two core categories set aside by the State. Air quality monitoring, air quality management planning and air quality information management are secondary categories that monitor, assess and regulate the compliance of the general public and organs of state with the Bill.

For the implementation of the Bill, a National Air Quality Advisory Committee and an air quality officer hierarchy "may" be assigned. This hierarchy begins at the national level and works its way down to the respective municipalities. The air quality officer has a responsibility to coordinate matters pertaining to air quality management at his or her particular level.

To aid in the management of air quality, the Bill allows for the designation of air pollution 'hot spots'. (The specific areas that are assigned undergo separate air quality management plans.) It also allows for the implementation of an activity list with restricting operations. This list prohibits any activity mentioned on the list to be carried out within the Republic without a license, including activities resulting in the release of offensive odours.

The license mentioned above stipulates the period of the license agreement, the revision date, the maximum allowable concentration of pollutants that may be discharged into the atmosphere and the penalties for non-compliance. It may also stipulate the control technology to be used on the site that is requesting the license, as well as some lawful requirements by an environmental enforcement officer in terms of the National Environmental Management Act.

The Bill also allows for specifically aimed measures to be put into place in order to help manage air quality. These measures are namely the control of specific emitters (i.e. vehicle emissions), control of noise and the control of odours. All of these are to be assigned under the consent of the environmental minister.

From the structural base set out, as stated above, the Bill then discusses offences and penalties. An offence is committed if an atmospheric emission license or the air pollution standards are not complied to and if the person involved gives misleading or false information. The penalty for an offence can vary from a monetary fine to imprisonment; this will depend on the severity of the impact (health or environmental) that has resulted.

The Brown Haze Two study supports NEMA and the Air Quality Bill in stating that the beneficiary of the environmental resource concerned is the public. The study further more supports the promotion of minimising or inhibiting adverse environmental impacts on the citizens of Cape Town. The Brown Haze Two study will therefore monitor the ambient air quality that exists in the Cape region and in doing so initiate the protection of the atmospheric resource.

Chapter 2 – Literature Review

2.1 Introduction

This chapter deals with specific background material for this study. A description of the Brown Haze, the meteorology of the Western Cape, as well as of Cape Town and the interaction between the meteorology and the Brown Haze will be discussed.

This chapter will also point out that the pollution phenomenon called 'haze' is not just well-known to Cape Town, but also affects other parts of the globe. Two previous haze studies, Phase One of the Brown Haze project and the Denver Brown Haze study are included in this review.

2.2 Description of the Brown Haze

The term atmospheric haze is the condition of reduced visibility caused by the presence of fine particles in the atmosphere, this can originate from natural or anthropogenic sources. This phenomenon is generally associated with diffuse or widespread atmospheric degradation as opposed to individual plumes (Boubel *et al.*, 1994).

The "Brown Haze" is a phenomenon that is associated with Cape Town and can be described as brown coloured smog. It occurs during the winter months, mainly May to September, due to the strong temperature inversions and windless conditions that can occur during these months. These conditions lead to the build-up of pollutants emitted into the atmosphere (Wicking-Baird *et al.*, 1997).

The Brown Haze is mostly dominant over the flat plains of the Cape Metropolitan Area. It is most intense over the morning periods and clears slightly as the day progresses. The intensity varies depending on the climate. (Wicking-Baird *et al.*, 1997) The climatic conditions also dictate the altitude range at which the Brown Haze will spread. In early morning, the haze is located close to the ground, below an approximate altitude of 200 m. As the day progresses the haze's vertical extent can reach an approximate altitude of 1 500 m. The Brown Haze is a negative visual effect that affects both the general population of Cape Town, as well as tourism.

The Cape Town Metropolitan council (CMC) have been doing routine monitoring of the Brown Haze since the first Brown Haze study and evidence shows that air quality is deteriorating. It is projected that without adequate control of such problems, air pollution could increase by at least 48% over the next decade, taking the air in some parts of the Cape Metropolitan Area to dangerously unhealthy levels (CMC, 2003).

Efforts have been made by the CMC, as well as, the Air Pollution Control Unit to improve the situation of the Brown Haze since the first study. Testing of diesel vehicles, improvements of traffic flow, improvement of vehicle and fuel technology, routine monitoring of industrial facilities, development of air quality management systems, assessment of air pollution legislation and expansion of the monitoring networks to thirteen monitoring locations have all been performed to improve the situation. Due to these undertakings the rate of increase of air pollution in the Cape metropolitan region is slowing down, this statement is presently a hypothesis formulated by the local council.

2.3 Meteorology of Cape Town

2.3.1 Description

The overall macro scale circulation for the Western Cape can be categorised into three distinctively different phases. The summer months, are characterised by a high south easterly airflow, which is caused by a ridging anticyclone over the South Atlantic Ocean (Wicking-Baird *et al.*, 1997). This system brings about high wind velocities and high atmospheric turbulence. The bulk of the second period is within the months of winter. North-westerly winds are dominant due to the pre-frontal systems that cause low temperatures, high rainfall and overcast conditions (Wicking-Baird *et al.*, 1997; Tyson, 1987). The final distinctive period comprises the months between late winter and early spring. The strong overnight temperature inversions are associated with light berg-wind conditions, ahead of migrating coastal lows (Wicking-Baird *et al.*, 1997). The coastal lows, which form with the aid of the escarpment topography, produce warm offshore airflow ahead of the system and cool onshore airflow ahead (Tyson, 1987). Berg winds are associated with the warm airflow moving offshore and they enhance the warming effect (Tyson, 1987). Stagnant conditions ahead of the system are common due to the presence of the anti-cyclones, which in turn causes light variable winds and an elevated temperature inversion.

When looking at the meso-scale meteorology of the Cape metropolitan region, the effects of the topography are important to consider. The topographical features that impact significantly on the micro climate for the region are Table Mountain, False Bay and Table Bay (figure 2). These features bring about complex wind circulation patterns, either recirculating or ventilation effects depending on the area.

All of the mentioned meteorological conditions affect the Brown Haze in some way. They affect the pollutant loading and the required conditions for its formation. The section that follows goes into detail of these requirements.

2.3.2 Relationship with the Brown Haze

The Brown Haze phenomenon occurs mostly in the late winter months and the early spring months. This is mainly due to the fact that the climatic conditions within these months offer favourable conditions for the phenomenon (Wicking-Baird *et al.*, 1997). Ambient pollutant concentrations are dependent on atmospheric conditions, such as wind and temperature.

The local atmospheric characteristics that are associated with pollution episodes are the berg winds, ahead of the coastal low pressure cells, from the North-North-East and a temperature increase of about 11°C from ground level to 500 m above the Earth's surface (Wicking-Baird *et al.*, 1997). The wind velocity, mechanical turbulence, the rate and height of emissions are also factors that govern the ambient pollutant concentrations, which in turn determine the intensity of the Brown Haze (Wicking-Baird *et al.*, 1997).

The mechanism behind the high pollution levels within the Brown Haze is best described in the initial Brown Haze report. "The warm berg winds cause dry night-time conditions in the lower atmosphere. Night-time radiative heat loss and sinking motion from the upper atmosphere combine under these conditions to form a strong ground based inversion. The conditions in the inversion are generally calm and so there is little dilution of emitted pollutants." (Wicking-Baird *et al.*, 1997) The build up of pollutants are then apparent as the emitted pollutants rise until their "initial buoyancy and vertical momentum are dissipated" (Keen, 1994).

2.4 Studies Completed

2.4.1 Cape Town Brown Haze Phase One Study

The study that will be discussed is from the first phase of the brown haze study. The first project dealt with a particular approach to discovering the sources and content of the brown haze. For the study review, the approach, the data collection procedures and the final outcome of the study will be discussed in detail. By looking at the first phase, it will enable one to focus the second study on points of importance and to place attention to those areas that were not fully dealt with.

The first phase of the Brown Haze project was mainly handled by a Brown Haze scientific team, which comprised of M. Wicking-Baird, M. de Villiers and Professor R Dutkiewicz. They approached the problem on the basis of a chemical mass balance (CMB) source apportionment study. This deals with quantifying the surrounding ambient air and relating its chemical breakdown to various contributions by emission sources, point and non-point.

The source apportionment was based on the fact that the $PM_{2.5}$ is the greatest importance to the Brown Haze. This is due to the fact that the Brown Haze is dependant on small particles, for reasons discussed previously and due to the fact that the $PM_{2.5}$ is of great concern when considering health effects. The method used was collecting chemical data from various sources and ambient sites with the help of filter papers. The chemical data from the respective sites were then placed into a computer model and the results that were extracted, indicated the percentage that each source was contributing to the Brown Haze.

Source sampling

The study commenced by collecting data for the respective sources that were felt to be major components of the Brown Haze. The sources that were characterised are as follows: various soils, road dust, sea salt, coal fired boiler emissions, Caltex and general oil fired boiler emissions, Caltex gas fired boiler emissions, Caltex furnace emissions, Caltex fluidised catalytic cracker unit emissions, Kynoch ammonium nitrate emissions, diesel combustion, petrol combustion, wood fires, grass fires and burning tyres.

The composition of the sources varied. For the oil-fired boiler emissions, significant proportions of aluminium, silicon, nickel, vanadium, sulphur, organic carbon and elemental carbon were expected to be present with vanadium being the recognised

tracer element. The companies from which samples originated from, were the Caltex refinery and African Products. It must be noted that the composition of the two profiles varied, this was because Caltex fires fuel oil is slightly different in composition to commercially available fuel oil and the condition of the firing in the two boilers varied in temperature. (Wicking-Baird *et al.*, 1997)

For the road dust samples, which were classified as crustal material, high proportions of aluminium, silicon, calcium and iron were expected. Note that the Caltex refinery catalyst dust profile also followed the crustal material proportions. (Wicking-Baird *et al.*, 1997) Three samples were collected and they varied with respect to location. One came from the city and the other two were collected from residential areas.

For the profile of the wood burning, high contents of potassium, chlorine, and organic and elemental carbon were present. This profile originated from the burning of Port Jackson and Rooikrantz wood. The tyre burning profile showed high levels of aluminium, silicon, iron, organic carbon and elemental carbon. Note that the tyre burning does not appear to produce as much chlorine as vegetative burning (Wicking-Baird *et al.*, 1997).

The vehicle profiles were sampled from the exhaust of the driving vehicle. The diesel vehicle profile was from a well-maintained vehicle that did not smoke badly, it had significant levels of sulphur, as well as organic and elemental carbon. While the petrol vehicle profile showed high levels of lead, bromine, organic carbon and elemental carbon (Wicking-Baird *et al.*, 1997).

All of these sources required the sampling techniques of either the isokinetic sampling method, resuspension sampling method or the controlled combustion in a chamber method (Wicking-Baird *et al.*, 1997). These techniques, as well as the sampling locations are described in greater detail in the initial phase of the Brown Haze project.

From the respective filters obtained from the sources mentioned above, X-ray fluorescence (XRF) and carbon analysis methods were used to determine the total particulate masses present. A few assumptions were made, the first being that a number of elements were assumed to occur only as oxides – namely silicon, aluminium, iron, vanadium, and calcium. The second being that a multiplication ratio of 1.2 was used to acquire an actual reading of the organic carbon present – this was to account for the organic hydrogen and organic carbon. (Wicking-Baird *et al.*, 1997) Improvement of these assumptions could result in improved data quality.

Ambient sample collection

The ambient air samples were collected by means of $PM_{2.5}$ samplers. The specimens were predominantly from four sites, namely the City Hall in the Central Business District, Goodwood, Table View and Wynberg. These sites all fall within the Cape Town Metropolitan Area. Note that a single sample was also taken at Guguletu.

The sampling duration was over a yearly period and the interval of the sampling was approximately twelve hours. Other parameters were also measured at the respective sites. These parameters included the ambient concentrations for a variety of trace gases, wind speed and direction, and temperature of the surrounding air.

At the Wynberg site, a residential area, PM_{10}, $PM_{2.5}$, NO_x and ozone were measured. In the Central Business District PM_{10}, $PM_{2.5}$, NO_x, non-methane hydrocarbons and weather data were collected. In the Table View residential area, which is located in close proximity to the Caltex refinery, as well as a fertiliser factory, PM_{10}, $PM_{2.5}$, NO_x, SO_2 and weather data were collected. In the third residential area, Goodwood, PM_{10}, $PM_{2.5}$ and NO_x were retrieved (Wicking-Baird *et al.*, 1997).

From the respective sites, a chemical mass balance model was used to determine the contribution of various sources to the brown haze. The $PM_{2.5}$ to PM_{10} ratio was used to aid in determining the mechanisms of the pollution. The ratio indicates what proportion of PM_{10} is made up by $PM_{2.5}$ (Wicking-Baird *et al.*, 1997).

The $PM_{2.5}$ is associated with emissions from combustion sources. Consequently, if the $PM_{2.5}$ to PM_{10} ratio is high, it would mean that the PM_{10} concentration was made up mainly of $PM_{2.5}$ and hence the particles originated from combustion sources. If the ratio is low, it indicates that the particulate pollution consisted of mainly coarse particles, indicating geological dust transported by berg winds (Wicking-Baird *et al.*, 1997).

The apportionment and the results

The apportionment, as described earlier, is the relationship of the source emissions to the final ambient air quality. The results obtained from the apportionment of the study, were broken up into two categories, firstly the overall apportionment and secondly the visibility apportionment. The visibility apportionment was derived from the conversion of the particulate matter less than 2.5 μm, by considering light extinction coefficients for various chemical species. Factors such as light scattering and absorption by gases were also taken into account. (Wicking-Baird *et al.*, 1997) This conversion was done to

illustrate the importance of the $PM_{2.5}$ and therefore to give an indication of the origin of the sources.

The results for the apportionment were split up into the contributions of crustal material, diesel vehicles, petrol vehicles, wood burning, sea salt, boilers, sulphate, nitrate and carbon (Wicking-Baird *et al.*, 1997).

The final $PM_{2.5}$ ambient source obtained by averaging the chemical data collected; is not an accurate method with respect to this case study, as height and time of emissions cause variations in the chemical data. The results show that diesel vehicles are the largest single source of $PM_{2.5}$, but it must be noted that petrol vehicles and wood burning are also significant contributors (Wicking-Baird *et al.*, 1997).

When collective modelling of all the results (source and ambient), the following significant findings were discovered. The results, set out in pie chart format, are from the initial Brown Haze report (Wicking-Baird *et al.*, 1997). Figure 3a represents the average $PM_{2.5}$ apportionment and Figure 3b the $PM_{2.5}$ visibility apportionment for the Brown Haze in Cape Town.

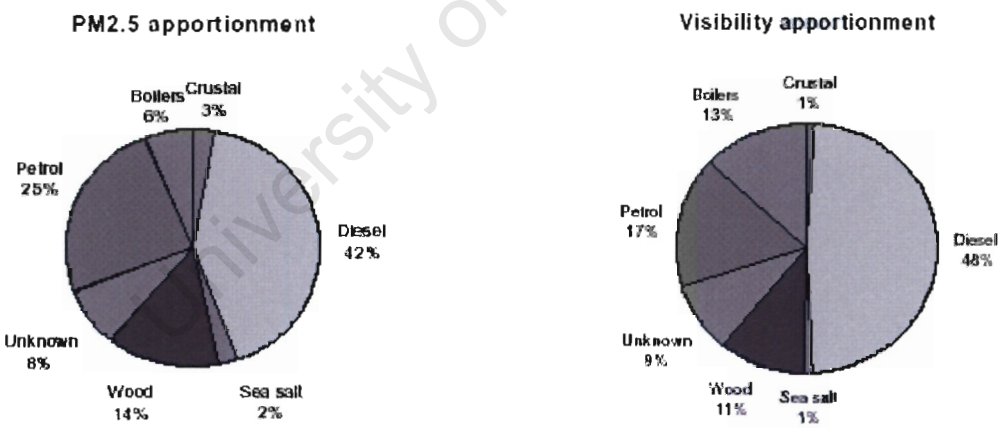

Figure 3: (a) $PM_{2.5}$ source apportionment for the Cape Town Brown Haze (b) Visibility source apportionment (After Wicking-Beard *et al.*, 1997).

From figure 3 it is clear that a large portion of the $PM_{2.5}$ apportionment and the visibility apportionment is due to diesel vehicles. Significant portions are also due to petrol vehicle emissions, as well as wood burning. (Note that a significant portion of both charts when modelling came out to be unknown. This portion is comprised of mostly organic carbon, which could be derived from industrial process emissions.) (Wicking-Baird *et al.*, 1997) Figure 4 incorporates the unknown portion as industrial process emissions. (Note that an estimated uncertainty value of 40% is integrated in figure 4.)

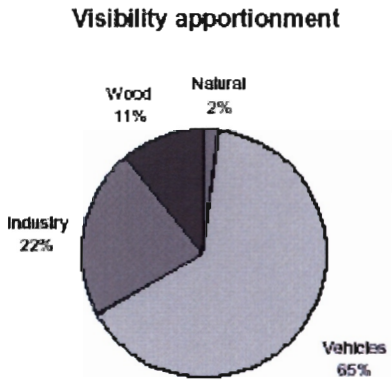

Figure 4: Overall visibility apportionment obtained from the Cape Town Brown Haze Phase One study (After Wicking-Baird *et al.*, 1997).

2.4.2 Denver Brown Cloud Study

The study took place in Denver, Colorado during years of 1987 and 1988. (Watson *et al.*, 1988). The Denver brown cloud is a term given to the white or brown haze which envelops the downtown areas of Denver. It is noticeable mostly over the winter months.

The aim of the project was to improve the understanding of the causes of the brown cloud. The project set out to acquire data in terms of visibility, air quality and meteorological measurements, to determine the contributions that the major pollution emission sources contributed to the brown cloud. It also desired to compare the contributions from power plants that burned coal to those that burned gas.

The project followed a receptor-oriented approach to apportion visibility extinction to pollutant emissions source types. The sources that were characterised are as follows: Raleigh scattering, nitrogen dioxide absorption, primary particles from vegetative burning, primary particles from mobile sources, and primary particles from power plant boilers, primary particles from suspended geological material, secondary particulate ammonium nitrate and secondary ammonium sulphate. (Watson *et al.*, 1988) The manner in which this apportionment is related to the particles is through the receptor model for PM_{10} developed by the Environmental Protection Agency (EPA). The model relates the chemical constituents which cause visibility extinction, to the source contributions.

The manner in which the study examined the change in power plant fuels was to compare the average chemical concentrations and visibility extinction between meteorologically stratified subsets for the gas and the coal burning samples. This

comparison was conducted during similar brown cloud episodes which occurred during gas and coal burning periods.

Measuring sites for ambient air analysis were representative of urban areas, as well as non-urban areas, and representative of the varying topography. Aerosols, gases and visibility were measured at each site. The elevations for aerosol and gas sampling ranged between 0 m (ground level) to 142 m above ground level. The sight path extinction measurements were taken at the 75 m down town site, to relate the point measurements of scattering and absorption to atmospheric transmittance (Watson *et al.*, 1988). The surface and upper air measurements of wind speed, wind direction, mixing height, atmospheric stability, temperature and relative humidity were also taken during the course of the project.

The results from the project showed that most of the sampling periods were found to have low extinction. Only approximately 15% of sampling days showed extinction values of any significance (Watson *et al.*, 1988). The facts presented below are indicative of the days that had brown clouds.

One factor that contributed to the low collection ratio of samples was the meteorology, as it played an important role in the formation and persistence of brown clouds (Watson *et al.*, 1988). Air was rarely stagnant over the downtown areas of Denver, even during the high extinction periods (Watson *et al.*, 1988). Return flow from the lower valley was a contributor to the high pollution levels that built up during the course of the day. The return flow brought about mixing between the primary and secondary particles and this, in turn, added significant fractions to the total light extinction. The major weather fronts cleared air pollution from Denver and reduced the extinction.

The primary sources that were the main cause of the visibility reduction in Denver were vegetative burning and mobile sources. A smaller contributor was the emitted dust, especially after roads were sanded. The direct emissions of fine particles from the coal fired power plants and the oil refineries showed to have insignificant impact on the brown cloud (Watson *et al.*, 1988).

The particles formed from gases also made significant contributions to the high extinction. The major portion of these gases was emitted by power plants, mobile sources, refineries, agricultural operations and natural sources (Watson *et al.*, 1988). Ammonium nitrate particles were the largest secondary contributors to visibility reduction (Watson *et al.*, 1988). Over one third of the oxides of nitrogen are emitted by cars and

trucks (Watson *et al.*, 1988). Power plants, oil refineries and space heating with natural gas also emitted oxides of nitrogen.

The main contributor to the sulphur dioxide levels was the coal fired power plants. Over half the sulphur dioxide emissions in Denver were attributed to the power plants. It was found that the fuel switching, between gas and coal, changed the sulphur dioxide emissions in the Denver area by more than 50 percent (Watson *et al.*, 1988). Other sulphur dioxide sources include the refineries, the diesel trucks and cement plants.

In concluding, it was found that there was not a single source which stood out as the main contributor to the brown cloud, hence, it was stated that pollution control efforts directed at only one source would not solve the problem (Watson *et al.*, 1988).

Chapter 3 – Sampling Methods and Strategy

This chapter introduces details of the Cape Town Brown Haze phase two field campaign which took place from the 29th July 2003 to the 26th August 2003 around the Cape Town metropolitan region. During the field campaign, aircraft were used to acquire the data needed to assess the current situation of the Brown Haze. The South African Weather Services (SAWS) Aerocommander 690A, as well as Powersonde model aircraft (figure 5), were used to obtain the respective samples and data readings.

Figure 5: The SAWS Aerocommander 690A used for airborne sampling in the Cape Town Brown Haze study. The two smaller aircraft are Powersonde model aircraft used in the field campaign.

The Aerocommander 690A set off on seventeen flights, recording non-haze days as well as haze days. In order to get a better perspective, the flight times varied. The Powersonde model aircraft flew seven flights ascending to a height of one kilometre. The objective for the Powersonde model aircraft was to obtain profile data, starting at low level, for both meteorological data and ozone concentration. The flight pattern for the Aerocommander flights (figure 6), could be described as a circuit pattern. The initial plan for the flight pattern was a grid formation over the whole Cape Town Metropolitan area, but this was altered due to air space restrictions over Cape Town International airport.

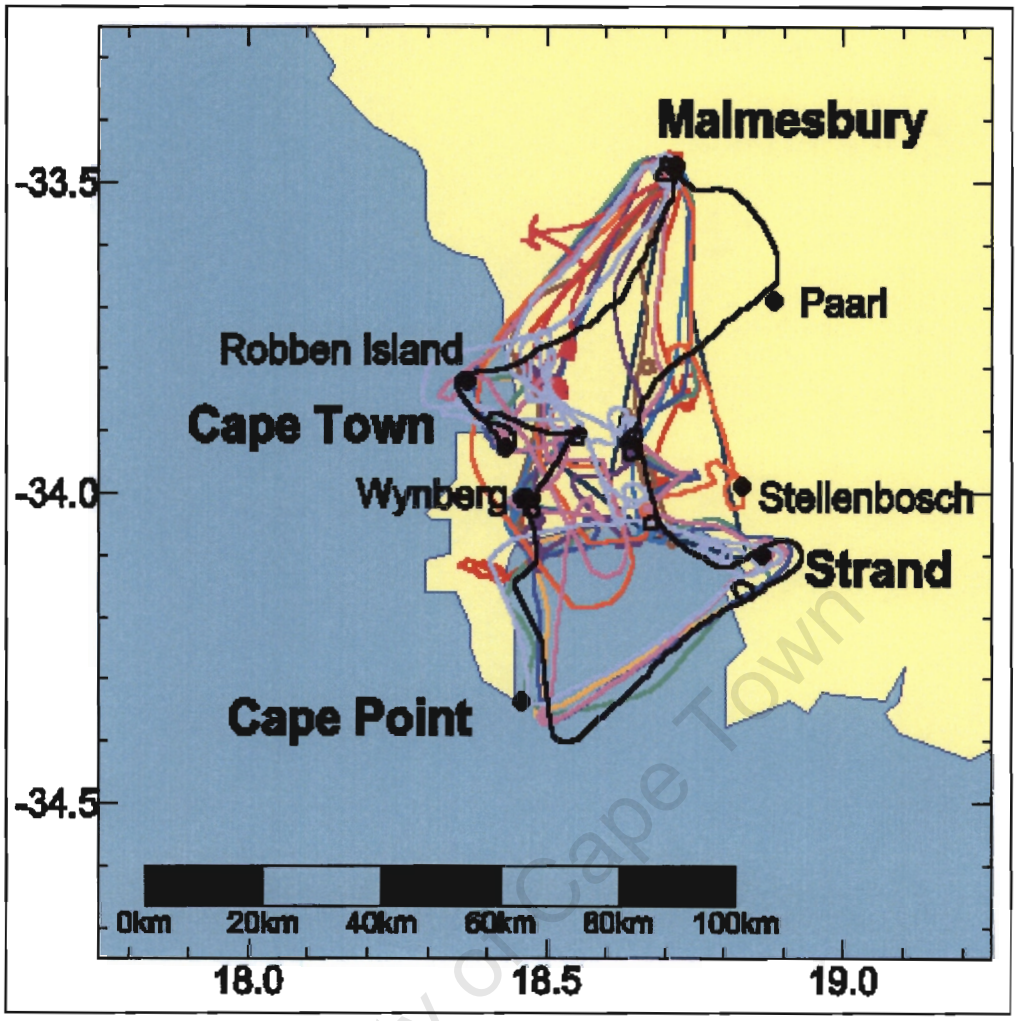

Figure 6: Aerocommander 690A flight patterns for the duration of the field campaign.

The purpose for the flights was to gather information on the vertical extent and the horizontal perspective of the Brown Haze for the day of interest. The movement and evolution of the Brown Haze influenced the flight paths and hence determined the sampling strategy for the day. Observations of the Brown Haze during the course of the day (figure 7 and 8) dictated that the commencement of the sampling flights should fluctuate to accommodate the variation of the Brown Haze with respect to time. Figure 7 shows that the Brown Haze was confined to low altitudes during the morning, where Figure 8 shows the Brown Haze at a higher altitude during the afternoon. The 22nd August 2003 was one day when two flights occurred, one in the morning and the other in the afternoon. These two flights, flights 14 and 15 respectively, are used in this thesis as a representation of the daily variation.

Figure 7: A view from the University of Cape Town of the Brown Haze over the Cape Flats region in the early morning of the twenty-third September 2003 at twenty-five minutes past eight o'clock (local time).

Figure 8: A view from the University of Cape Town of the Brown Haze over-looking the Cape Flats region in the afternoon of the fifteenth September 2003 at eight minutes past twelve o'clock (local time).

The targeted zones during the flights included areas upwind, areas downwind, areas within the haze (including hot spot industrial areas) and areas outside the haze. The location of the vertical profiles varied depending how the meteorological conditions affected the haze. The wind directions determined the location of the up-gradient location and the down-gradient location. For example, if a south easterly wind was blowing, Cape Point would be the location of the up-gradient vertical profile location and Robben Island would be the location for the down-gradient location. The maximum altitude for the vertical profiles was determined by the top of the haze. Sampling extended into the cleaner layer above, often exceeding a 2 km altitude. Simulation landings at various local airfields were carried out in order to acquire data closer to the surface, which would otherwise have been out of bounds in terms of the air navigation regulations.

To determine background conditions influenced by urban sources, control areas were sampled, selected as over Cape Point and over the Atlantic seaboard around Robben

Island. These profiles were likely to show the natural levels of aerosols at various altitudes and hence highlight the severely polluted altitude zones. A comparison of sampling on a non-hazy (13th August 2003 – Flight 12) to a hazy day (15th August 2003 – Flight 13)) was similarly made with respect to the entire spatial distribution of the Brown Haze. While 17 flights were made altogether during the campaign, flights 12, 13, 14 and 15 are used for detailed evaluation in the remainder of the thesis.

The Aerocommander 690A was equipped with various instruments that analysed for ozone, sulphur dioxide, carbon monoxide, nitrogen oxides and carbon dioxide. Other gaseous compounds such as methane and volatile organic carbons (VOCs) were also sampled using gas canisters for later analysis. The VOC concentrations were measured using a Fourier-transform infrared spectrometer FTIR which analysed for 280 species. The Aerocommander 690A was also equipped for analysis of aerosol particles, the major instruments used included the passive cavity aerosol spectrometer probe (PCASP) (which analysed for the 0.1 to 3 μm sized particles), cloud condensation (liquid sized particles ranging from 0.011 to 3 μm), Continuous flow Condensation Nuclei Counter (CCN) and the Airborne Streaker sampler (ABS) (filter sampler). Powersonde model aircraft were used to measure the following parameters; ozone, temperature, pressure and later in the field campaign VOCs using flask sampling.

Air samples were taken into the aircraft via inlets or directly into the instruments. The inlets were placed on the nose and on the roof of the plane. Inlets for the particle and gaseous instruments were positioned on the top of the Aerocommander. The general state parameter sensors (temperature, pressure and humidity), were located on the nose of the Aerocommander.

3.1 Analytical Methods

Continuous monitors are classified by the properties that they measure with respect to mass (i.e., inertial mass, beta-ray attenuation, pressure drop), interactions with light (i.e., scattering and absorption), condensation, mobility (e.g. electrical mobility, differential mobility), chemical components (e.g. single particle characteristics, carbon, sulphur, nitrate, and elements), and precursor gases (e.g. ammonia, nitric acid, sulphur dioxide). There are several approaches to measuring the same property, hence an explanation of the chosen instrumentation to be used in the collection of data for the Brown Haze, will be discussed in detail later in this section. A brief explanation of the two forms (particle and gaseous) of analysis will now be discussed.

3.1.1 Particle analysis

Particles in the atmosphere vary in size, chemical composition, and optical properties. Aerosol diameters range over five orders of magnitude, from 0.01 μm to around 100 μm. Various continuous or manual aerosol sampling techniques (figure 9) are available to analyse for the respective aerosol ranges.

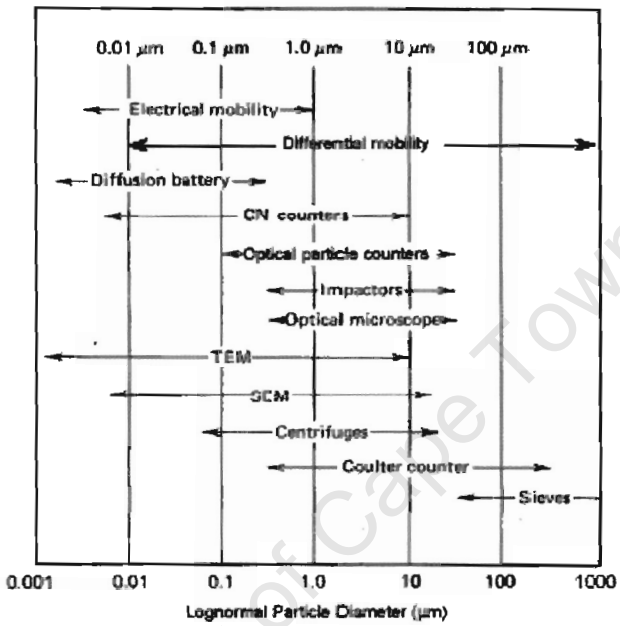

Figure 9: Various continuous or manual aerosol sampling techniques available to analyse the respective aerosol ranges. (From US EPA, 1998, via Willeke and Baron, 1993.)

This section further discusses the physical (e.g. particle size), and optical (e.g. light scattering, light absorption) properties of aerosols.

Particle size is an important parameter in determining emission sources, atmospheric processes, visibility impairment, as well as human respiratory system responses and associated health effects (US EPA, 1998). At one time the quantity of atmospheric particles can vary into the hundreds of millions in a certain volume of air. The largest number of particles is in the nuclei or ultrafine size fraction (particle diameters less than 0.1 μm). Ultrafine particles are often observed near emission sources and possess a very short lifetime, with duration of less than one hour. Ultrafine particles rapidly condense on or coagulate with each other, forming particles in the accumulation mode (0.08 to ~2 μm). The accumulation range particles (0.08 to 2 μm) can also result from condensation of volatile species and from gas-to-particle conversion. Particles in the accumulation mode scatter and absorb light more efficiently than the larger or coarse

particles. The nucleation and accumulation ranges constitute the $PM_{2.5}$ size fraction. Particles larger than 2.5 μm are called "coarse" particles; they result from grinding activities and are dominated by materials of geological origin (US EPA, 1998).

Particle Interactions with Light

An apparent and more direct indicator for assessing the Brown Haze is through human visibility. Visibility degrades when particle concentrations increase. This visibility is determined through the reflection and absorption of light as it falls on an object. These interactions are a function of wavelength. Visible light occupies a region of the electromagnetic spectrum with wavelengths between 400 nm and 700 nm, partially overlapping particle diameters in the accumulation mode (US EPA, 1998).

Light is scattered when diverted from its original direction by matter. The presence of atmospheric gases such as oxygen and nitrogen limits horizontal and vertical vision (US EPA, 1998). Light is also scattered by particles suspended in the atmosphere, and the efficiency of this scattering is largest for particles with sizes comparable to the wavelength of light (approximately 500 nm). The degree to which particles scatter light depends on their size, shape, and index of refraction (which depends on their chemical composition) (US EPA, 1998). Light passing through the atmosphere is absorbed primarily by nitrogen dioxide gas, and by non-transparent geological and black organic particles (US EPA, 1998).

3.1.2 Chemical analysis

The relative abundances of chemical components in the atmosphere closely reflect the characteristics of emission sources. These chemical compositions need to be quantified in order to establish causality between exposure and health effects. Major chemical components of $PM_{2.5}$ or PM_{10} mass in urban areas consist of nitrate, sulphate, carbon, geological material, sodium chloride, and liquid water. PM concentration and chemical composition vary in time and space due to changes in emission density, meteorology, and terrain features (US EPA, 1998).

3.2 Instrumentation

In this section a brief overview of the instruments used in the analysis phase of the thesis will be discussed. The first four instruments are descriptive of the physical attributes of particles, whilst the remaining instruments are used in describing the chemical attributes of the pollution.

3.2.1 Particle analysers

The instruments used to assess the physical attributes are based on the properties of visible-light scattering. This is done by illuminating particles, individually or as a group, and measuring the intensity at different orientations from the incident light source. The intensity of scattered light is related to mass concentration by electromagnetic theory (US EPA, 1998). The instruments that use such concepts are the PCASP and the CCN counter. The other particle analyser mentioned, the ABS, uses a filter collection device.

PCASP

The model used for the analysis of particles within the range of 0.1 to 3 μm is the PCASP 100X (figure 10). It is designed to allocate detected particles into fifteen size channels. The spectrometer has a size resolution of 0.02 μm in the smallest channel. The maximum count rate for the instrument is 20 000 counts per second and the sample volume flow rate is 1 cm^3/sec. The PCASP-100X operates best when temperatures range between -40°C to 40°C and up to an altitude of 12.1 km (Particle Measuring Systems Inc.).

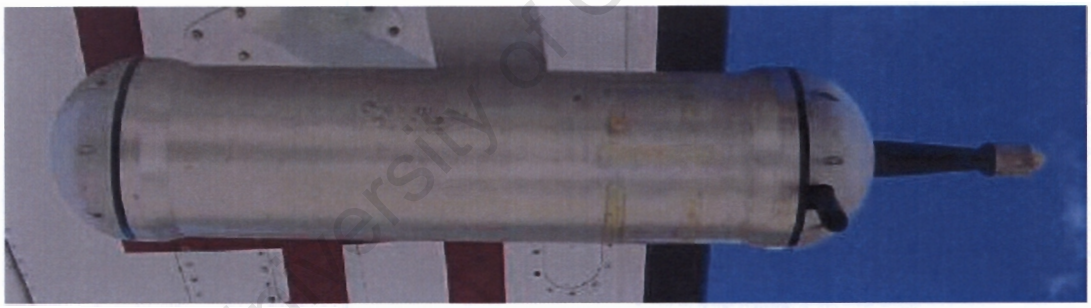

Figure 10: The PCASP instrument attached to the right wing of the Aerocommander.

The instrument operates on the principle that the light scattered by a particle within an active laser cavity is a direct function of its size. The laser contained by the PCASP-100X is a classical passive cavity with a He-Ne high order multimode tube which is enveloped with stainless steel. The laser alignment is achieved with sensitive adjustment on the crystal oscillator assembly. The PCASP-100X uses a combination reflecting-refracting imaging system in its collecting optics. This high efficiency light gathering system collects more than one-half of the total light scattered even by the smallest particle with over 2π steradians collecting solid angle (Particle Measuring Systems Inc.).

The method of particle input is with an aerodynamically focused jet which constrains particle flow to a 150 μm diameter stream surrounded by a filtered sheath flow. Particles

produce pulses of radiant energy during transit through the laser beam. The light obtained off the particles is channeled with the aid of an aspheric lens and a parabolic mirror to a single silicon photodiode detector which converts the collected light into signal photocurrent (sized with a 16-channel pulse height analyzer) (Particle Measuring Systems Inc.).

CCN counter

Continuous flow Condensation Nuclei Counters (CCN) sense ultrafine particles by causing them to grow to a size that is efficiently detected by light scattering. Particles in a sampled air stream enter a saturator where alcohol vapours at a temperature above 35°C create a saturated atmosphere. Particles then pass into a condenser tube where alcohol vapour condenses on the particles causing them to grow, they are then detected and classified.

CCNs detect particles with 0.003 to 1 µm diameters. For low particle concentrations, the instrument operates in a counting mode, registering individual light pulses. For concentrations above 1 000 particles/cm^3, the viewing volume of particles becomes saturated and individual particles can no longer be counted. Hence, the CCN switches to the photometric mode where the power of the light scattered by all particles present in the viewing volume is measured.

In the counting mode, a CCN can be very precise, but the counting efficiency for ultrafine particles depends substantially on the instrument design. In the photometric mode, the CCN must be calibrated with aerosol of known concentration (for example, by using an electrostatic classifier) (US EPA, 1998).

Airborne Streaker Sampler

The airborne streaker sampler (ABS) was mounted inside a capsule which was attached to the left wing of the Aerocommander (Figure 11).

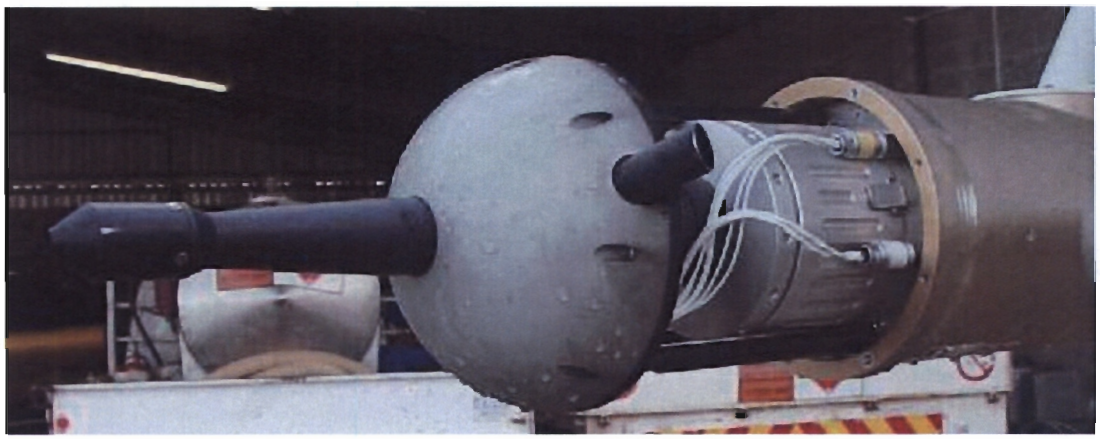

Figure 11: The ABS instrument was attached to the left wing of the Aerocommander.

The ABS consists of size-selective inlets, filter media, filter holders, and flow movers/controllers. The body of the ABS unit has a cylindrical form with a diameter of approximately 100 mm and a length of about 200 mm. It contains a clock motor that advances two particle collection substrates mounted within the streaker. Sample air flow rates can be verified by a flow meter, temporarily attached to the inlet of the streaker sampler at the beginning and end of sampling on each substrate, or at times in between. The air flow rate through the streaker sampler is primarily controlled by the porosity of the filter and the area of the sucking orifice.

The collection of the ambient particles occurs on two impaction stages and a Nuclepore polycarbonate-membrane after-filter. From this elemental composition analysis is done on the filters by either particle-induced x-ray emission (PIXE) analysis or scanning electron microscope (SEM). The SEM unit was chosen to perform the elemental analysis. This process will be described in greater detail in the next section.

The method of particle selection or collection through the ABS is executed by firstly advancing through the first impaction stage, which has a 10 µm cut point and collects particles on an oiled frit that does not move. The particles collected on this stage are discarded. The second impaction stage has a 2.5 µm cut point and collects coarse particles on a rotating Kapton substrate that is coated with Vaseline to minimize particle bounce. The second impaction stage is followed by a 0.4 µm pore size Nuclepore polycarbonate-membrane filter that has an 8 mm long negative pressure orifice behind it to collect fine particles (US EPA, 1998).

Scanning Electron Microscope

The scanning electron microscope (SEM) unit that was used at the University of Cape Town comprises of the Leica S440 digital scanning electron microscope and three major subsystems: a Fisons Kevex Energy Dispersive X-Ray Analysis System; a Fisons LT7400 Cryo Transfer; and an Oxford Monochromator Cathodoluminescent system.

The microscope is capable of a resolution of 3 nm at 40 kV with a LaB6 filament and is digital in every respect. This enables experiments to be automated and it enables the images to be analysed directly. Line averaging and frame averaging can be applied to the image in addition to increasing the dwell time in order to reduce the noise without damaging the specimen. The digital images can also be stored on magnetic disc and can be saved on a variety of different mediums.

The five most important hardware requirements include the specimen holder, phosphor screen, a low light video camera, a vacuum system and an electron gun. The phosphor screen is mounted internally whereas the video camera is mounted on the outside of the chamber. Despite the large chamber on the LEICA 440 SEM, space has been restricted in the present system due to the configuration of SE, BSE, X-ray, CL and Mono-CL detectors, as well as a cryoprep chamber and stage, and an infra-red chamberscope. The specimen holder tilt angle is fixed at 70.5° when the microscope stage is horizontal. In view of the positioning of the other detectors within the chamber, and the need to acquire SE images, the EDR port was selected to mount the video camera. A 50 mm diameter lead glass window has been fitted to the EDR port, and the video camera (HAMAMATSU C2400-08 SIT camera) is supported by a stainless steel arm attached to the port.

The electron gun is the source of the electron probe. A common type of gun utilises a tungsten hairpin emitter. The mechanism behind the electron emissions is due to a sharply bent piece of 120 µm wire which is heated at 2 700 – 2 900 K in a vacuum usually better than 0.1 mPa. The more weakly-bound electrons are thus given sufficient energy to escape the solid state.

The available detectors include the secondary electron detector (those emitted electrons having an energy less than or equal to 50 eV and which give insight into the surface topography of the specimen), the backscattered electron detector (those emerging electrons having an energy greater than 50 eV and which displays regions of altered atomic composition due to the energy emitted being sensitive to the atomic number of the atoms in the specimen), a transmission detector, a specimen current amplifier, the

Si(Li) X-ray detector (which is a characteristic of the atom type and thus can be used to quantify the atomic composition), a cathodoluminescence detector with ellipsoidal mirror and spectrometer and a long working distance cathodoluminescence detector.

An infrared video camera enables the inside of the chamber to be monitored continuously. The design of the secondary electron detector enables specimens to be examined horizontally, thus overcoming the geometric distortions introduced by viewing tilted specimens. Signals from any two of the SE detector, BS detector or CL detector can be viewed simultaneously. The X-ray detector is fitted with a BN window and can detect elements with atomic numbers as low as boron.

The preparation of the filter samples was performed by cutting out the filter samples and mounting them onto aluminium sample stubs 10 mm in diameter, using water-based glue, which was mixed with colloidal carbon. The filter samples where then coated with carbon in an evaporation coater. This was done to reduce charge buildup on the insulating filter substrate during electron beam bombardment. Once this was done the filter stubs were ready for analysis.

The calibrations and corrections that are needed to be performed on the SEM on a regular basis are the calibration of the probe diameter (which is a function of kV, aperture size, working distance and beam current), the filament saturation and astigmatism correction (which enables the best obtainable image quality) and lastly the magnification calibration and distortion correction (errors of up to 25% can be recorded). Distortion takes place at low magnification (lower then 500 times) and hence, there is no need to worry about this error, as the samples were all taken at x500 or greater magnification.

3.2.2 Gaseous analysers

The direct-reading gaseous analysers were onboard the Aerocommander aircraft. The instruments that are relevant to the analysis of the Brown Haze are the ozone analyser, the sulphur dioxide analyser, the carbon monoxide analyser, the nitrogen oxides analyser and the carbon dioxide analyser.

These chosen instruments encompass various features that form part of the respective gaseous analysers. They are the multi-line alphanumeric display, menu-driven software, field programmable ranges, dual range mode, auto range mode, multiple analog outputs, high sensitivity, fast response time and the linearity through all the ranges. Additional features, specific to the type of analyser, are discussed in the respective sections below.

All of the above mentioned gaseous instruments onboard the Aerocommander were calibrated and corrected for by the manufacturer "*Thermo Environmental Instruments Inc.*". The corrections, temperature and pressure, for all gaseous instrumentation took place prior to the routine calibration procedures for the instruments. The temperature correction provides compensation for any changes to the instrument's output signal due to internal instrument temperature variations. Pressure correction provides compensation for any changes to the instrument's output signal due to optical chamber pressure variations. Both these corrections are corrected for empirically.

The respective calibrations for the various analysers were conducted under the required regulations. The ozone analyser was calibrated under a current EPA approved procedure using a UV photometer as the calibration standard. The carbon dioxide and carbon monoxide analysers used an approved cylinder as the standard – these cylinders were up to the specification of the National Institute of Standards and Technology (NIST) in Air Standard Reference Material (SRM) or to the NIST/EPA approved gas manufacturer's Certified Reference Material (CRM) standard. The sulphur dioxide analyser used an SO_2-free (less than 0.0005 ppm) air supply for the zero calibration, preceded by a SO_2 calibration gas of a known concentration. The calibration technique that was used for the nitrogen oxides analyser was based on the rapid gas phase reaction between NO and O_3 which produces stoichiometric quantities of NO_2 in accordance with the reaction: $NO + O_3 \rightarrow NO_2 + O_2$. The cylinders used for this calibration were also traceable to a National Institute of Standards and Technology (NIST) Standard Reference Material (Thermo Environmental Instruments Inc. Instruction Manual, 2000a, b, c, d, e).

Ozone analyser

The instrument used was the Thermo Environmental Instruments Model 49C, which offered additional features, such that the dual cell measurement cancels potential interference, the temperature and pressure correction is automated and the instrument is approved by the US Environmental Protection Agency (Thermo Environmental Instruments Inc. Instruction Manual, 2000e).

Some specifications that the Model 49C possess include a precision of 1 ppb, a lower detectable limit of 1.0 ppb, a sample flow rate of one to three litres per minute, a range between 0.05 to 200 ppm and an operating temperature between 20°C to 30°C (Thermo Environmental Instruments Inc. Instruction Manual, 2000e).

The Model 49C uses the principle that ozone molecules absorb Ultra Violet (UV) light at a wavelength of 254 nm. The degree to which the UV light is absorbed is directly related to the ozone concentration. The Beer-Lambert law illustrates this relationship:

$$\frac{I}{I_0} = e^{-KLC}$$

where: K = molecular absorption coefficient at 0°C and 1 atmosphere (308 cm^{-1}); L = length of cell (380 mm); C = ozone concentration in parts per million; I = UV light intensity of sample with ozone (sample gas); I_o = UV light intensity of sample without ozone (reference gas).

The mechanism behind the analysis is such that a sample is drawn into the Model 49C through the sample bulkhead and is split into two gas streams. One gas stream flows through an ozone scrubber to become the reference gas (I_o). The reference gas then flows to the reference solenoid valve. The sample gas (I) flows directly to the sample solenoid valve. The solenoid valves alternate the reference and sample gas streams between cells A and B every 10 seconds. When cell A contains reference gas, cell B contains sample gas and vice versa. The UV light intensities of each cell are measured by two detectors A and B. When the solenoid valves switch the reference and sample gas streams to opposite cells, the light intensities are ignored for several seconds to allow the cells to be flushed. (Thermo Environmental Instruments Inc. Instruction Manual, 2000e).

Sulphur dioxide analyser

The instrument used was the Thermo Environmental Instruments Model 43C, which offered additional features, such that the instrument is totally self-contained, it possesses an internal sample pump, it is insensitive to change in flow and temperature and the instrument is approved by the US Environmental Protection Agency (Thermo Environmental Instruments Inc. Instruction Manual, 2000c).

Some specifications that the Model 43C possesses, include a precision of 1 ppb or one percent (which ever is greater), a lower detectable limit of 2.0 ppb in a 10 second average time, a sample flow rate of 0.5 to 1.0 litre per minute, a range between 0.05 to 100 ppm and an operating temperature between 20°C to 30°C (Thermo Environmental Instruments Inc. Instruction Manual, 2000c).

The Model 43C uses the principle that SO_2 molecules absorb ultraviolet (UV) light and become excited at a particular wavelength, they then decay to a lower energy state

emitting UV light at a different wavelength (Thermo Environmental Instruments Inc. Instruction Manual, 2000c).

The sample is drawn into the Model 43C through the sample bulkhead. The sample flows through a hydrocarbon kicker, which removes hydrocarbons from the sample. The SO_2 molecules then pass through the hydrocarbon kicker unaffected and flow into the fluorescence chamber, where pulsating UV light excites the SO_2 molecules. The condensing lens focuses the pulsating UV light into the mirror assembly, which only reflects the wavelengths of the excited SO_2 molecules (Thermo Environmental Instruments Inc. Instruction Manual, 2000c).

As the excited SO_2 molecules decay to lower energy states they emit UV light that is proportional to the SO_2 concentration. The bandpass filter allows only the wavelengths emitted by the excited SO_2 molecules to reach the photomultiplier tube (PMT). The PMT detects the UV light emission from the decaying SO_2 molecules. The photodetector then continuously monitors the pulsating UV light. The Model 43C outputs the SO_2 concentration to the front panel display and the analog outputs (Thermo Environmental Instruments Inc. Instruction Manual, 2000c).

Carbon monoxide analyser

The instrument used was the Thermo Environmental Instruments Model 48C, which offered additional features, such that the instrument was highly specific to CO, it possesses self aligning optics, it automatically corrects for temperature and pressure variations and it is approved by the US Environmental Protection Agency (Thermo Environmental Instruments Inc. Instruction Manual, 2000d).

Some specifications that the Model 48C possesses, include a precision of approximately 1 ppb, a lower detectable limit of 0.04 ppm, a sample flow rate of 0.5 to 2.0 litres per minute, a range between 0 to 10 000 ppm and an operating temperature between 20°C to 30°C (Thermo Environmental Instruments Inc. Instruction Manual, 2000d).

The Model 48C uses the principle that carbon monoxide (CO) absorbs infrared radiation at a wavelength of 4.6 μm. Infrared absorption is a non-linear measurement technique, hence an exact calibration curve has been used to accurately linearise the instrument output over the instruments range (Thermo Environmental Instruments Inc. Instruction Manual, 2000d).

The sample is drawn into the Model 48C through the sample bulkhead. The sample then flows through the optical bench where alternating CO and N_2 filtered radiation from an infrared source is absorption by the sample gas. The infrared radiation then exits the optical bench and falls on an infrared detector. The chopped detector signal is modulated by the alternation between the two gas filters with amplitude related to the concentration of CO in the sample cell. Other gases do not cause modulation of the detector signal since they absorb the reference and measured beams equally. Thus the Gas Filter Correlation (GFC) system responds specifically to CO (Thermo Environmental Instruments Inc. Instruction Manual, 2000d).

3.2.2.4 Nitrogen Oxides Analyser

The instrument used was the Thermo Environmental Instruments Model 42C, which offered additional features, such as independent NO, NO_2 and NO_x ranges, a replaceable NO_2 converter cartridge and it is approved by the US Environmental Protection Agency (Thermo Environmental Instruments Inc. Instruction Manual, 2000b).

Some specifications that the Model 42C possesses, include a precision of approximately 0.4 ppb, a lower detectable limit of 0.4 ppb, a sample flow rate of 0.6 litres per minute, a range between 0 to 100 ppm and an operating temperature between 15°C to 35°C (Thermo Environmental Instruments Inc. Instruction Manual, 2000b).

The Model 42C uses the principle that nitric oxide and ozone react to produce a characteristic luminescence with intensity linearly proportional to the NO concentration. Infrared light emission results when electronically excited NO_2 molecules decay to lower energy states (Thermo Environmental Instruments Inc. Instruction Manual, 2000b).

The ambient air sample is drawn into the Model 42C through the sample bulkhead. The sample flows through a particulate filter and then to the mode solenoid valve, which routes the sample either straight to the reaction chamber (NO mode) or through the NO_2-to-NO converter and then to the reaction chamber (NO_x mode). A flow sensor prior to the reaction chamber measures the sample flow, which in turn regulates the ozonated dry air. The ozonator generates the necessary ozone concentration needed for the chemiluminescent reaction. The ozone reacts with the NO in the ambient air sample to produce electronically excited NO_2 molecules. A photomultiplier tube (PMT) housed in a thermoelectric cooler detects the NO_2 luminescence. The NO and NO_x concentrations are stored in memory and the difference between the concentrations is the resulting NO_2 concentration (Thermo Environmental Instruments Inc. Instruction Manual, 2000b).

3.2.2.5 Carbon Dioxide Analyser

The instrument used was the Thermo Environmental Instruments Model 41C, which offered additional features, such as self aligning optics and automatic temperature and pressure correction (Thermo Environmental Instruments Inc. Instruction Manual, 2000a).

Some specifications that the Model 41C possesses, include a precision of approximately 1 percent, a lower detectable limit of 100 ppb, a sample flow rate between 0.5 to 2.0 litres per minute, a range between 0 to 2 000 ppm and an operating temperature between 15 to 35°C (Thermo Environmental Instruments Inc. Instruction Manual, 2000a).

The Model 41C High Level uses the principle that carbon dioxide absorbs infrared radiation. Infrared absorption is a non-linear measurement technique, hence an exact calibration curve has been used to accurately linearise the instrument output over the instruments range (i.e. up to a concentration of 2 000 ppm) (Thermo Environmental Instruments Inc. Instruction Manual, 2000a).

The sample is drawn into the analyzer through the sample bulkhead. The sample then flows through the optical bench where alternating CO and N_2 filtered radiation from an infrared source are absorbed by the sample gas. The infrared radiation then exits the optical bench and falls on an infrared detector. The chopped detector signal is modulated by the alternation between the two gas filters with amplitude related to the concentration of CO_2 in the sample cell. Other gases do not cause modulation of the detector signal since they absorb the reference and measured beams equally. Thus the Gas Filter Correlation (GFC) system responds specifically to CO_2 (Thermo Environmental Instruments Inc. Instruction Manual, 2000a).

Chapter 4 – Results

The results chapter presents data from the chosen flights. These flights were used as a comparison to determine the characteristics of the Brown Haze on a haze day in relation to a non-haze day and changes in the Brown Haze characteristics with respect to time of day.

Flights 14 and 15 were utilized to determine the fluctuation in the pollution levels from early morning to the afternoon and flights 12 and 13 were used to determine the difference between a haze day and a non-haze day. Table 1 shows the flight details for these four flights and the path flights are illustrated in figure 12. The two flights chosen for the haze and non-haze day comparisons were at approximately the same time of day. The 13th August 2003, was chosen as a non-haze day as a cold front had passed through a day prior. A cold front has a cleansing effect on the atmosphere as it replaces air that may have accumulated urban emissions, with an air mass that originates over the remote ocean, as well as it scrubs out pollutants with rain, which is usually associated with cold fronts. During the course of the flight, clearer visibility was apparent in flight 12.

Table 1: Flight details used in the profile comparisons.

Date	Flight Number	Haze characteristics	Take Off Time (UTC)	Duration (h:min:s)
13 August 2003	12	Non-haze day	12:33:00	01:45:00
15 August 2003	13	Haze day	13:38:00	02:20:00
22 August 2003	14	Haze day	06:55:00	02:15:00
22 August 2003	15	Haze day	14:10:49	01:20:00

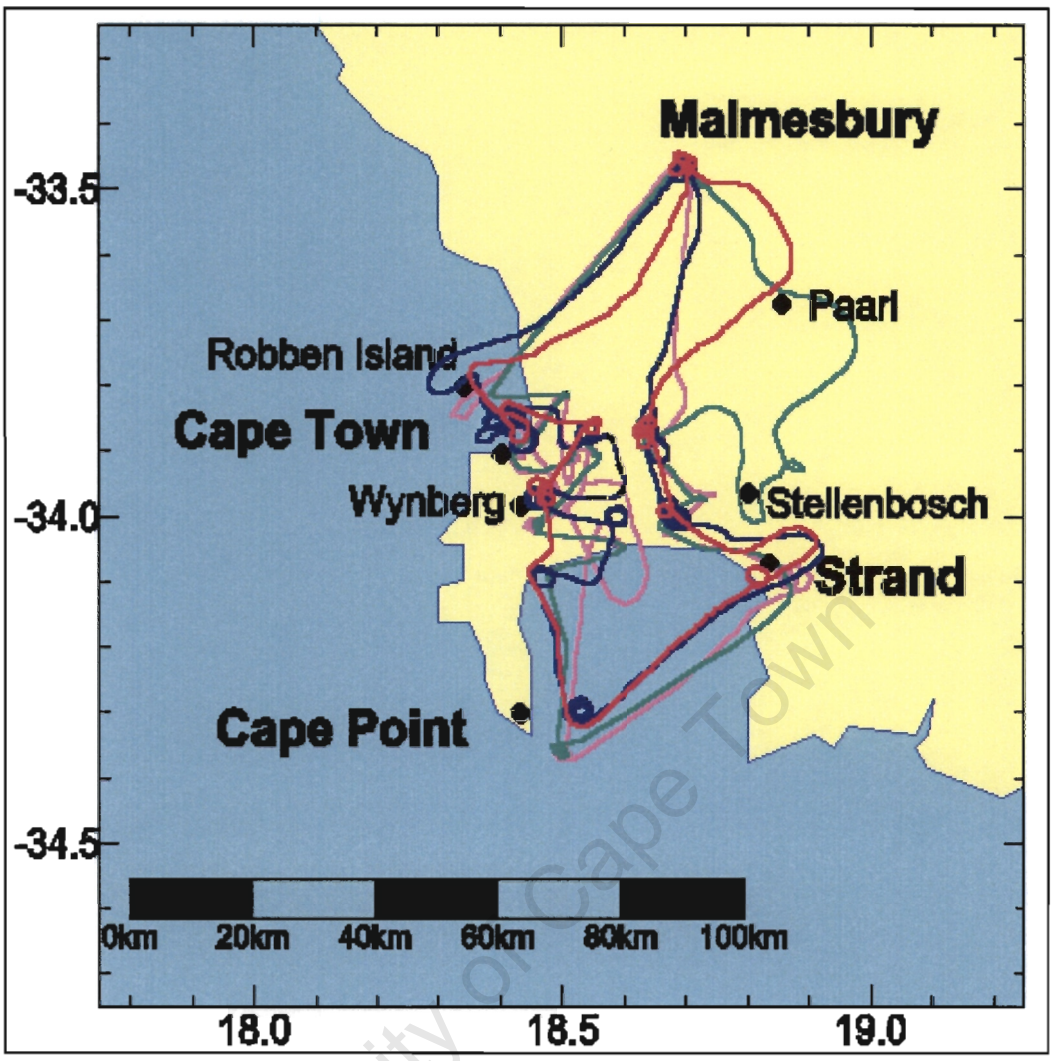

Figure 12: The flight paths for the flights 12, 13, 14 and 15 selected for interpretation in this dissertation.
(Flight 12 - green, flight 13 - pink, flight 14 - blue and flight 15 - red.)

4.1 Meteorological Data

4.1.1 Weather conditions

The surface wind speed and direction within the Cape region varies from area to area due to the topography of the surrounding mountains. Surface weather data was obtained from two South African Weather Services weather stations, at Strand and at Cape Town. The Cape Town station is located in the suburb of Gardens and the Strand station is located inland off the Strand beach. Both sites are good representations of the topography that surrounds them. The Strand station provides a representation of the weather experienced on the Cape flats. The Cape Town station is representative of areas surrounded by mountains. The climate number for the Cape Town station is 0021178A3 and 0005609 8 for the Strand station.

The wind direction diagrams, found in the compilation in Appendix A, are represented by the number of hours the wind was blowing in a given direction during the course of the chosen day (The wind roses also indicate the dominant wind directions that endured during the various flight hours – these are marked in red or yellow). The wind speed statistics for the particular wind directions are represented in tabular form. Table 2 shows the average wind speed, standard deviation of the wind speeds, as well as the minimum and maximum wind speeds for the various wind directions. The wind speed averages were derived from the flights discussed in the dissertation, which occurred over a one month period. Calm conditions are represented on the respective wind direction diagrams and the wind speed table by a null value.

Table 2: Wind speed (m/s) data, recorded for the days of interest, for the various wind directions.

Average Wind Speed (m/s)				
Direction	**mean**	**std dev**	**min**	**max**
N	28.78	12.17	15.00	45.67
NNE	21.44	10.51	11.00	41.00
NE	18.68	6.73	14.00	32.00
ENE	19.01	9.21	12.00	40.13
E	21.04	11.34	14.50	38.00
ESE	17.00		17.00	17.00
SE	*			
SSE	20.33	7.54	15.00	25.67
S	14.00	7.65	3.00	24.00
SSW	*			
SW	30.39	15.59	6.00	49.00
WSW	15.14	4.96	12.00	25.00
W	*			
WNW	23.33		23.33	23.33
NW	44.15	24.47	16.67	74.33
NNW	26.83	21.82	4.00	52.67

(The symbol, *, indicates that there were calm conditions during the flight duration).

From the wind rose diagrams (Figures 13, 14 and 15) for the respective days, it can be seen that the predominant surface wind for the Cape and the Strand region is from a north easterly/north north easterly direction. This indicates a continental wind direction. There is also evidence that the south westerlies (maritime winds) have an influence on the wind flow patterns in the Strand region. From the wind speed table, table 2, the

strong nature of both wind types indicate that they will have an influence on the pollution levels within the study area.

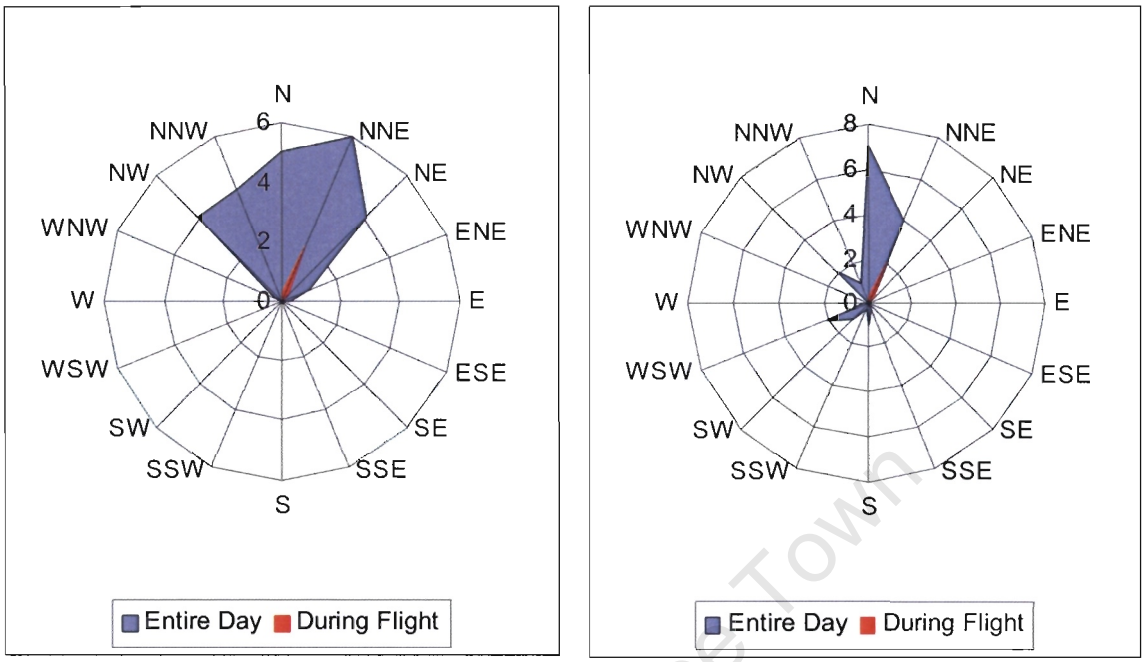

Figure 13: Wind rose diagrams of the surface winds for the 24 hour duration on 13th August 2003: (a) (left) Cape Town weather station; (b) (right) Strand weather station.

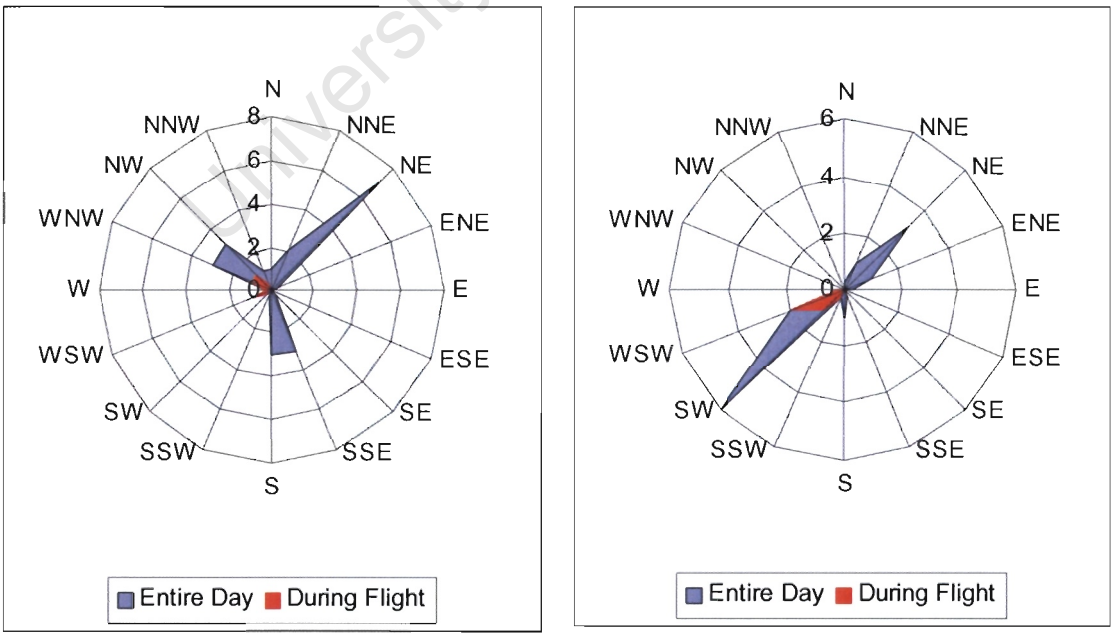

Figure 14: Wind rose diagrams of the surface winds for the 24 hour duration on 15th August 2003: (a) (left) Cape Town weather station; (b) (right) Strand weather station.

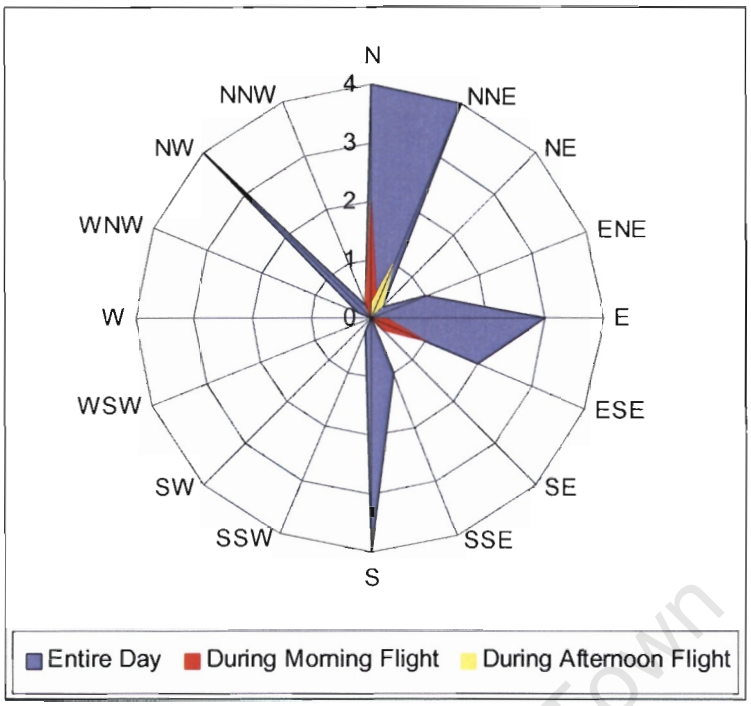

Figure 15: Wind rose diagram of the surface winds, taken at the Cape Town weather station, for the 24 hour duration of the 22nd August 2003.

4.1.2 Inversion layers

For the flights of interest, potential temperature graphs have been created within the flight altitudes. Daily comparisons, Figure 16, were used to determine if the pollution layer was indeed rising. Figure 16a shows that the inversion layer is at an altitude of 90 m. If newly formed pollution is being emitted into the atmosphere during the night and in the early hours of the morning, it most certainly will not rise above the inversion layer and hence be trapped in the zone below the inversion layer. Figure 16b indicates that the significant inversion layer has risen from the morning level to an altitude of 290 m. This expansion of the near surface layer dilutes the Brown Haze, illustrated also by photographs of the haze in early and late morning (figure 7 and 8).

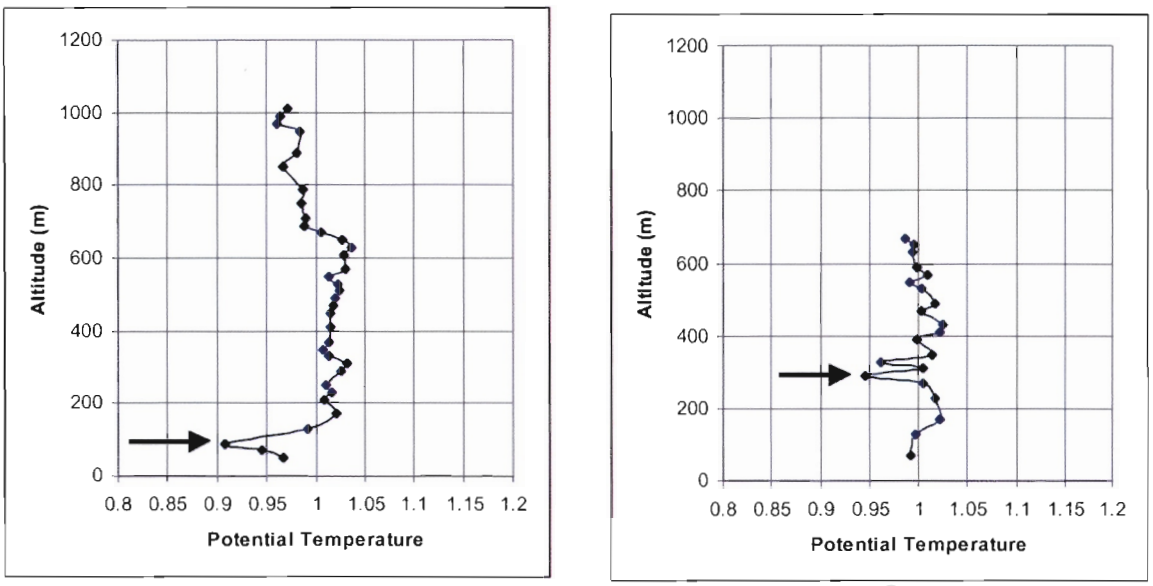

Figure 16: Potential temperature profiles at Cape Point on 22nd August 2003: (a) Early morning (08:15:00 UTC); and (b) Afternoon of the same day (14:46:45 UTC). (The arrow is an indication of the inversion layer altitude).

Table 3 shows the significant inversion layer heights for the respective flights, which were extracted from the potential temperature graphs similar to figure 13. Similar daily trends can be seen when comparisons are done for the morning (flight 14) to the afternoon flights (flights 12, 13 and 15). Most often the lowest significant inversion layer in the afternoon is at a higher altitude than in the morning. (The values that are preceded by a greater or a less than sign, are values that are estimates as to the location of the inversion layer. Insufficient data were obtained because the Aerocommander 690A restricted its flight altitude for that area on that particular flight.) The entire set of potential temperature profiles can be found on the compact disc (Appendix CD-ROM) (The profiles are labelled "g pot T" in Excel format under the respective day).

Table 3: Summary of the significant inversion layers endured during the respective flights.

	Inversion Altitudes (m)			
Region	**Flight 12**	**Flight 13**	**Flight 14**	**Flight 15**
Cape Point	600 - 1100	400 - 1000	< 125	280 - 350
Strand	< 150 > 450	450 – 600 1100 - 1400	< 210 > 470	125 - 175 510 - 560
Robben Island	200 - 280	320 - 1650		
Wynberg			220 – 370	< 300 380 – 410 > 600

4.2 Particulate Matter

4.2.1 Profiles

Vertical profiles varied in range of altitude, according to the pollution vertical profile at the time of the flight, due to the level at which the Aerocommander could safely operate over the urban and mountainous areas and air traffic control restrictions imposed by Cape Town International Airport. Vertical profiles of pollutants were calculated for the days of interest. The areas chosen for the comparisons are namely Strand, Robben Island, Wynberg and Cape Point. These areas were chosen as they represent a spread of the horizontal extent of the Brown Haze. Their locality is such that they are spread far apart to allow for comparisons of an upwind profile (control profiles) and a downwind profile (inside the haze), depending on the wind direction.

The profiles calculated for the analysis of the particles are: the CN profile (which takes into account the total number of particles), the 0.1 to 3 µm diameter particle number concentration profile (obtained from the PCASP) and the 0.1 to 3 µm volume profile (which is further divided into two portions, the fine and coarse particle volumes). The 0.1 to 3 µm volume profiles were obtained from the particle number concentrations by calculating the mean particles size from the respective channel and multiplying that by the total number of particles recorded by the PCASP within the specific channel. The 0.1 to 3 µm volume profile was then categorised into two fractions by determining the portion of particles not detected within the same profile for the number concentrations for the PCASP. These new categories will be used throughout the discussion on PM vertical profiles and are different to the conventional definitions of fine and coarse particles, stated previously. The particle concentrations for particles greater then 0.9 µm were insignificant, hence the volume profile for the same fraction was divided into the fine (0.1 to 0.9 µm) and the coarse (0.9 to 3 µm) particles.

For the flights of interest, the CN profile varied considerably with altitude. This could be due to the stability of the air, as an inversion layer would inhibit the mixing of the atmosphere with height. Most of the profiles unfortunately do not give a good representation of the height where the particle counts are at an atmospheric background value. Flight 13 - Robben Island is the only flight profile which gives some indication (figure 17). Figure 17 shows high concentration below 300 m, a clean slot from 300 m to 600 m, a second layer of high concentration from 600 to 900 m, followed by fragmented high concentration zone from 1 100 to 1 400 m. Above 1 700 m a clean layer of the mid-

troposphere is reached (This clean layer shows a background value above the polluted air mass).

The surface wind conditions for flight 13 (15th August 2003) (figure 14a) were predominantly a north easterly wind for the majority of the early morning. The surface winds changed to a north westerly direction for the remainder of the day until the flight. The flight took place during the occurrence of a north westerly and a west north westerly wind. The wind patterns give some indication as to why high particle number concentrations were obtained close to the surface (Robben Island was located down wind of the northern suburb areas of Cape Town for the majority of the morning).

The zones mentioned for figure 17 correspond to the inversion layers for the same profile (figures 17 and 18). Figure 18 also indicates the clean air slot, with inversion layers above and below.

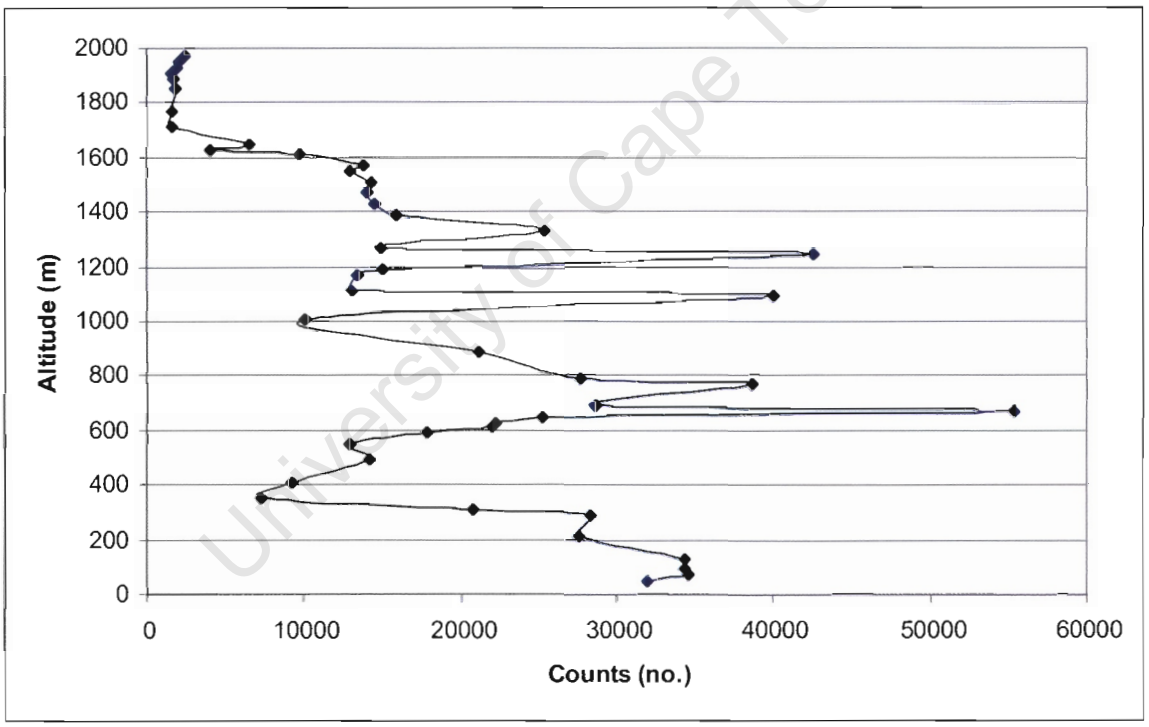

Figure 17: A vertical profile of the particle number concentration over Robben Island for Flight 13 at 12:49:00 UTC.

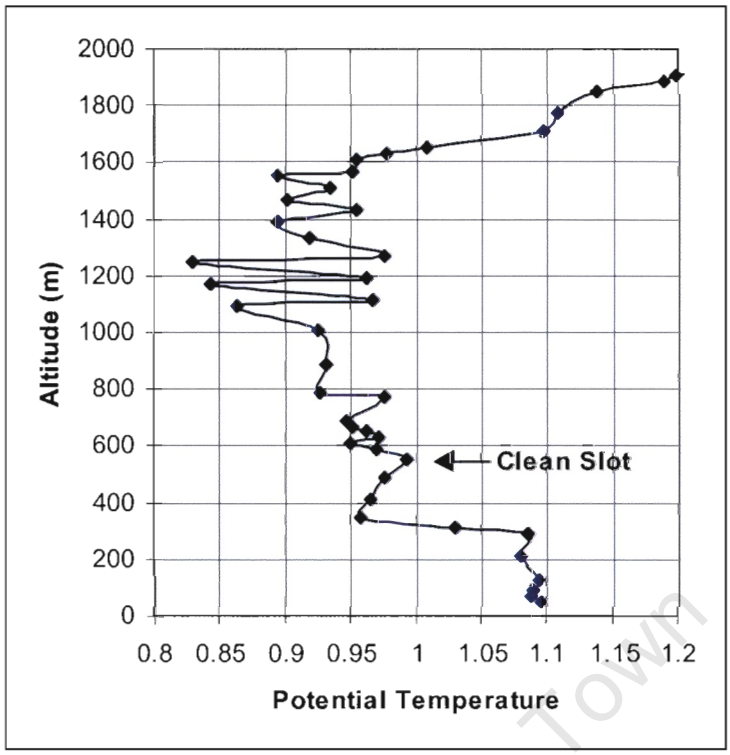

Figure 18: A vertical profile of the potential temperature graph showing the inversion layers over Robben Island for Flight 13 at 12:49:00 UTC.

Cape Point, flight 13, was the only region were atmospheric background values were obtained for altitudes below 800 m. This was due to the fact that for this particular day the wind conditions dictated that the majority of the pollution levels accumulated over the Strand region, hence, the location at which the greatest particle count (63 640 counts cm^{-3}) was recorded was at an altitude of 870 m over Strand. A typical value of the atmospheric background particle counts would be in the region of 1 800 counts cm^{-3} (figures 17 and 19).

The surface wind conditions for flight 13 over the Cape Town region are explained with figure 17. The surface wind conditions for the Strand region (figure 14b) were slightly different, as the dominant surface wind for the day was a strong south westerly wind. This wind direction dictated that the pollutants from the Cape region were directed into the Strand region. The additive effect of both the wind direction and the trapping effect of the surrounding mountains allowed for an accumulation of pollutants in the Strand region.

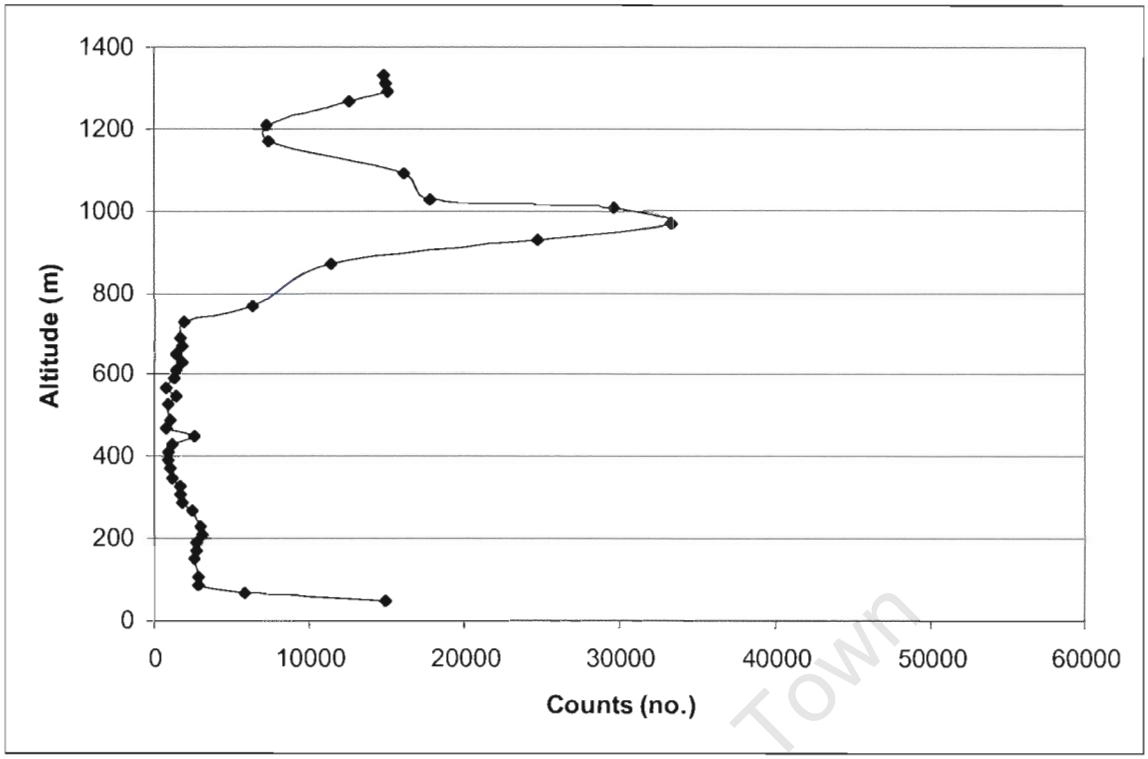

Figure 19: A vertical profile of the total particle number concentration over Cape Point (flight 13 at 14:01:24 UTC), representing clean background conditions at altitudes lower than 800 m.

The number concentration profile values never indicated any significant quantity above an altitude of 1400 m (figures 20 and 21). Comparisons for the haze day and the non-haze day (figures 20 and 21), indicate that the haze days show a significant difference in particle concentrations. The surface winds differed between the non-haze and haze days. The surface winds for the non-haze day (13th August 2003) (figure 13), at the Strand and Cape Town stations, showed that very strong northerly winds flushed pollutants out of the regions (Strand and Robben Island). The haze day (15th August 2003) had slower wind speeds (figure 14), which allowed the pollutants to be detected in the vicinity of the source.

The regions that showed significant concentration values were Strand and Robben Island (Also see the vertical profile for the particle number concentrations obtained, figure 17). Values exceeding 3000 counts per cubic centimetre were recorded on flight 13 for Strand and Robben Island (figures 20 and 21) and on flight 14 for the Strand region. The highest recorded value (5771) was obtained on flight 14 at an altitude of 489 m. The relative profiles can be found on the compact disc (CD-ROM Appendix) (The profiles are labelled "AQ" in Excel format under the respective day).

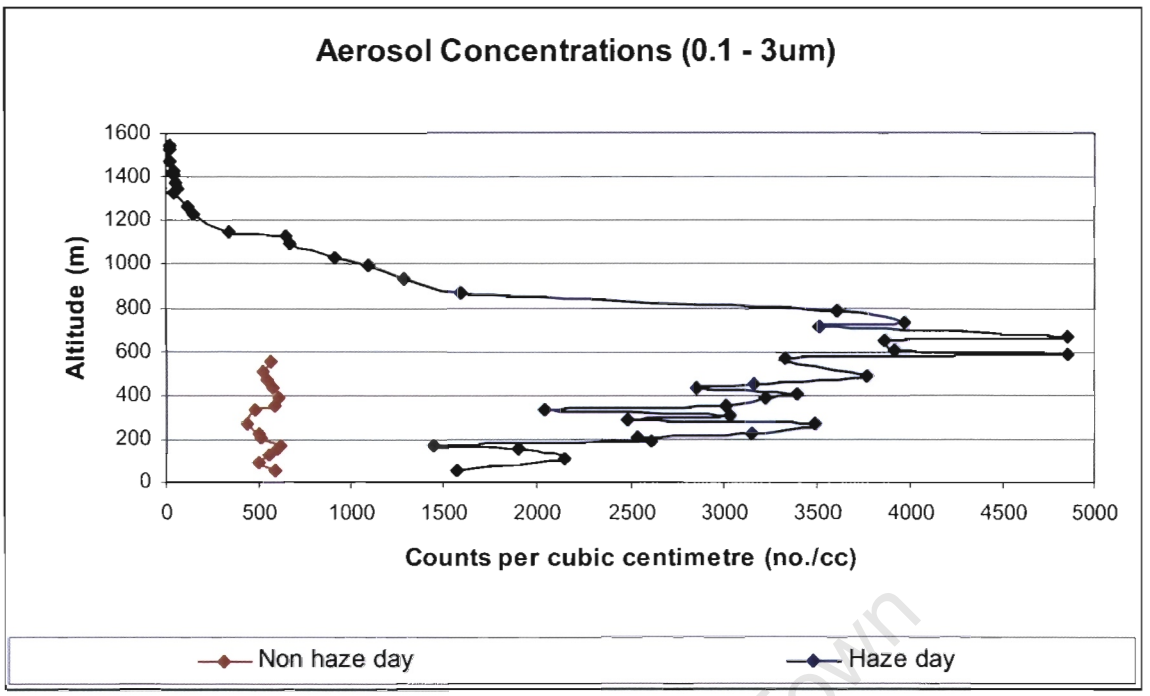

Figure 20: Comparison over the Strand region of haze (flight 13 14:25:54 UTC) and non-haze day (flight 12 13:25:51 UTC) total aerosol number concentrations between 0.1 to 3 μm.

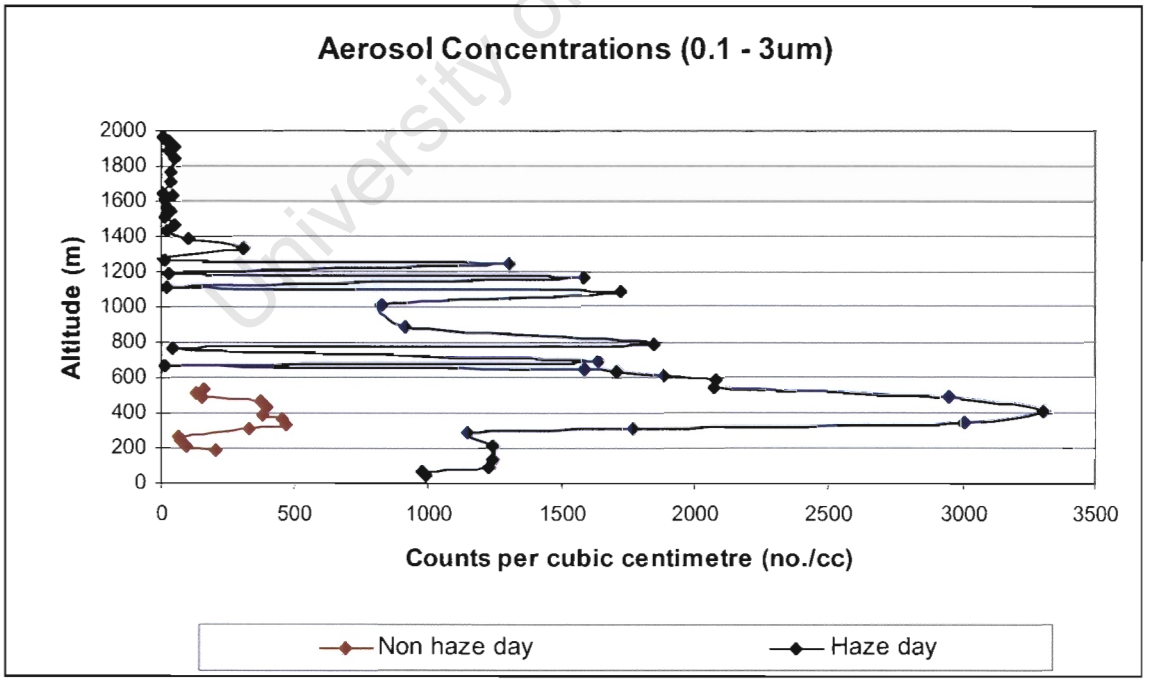

Figure 21: Comparison over Robben Island of haze (flight 13 12:49:44 UTC) and non-haze day (flight 12 12:39:21 UTC) total aerosol number concentrations between 0.1 to 3 μm.

The volume profiles for the 0.1 to 3 µm particles illustrate that the coarse fraction (0.9 to 3 µm) have a greater influence on the total particle quantity than anticipated. The coarse fraction either contributes similar values, in comparison to the fine particles, or values greater then those of the fine fraction. This is understandable, as the volume of a coarse particle can be as much as 15000 times greater than that of a fine particle. The normalised size distribution graphs, which were acquired with the aid of the volume profiles, can give a better indication for the reasons behind this occurrence.

4.2.2 Size distribution

The normalised size distributions consist of size distributions for various heights within a profile. The height ranges for the distributions were chosen specifically from the volume profiles, the potential temperature profiles and from the CN profiles. This was to determine if any anomalies existed between the stable and unstable air masses and to determine if a trend existed between the fine and coarse particles with altitude.

The mode diameter of a volume distribution is the diameter at which the volume size distribution reaches a local maximum. For most of the distributions, two modes were apparent, at 0.2 to 0.3 µm (fine mode) and at ~2.5 µm (coarse mode). The fine mode consists predominantly of combustion aerosols, while the coarse mode consists of dispersal aerosols (i.e. wind blown dust or sea salt). The maximum mode of the particle diameter for the majority of the volume-normalised size distribution curves is between 1 and 3 µm (coarse mode). Flight 15 (Wynberg), flight 15 (Cape Point), flight 14 (Wynberg) and flight 13 (Cape point) all show some or all of the size distribution magnitudes exceeding a maximum mode of 3 µm. Flight 14 (Strand) was the only flight which showed a different pattern (figure 22) – its maximum mode for two of the three height ranges was between a diameter of 0.2 and 0.3 µm.

When comparing the morning normalised volume size distribution curves to the afternoon, a general trend was observed with increasing altitude. The afternoon normalised volume size distribution curves showed a similar pattern for the fine fraction at the various altitudes (figure 23), whereas the morning normalised volume size distribution curves indicated a change in the fine concentration of particles with altitude.

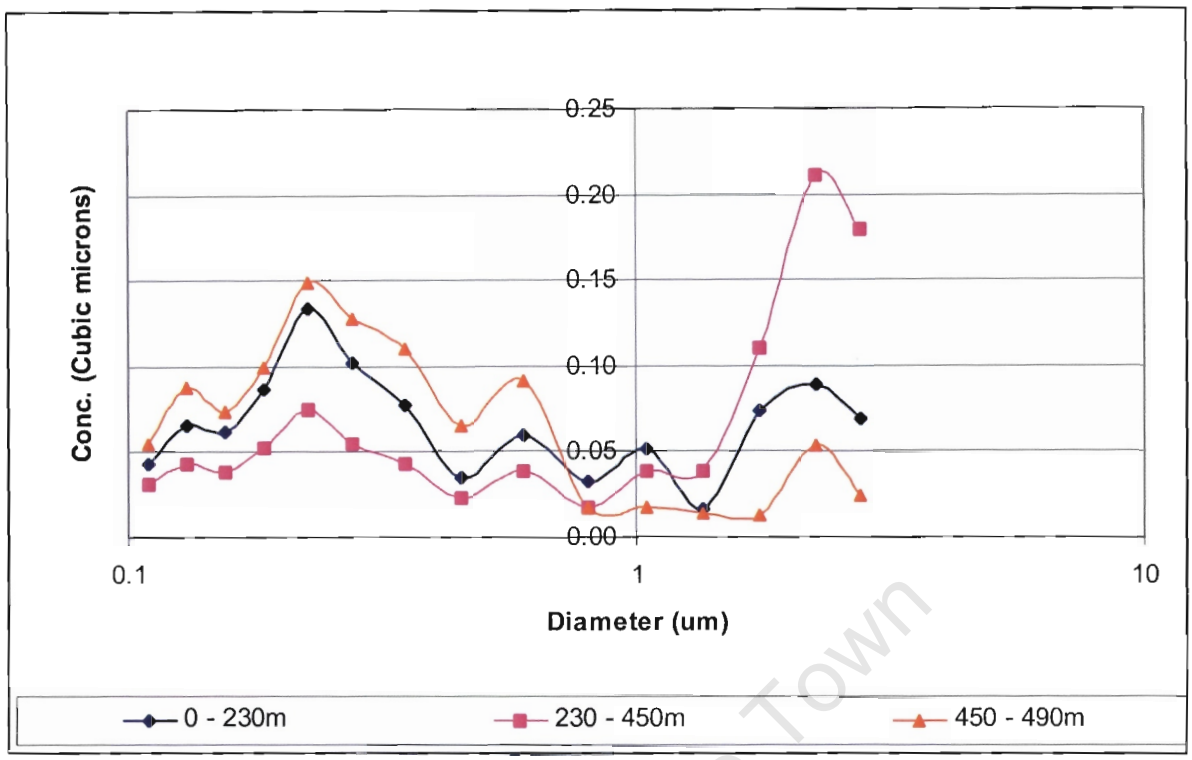

Figure 22: Normalised size distribution for the Strand on flight 14 (morning).

Figure 24 illustrates a decrease in fine particle concentrations and an increase in coarse particle concentrations with altitude. Sea salt particles from breaking bubbles at the ocean surface are the most likely components of the coarse mode particles over Cape Point. The decreasing fine mode and the increasing coarse mode scenario is generally not the case in an ideal atmosphere, as the residence time of coarse particles are expected to be lower than finer particles. This then signifies that various sources are emitting fine particles of these fractional magnitudes during the morning periods. The low inversion layer traps the emissions from these sources in the morning. These inversion layer(s) rise or break up during the course of the day (figure 16), and hence the particles tend to dissipate leaving no trace of these particles in the afternoon. Figure 25 is a comparative normalised volume size distribution curve, which could explain the above anomaly, as this figure is representative of the background values seen in figure 19. From figure 25, the background concentrations for the fine mode concentration are not greater than 0.11 μm^3. This then verifies that a source of particles has added additional fine particles to those already present in the morning normalised distribution (figure 24).

The respective volume normalised size distribution curves can be found on the compact disc (Appendix CD-ROM) (The curves are labelled "nSD" in Excel format under the respective day).

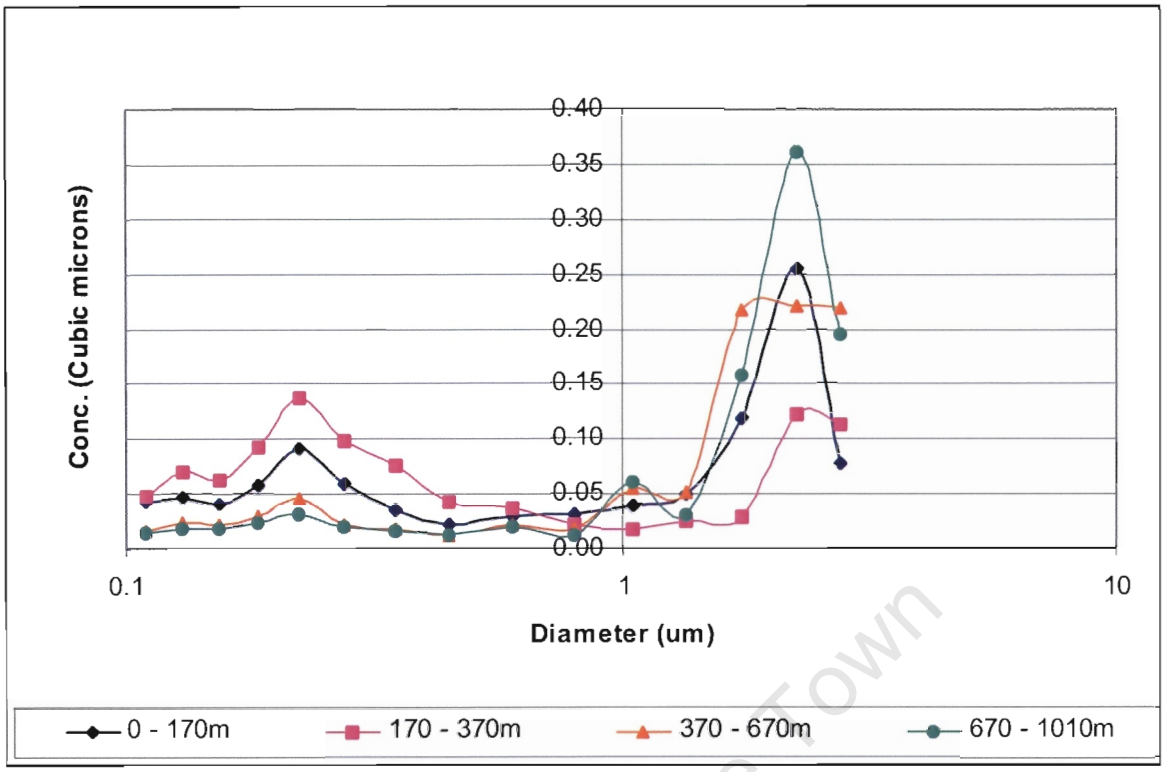

Figure 23: An afternoon normalised size distribution curve for Cape Point (flight 15).

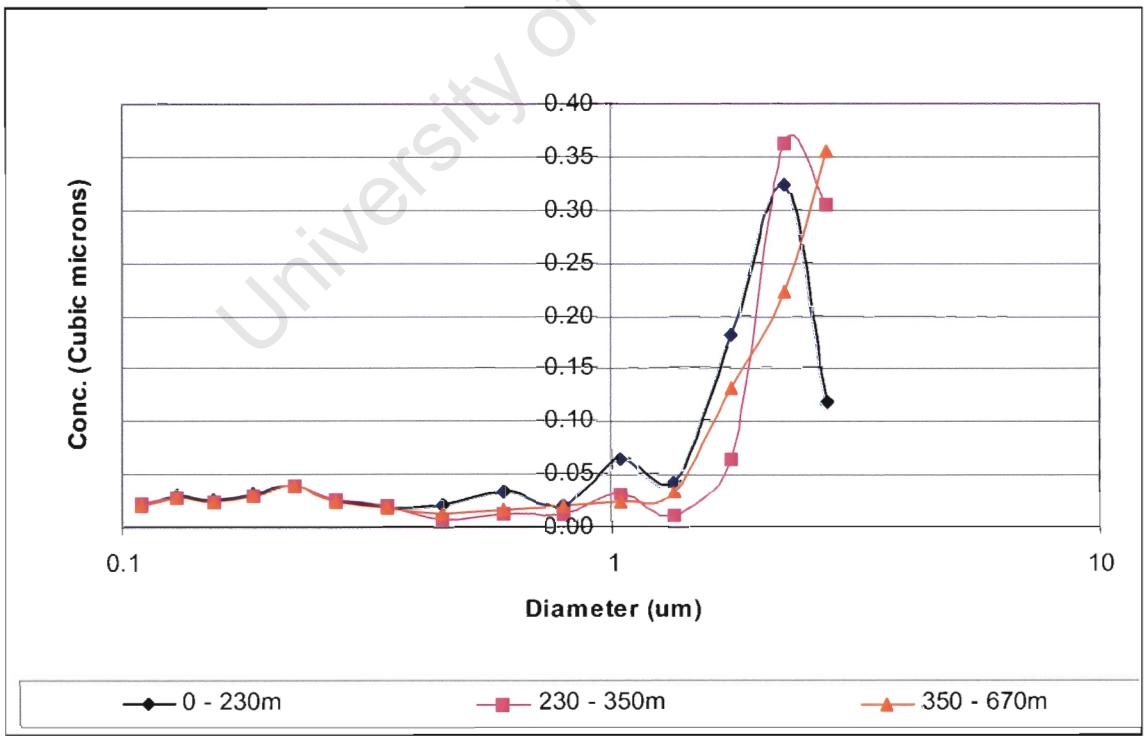

Figure 24: A morning normalised size distribution curve for Cape Point (flight 14).

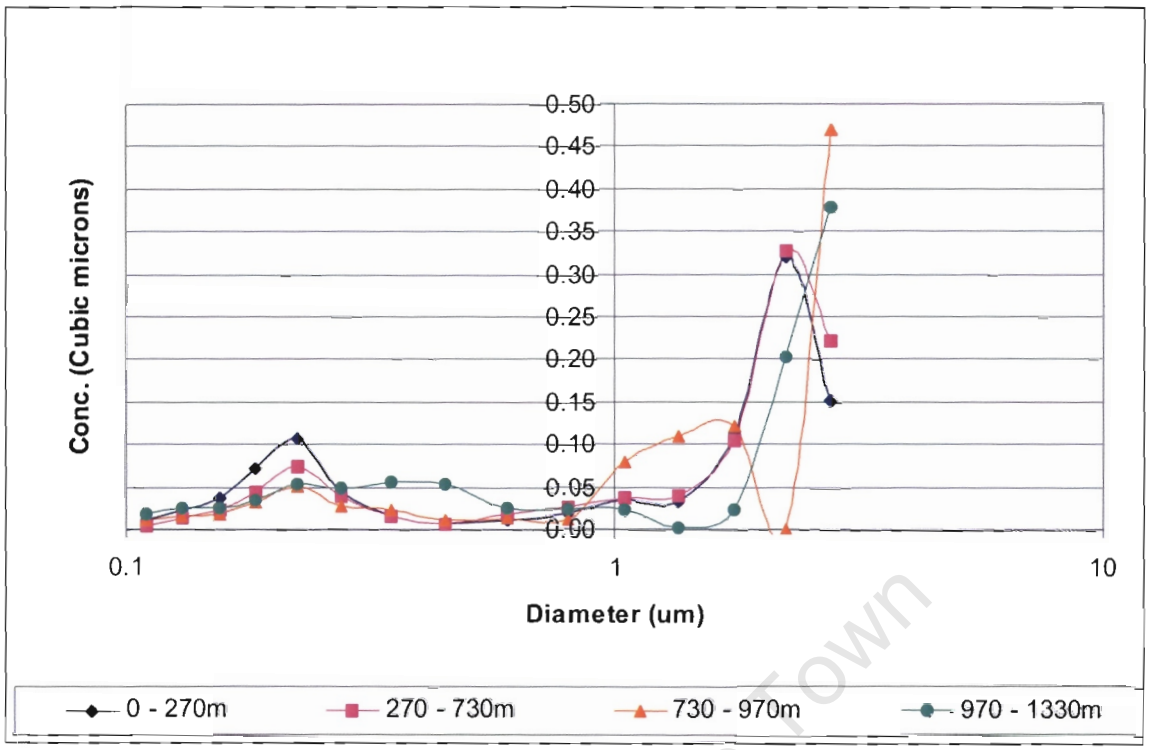

Figure 25: An afternoon normalised Size Distribution curve for Cape Point (flight 13).

4.3 Chemical Composition of Brown Haze

The fine particle (less than 1 µm) elemental composition was determined from the 0.4-µm-pore-size Nuclepore polycarbonate-membrane filter using the Scanning Electron Microscope (SEM). The procedure of the SEM analysis is given in detail in Chapter three. As stated in the procedure, the technique uses a carbon coating to provide an electrically conducting layer over the filter. The coating, as well as the content of the filter (predominantly carbon) interrupts the accuracy of the elemental analysis of carbon. Hence, the SEM is accurate for elements with an atomic number greater than or equal to eight (oxygen) on the periodic table. The approximate error for the readings is 2 percent. (Take note that a value less then 1% indicates that the element was a trace element.)

The analysis of the two filter samples, flight 8 and flight 17, occurred on the 1st December 2003. Flight 8 occurred on the 6th August 2003 and five ABS specimens were taken. The five specimen durations, occurrence and areas flown over, are included in table 4. The flight paths are included in figure 26.

Flight 17, which was the last flight of the field campaign, occurred on the 26th August 2003 and two ABS specimens were taken. The first specimen was acquired at 7:41:52 UTC when flying over the following areas: the city centre, Ysterplaat runway (which included a missed approach), Goodwood, Athlone (which included routing over

the Athlone power station), Wynberg, Mitchell's Plain and the Cape Town International Airport runway. The duration of the first specimen was approximately 30 minutes. The second specimen was logged at 8:36:11 UTC and included the following areas: Somerset West, Strand, Khayelitsha, Cape Town International airport and Bellville (the two companies, Consol Glass and African Products were included). The specimen was collected over a 23 minute interval.

Table 4: Details of the ABS filter sampling for the 6th August 2003.

Specimen Number	Starting time (UTC)	Duration (min)	Areas flown over included:
1	6:11:00	14	Cape Town Waterfront, Table Bay, Goodwood, Athlone (including the Power Station) and Wynberg
2	6:26:46	6	Mitchell's Plain
3	6:45:08	8	False Bay, Gordon's Bay, Along False Bay coastline, Khayelitsha (including through a biomass plume) and Somerset West
4	6:53:30	5	Stellenbosch
5	7:09:46	5	Areas including and in between Bellville and Malmesbury

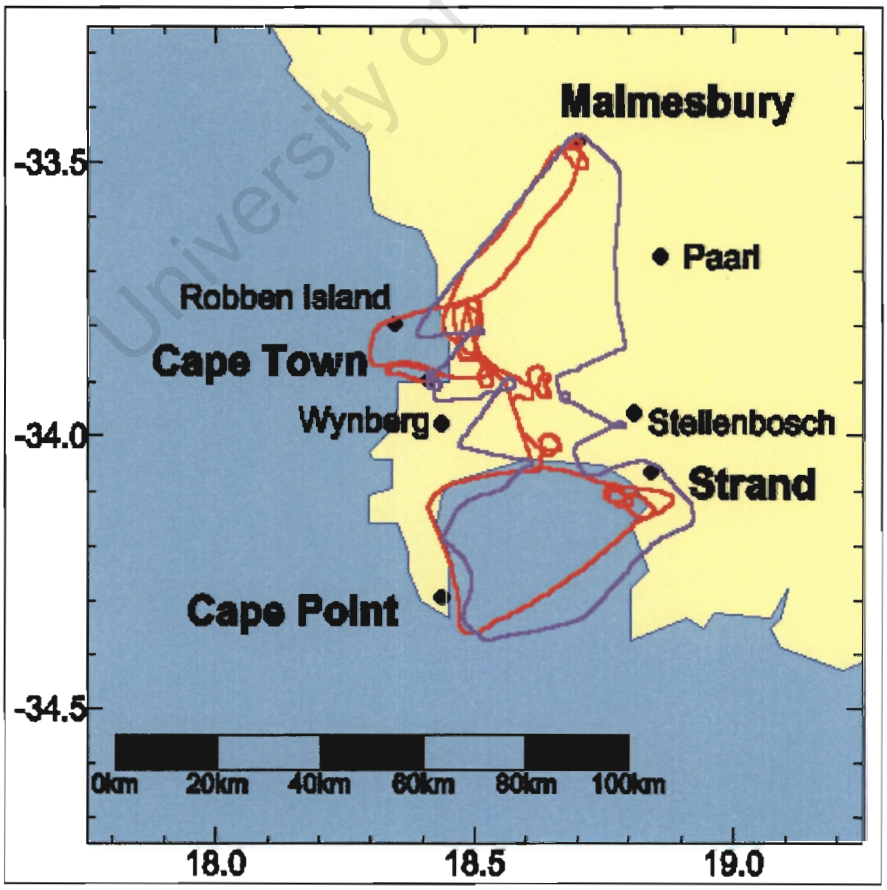

Figure 26: Flight paths for the two SEM flights, flight 8 in purple and flight 17 in red.

For the analysis of the elemental composition for the various specimens the filament voltage was set to 20 kV. The backscatter detector was used in the identification of the sample and the secondary detector was used to identify the topographical detail. The results for the particles analysed from the filters included evidence of common sea salt (NaCl) and soil (silicon based) particles. Examples of these salt particles are in samples, 26-02a (figure 27), 26-02c, 06-03a, 06-04a, 06-04c and 06-05a and examples of the general soil particle were seen in samples, 06-01b, 06-01c (figure 28) and 06-05b. Some other samples on the ABS filters showed signs of industrial activities (traces of Ni and Zn) (samples 06-03c and 06-05c respectively), agricultural activities (trace of K and/or P (sample 26-02b)) and vehicle emissions (Pb and Br) (sample 26-01b) (figure 29). The analysis reports and data sheets for samples 26-01b, 26-02a, 06-01c, 06-03c and 06-05c can be referred to in Appendix B. The rest of the particles analysed by the SEM can be seen in the folder "SEM" on the compact disc (Appendix CD-ROM).

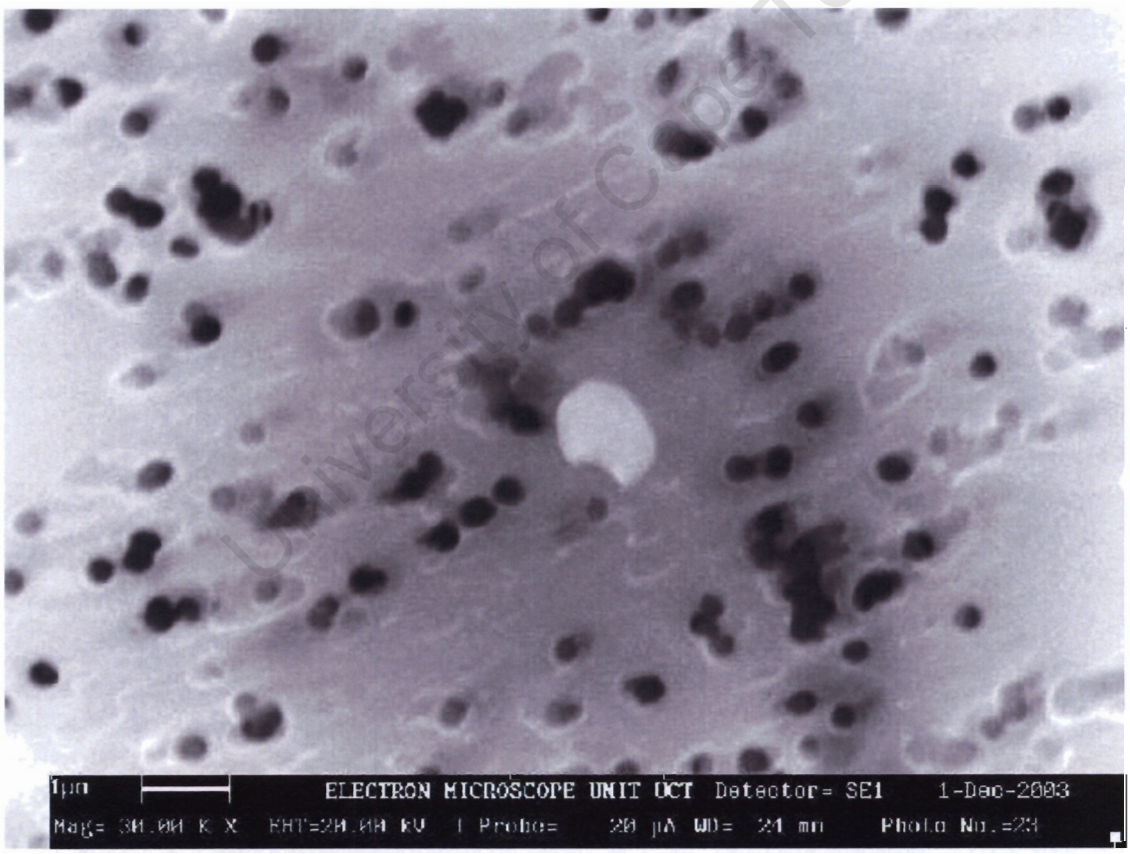

Figure 27: A common sea salt particle.

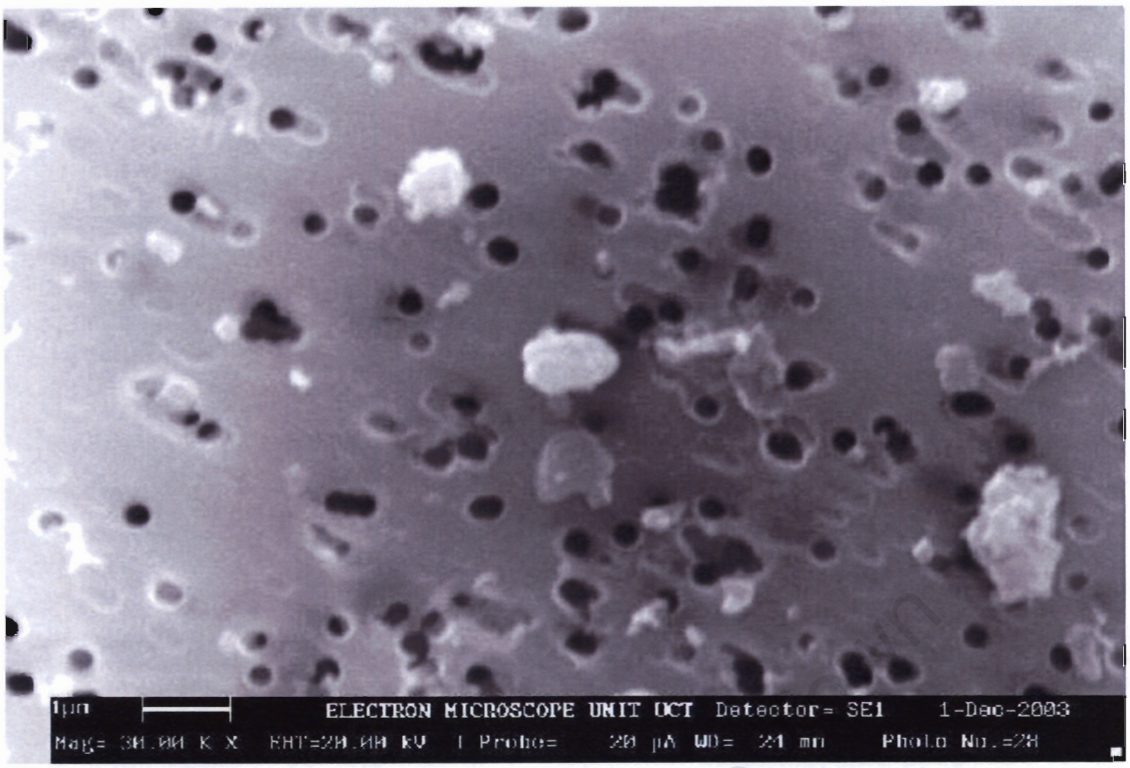

Figure 28: A common silicon based soil particle. (Particle analysed is the most centred particle.)

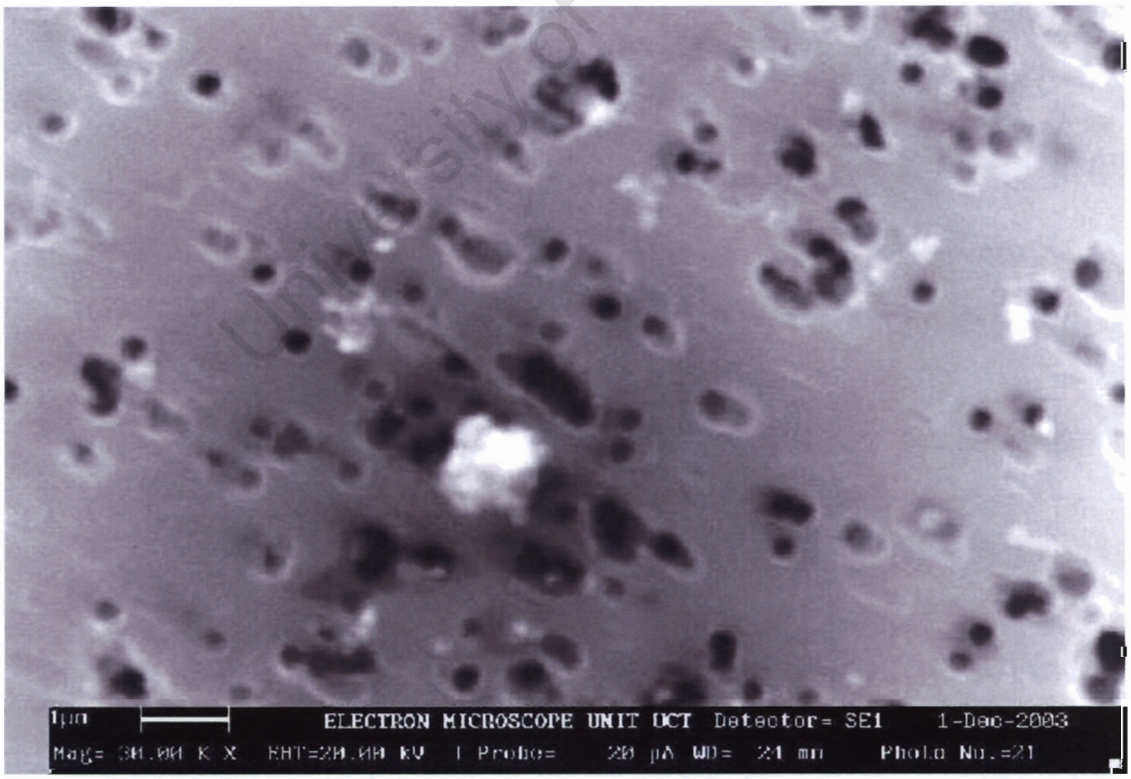

Figure 29: A vehicle related particle. (Contains high Pb and Br concentrations.)

4.4 Gases

The gases that have been identified to contribute to the atmospheric pollution are SO_2, CO, CO_2, O_3 and NO_x. They are recorded as they give an indication of the sources of the pollutants.

Visibility can be reduced from particular gases present in the atmosphere. Of all gases , NO_2, has the greatest effect due to their specific absorption and light scattering properties. This absorption of various wavelengths of light is responsible for the atmospheric colorations (Seinfield, 1986). It is furthermore important to note that the visibility effect by NO_2 is insignificant in comparison to the particles contribution to the visibility.

For the formulated profiles for the haze and non-haze days, as well as the daily profiles, the SO_2, CO_2 and the CO concentrations did not fluctuate as much as the NO_x and O_3 concentrations within the same profiles. The tables that follow give a representation of the CO, CO_2 and SO_2 values that could be expected within the various profiles flown. Tables 5, 6, and 7 show the average values and standard deviations for the CO, CO_2 and SO_2 concentrations respectively.

Table 5: CO concentrations (ppm) for the flight profiles.

CO Concentrations (ppm) for flight profiles			
Flight number	**Area**	**Average**	**Std dev**
12	Cape Point	2.630	0.021
12	Robben Island	2.563	0.012
12	Strand	2.667	0.026
13	Cape Point	2.690	0.026
13	Robben Island	2.674	0.086
13	Strand	2.804	0.086
14	Cape point	2.893	0.025
14	Strand	2.885	0.018
14	Wynberg	3.051	0.122
15	Cape Point	2.881	0.037
15	Strand	2.930	0.044
15	Wynberg	2.840	0.020

Table 6: CO_2 concentrations (ppm) for the flight profiles.

CO_2 Concentrations (ppm) for flight profiles			
Flight number	**Area**	**Average**	**Std dev**
12	Cape Point	335	1.039
12	Robben Island	331	0.590
12	Strand	336	0.820
13	Cape Point	329	0.850
13	Robben Island	326	3.072
13	Strand	331	1.769
14	Cape point	330	0.808
14	Strand	329	1.082
14	Wynberg	337	1.419
15	Cape Point	317	0.396
15	Strand	316	1.048
15	Wynberg	317	1.154

Table 7: SO_2 concentrations (ppb) for the flight profiles.

SO_2 Concentrations (ppb) for flight profiles			
Flight number	**Area**	**Average**	**Std dev**
12	Cape Point	0.346	0.263
12	Robben Island	0.311	0.326
12	Strand	0.572	0.287
13	Cape Point	0.858	0.740
13	Robben Island	0.824	0.528
13	Strand	1.629	0.817
14	Cape point	0.317	0.260
14	Strand	0.370	0.243
14	Wynberg	8.330	3.687
15	Cape Point	0.513	0.192
15	Strand	1.855	0.744
15	Wynberg	0.544	0.328

The gaseous concentrations that varied considerably, on flights 12, 13, 14 and 15, were NO_x compounds (NO and NO2), as well as ozone. Figure 30 shows the inverse relationship between the ozone concentrations and the NO_x particles. It also demonstrates the relationship the NO_x has with other particles in the Brown Haze. When using both figures 17 and 30, the latter relationship is clear, especially near ground level, as well as at 700 m, 1050 m and 1250 m.

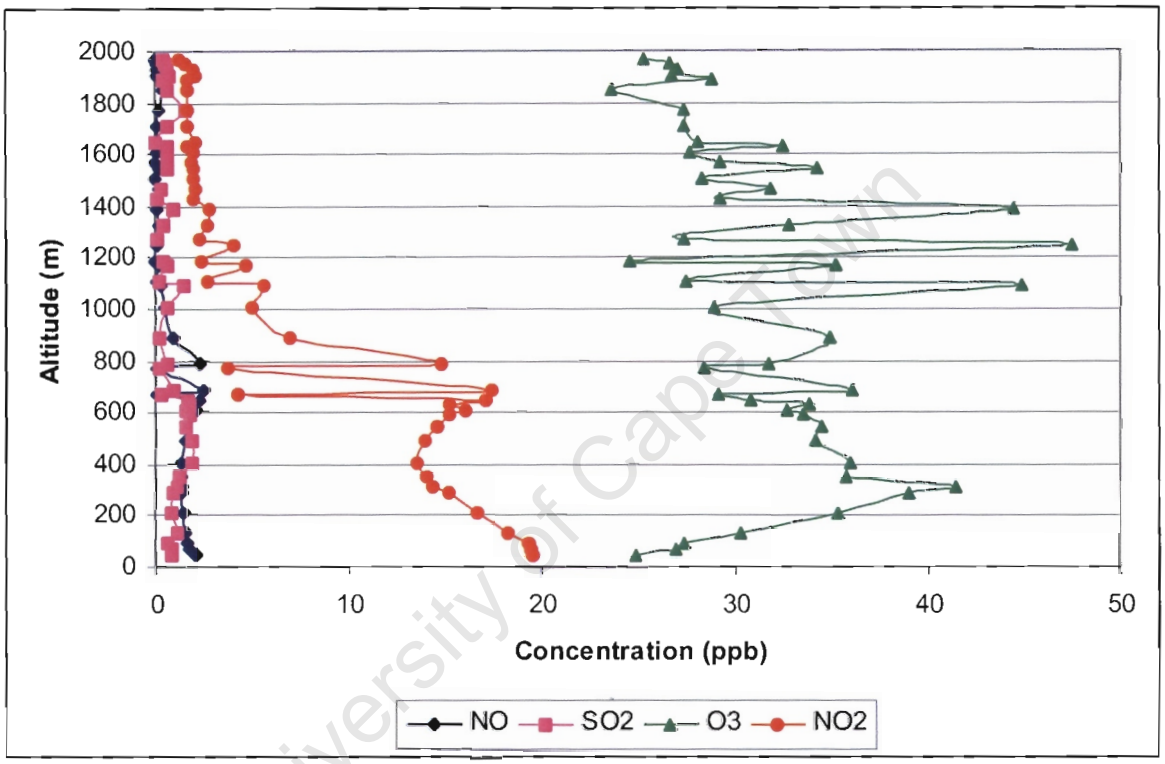

Figure 30: Gas concentrations (ppb) over Robben Island for flight 13.

Ozone concentrations ranged between 13 ppb and 47 ppb. The 47 ppb was recorded on flight 13, at Robben Island (figure 30), at an altitude of 1250 m. The 13 ppb was recorded on flight 14, on the Wynberg profile, at an altitude of 170 m. The NO_x compounds had a significant fluctuation, ranging from near zero values at Cape Point to a value of 60 ppb for the NO concentration and 111 ppb for the NO_2 concentration. Both these values are illustrated in figure 31 and were obtained at an altitude of 170 m, during the Wynberg profile on flight 14.

The complete set of the gas vertical profiles for the respective flights can be seen on the compact disc (Appendix CD-ROM). The curves are labelled "CO", "CO2" and "Gas" in Excel format.

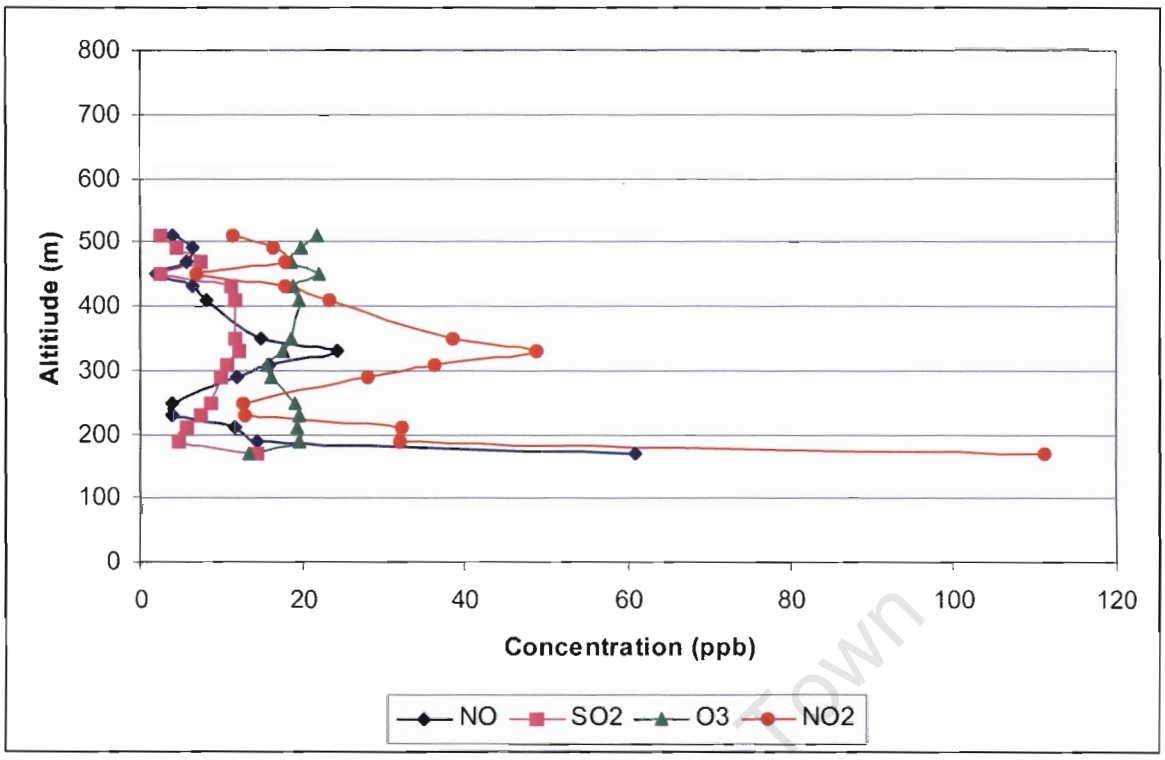

Figure 31: Gases concentration profiles for the morning haze episode at Wynberg (flight 14).

Chapter 5 – Discussion and Conclusions

5.1 Field Campaign Objectives

The Brown Haze Two field campaign was a successful endeavour, as the required information needed to characterise and assess the Brown Haze was obtained. As with every project, inevitable hitches can be expected. The total number of air time hours flown by both the Aerocommander 690A and the Powersonde model aircraft's were sufficient for retrieving the relevant data, but was not up to the target requirements. This was primarily due to the difficulties encountered during the field campaign.

Some of the problems encountered by the Aerocommander 690A included mechanical or electrical faults, climatic influences and a collapsing runway. The field campaign took place toward the end of the Western Cape rainy season. However, the 2003 rains arrived late and reduced the flight hours. Extensive rains weakened the runway, which at the end could not take the strain due to the Aerocommander's weight. Persistent electrical faults in the Powersonde equipment meant that some of the field campaign plans were not achieved. However, as this was the first full field campaign in which the Powersondes had been deployed, this was not unexpected.

5.2 Brown Haze

The implications of the haze in many regions of the world are significant enough to affect the global radiation budget, agriculture and health (Ramanathan and Crutzen, 2003). All of these impacts pose a potential threat to mankind, as mentioned in the health impacts section, some anthropogenic aerosols can lead to mortality. The effect of haze is connected to both the pollution levels present, as well as the climatic change induced, hence, both should be dealt with under one common framework (Ramanathan and Crutzen, 2003). Anthropogenic aerosols are found in and downwind of all inhabited regions on the planet and they are commonly spread over a large region (Ramanathan and Crutzen, 2003). The regional climatic changes are influenced more strongly by the absorbing aerosol particles than the greenhouse gases (Ramanathan and Crutzen, 2003).

5.2.1 Climatic conditions

The atmospheric climatic conditions are always changing due to wind fluctuations and solar heating of the Earth's surface. These changes bring about dynamic temperature behaviours in the lower layers of the atmosphere. The wind components and the temperature inversions are two climatic conditions that are incorporated within the assessment of the Brown Haze.

An inversion forms either from cooling below or heating from above (when the temperature of the atmosphere increases with height). The air within these inversion layers is stable, hence, little mixing of pollutants takes place. This inhibited mixing between the inversion layers is a major contributor to the accumulation of pollutants and therefore needs to be identified.

The variations in the temperature profiles from the earth's surface can be highlighted by using an indicator known as potential temperature. Potential temperature relates the actual temperature profile to the adiabatic lapse rate (Seinfield, 1986). Hence, it becomes an indicator of how stable the atmosphere is.

$$\text{Potential Temperature} = \frac{T_{measured}}{\Gamma z + T_0}$$

where T is the actual temperature measured, T_0 is the starting adiabatic temperature at z_0, z is the altitude (m) and Γ is the adiabatic lapse rate.

When the potential temperature is greater than one, the atmosphere is said to be unstable. If the potential temperature is equal to one, then the surrounding air has a neutral stability. If the potential temperature is less than one, the atmosphere is said to be stable (an inversion layer is present).

From the results for the temperature inversions, highlighted with the concept of potential temperature, a general trend was established for 22nd August 2003. The comparison of the morning (flight 14) to afternoon (flight 15) potential temperature graphs, showed that the inversion layer increased in height and became weaker during the course of the day. This is especially evident with the Cape point data for the same day (figure 16).

Wind conditions can also influence the quantity of pollution within the atmosphere. A non-haze day (flight 12) occurred when a strong continental wind influenced the pollution concentration (figure 13). The wind for the 13th August 2003 had an average wind speed of 28±15 m/s. For the flights (13, 14 and 15) on the visibly haze days (15th and 22nd

August 2003), the wind direction varied from maritime winds to continental winds (figures 14 and 15 respectively). The 15th August 2003 had an average wind speed of 18±6 m/s. The 22nd August 2003 had an average wind speed of 19±8.5 m/s. This then shows that when the wind speed is strong, a flushing effect occurs and during mild to calm wind conditions pollution concentrations become more prevalent.

5.2.2 Major sources

Gases

The most abundant trace substance in the lower atmosphere is CO_2. This is followed by CO (Seinfield, 1986). This fact is supported by the concentration levels of the Brown Haze. The CO and CO_2 concentration were in the ppm range, while the other gases sampled where in the ppb range. When comparison of the CO levels is performed with respect to the time of day, it shows that higher levels of CO are generally seen during the morning in densely populated areas. Table 5 highlights the Wynberg region for having the highest recorded value, which was obtained during the morning period and was observed at a low altitude. This information gives testimony to the fact that vehicle emissions and domestic fire burning are known to contribute to high levels of CO within the atmosphere. The wind direction for the day (figure 15) was from a northerly and east south easterly direction, which indicates that the pollution originated from these areas. Note that all the major roads in the region, namely the N1 and N2, are located specifically upwind of Wynberg. The residential areas, which use coal and wood for heating during the cold winter months, are located to the east. The CO_2 concentrations, found in table 6, illustrate similar trends to the CO concentrations. The CO_2 profiles for all of the respective days (found on the CD), show decreasing values of CO_2 concentration with altitude.

Ozone is naturally present in the clean troposphere at concentrations ranging between 20 to 80 ppb (Seinfield, 1986). The range is dependant upon the seasons as the combination of tropospheric chemistry and transports from the stratosphere influence the seasonal concentrations (Seinfield, 1986). One such tropospheric chemical cycle is between O_3 and NO_x compounds. When NO_2 is present with sunlight, ozone formation occurs as a result of the photolysis of NO_2 (Seinfield, 1986). When O_3 has formed, it then reacts with NO to regenerate NO_2.

The relationship between the NO_x and the O_3 can be best seen in the Cape Point region for flights 12, 13, 14 and 15, for example figure 30. The data obtained for these flights

indicate that the relationship is best illustrated at lower altitudes (less than 800 m). The relationship is also demonstrated in the Wynberg region on flight 14 (figure 31). The highest recorded values for both NO and NO_2, NO_x in total, were obtained on this flight at an altitude of 170 m.

On flight 14, SO_2 levels were also seen to be much greater in the morning. The highest recorded value was 14 ppb at an altitude of 170 m. High levels of SO_2 are attributed to the energy sector, where it could originate from coal burning or from the petroleum industry.

Particles

From the CN counter values, a pattern emerges between the morning and afternoon levels. At low altitudes, the CN count indicates lower quantities for the morning compared to the afternoon. This is illustrated on flight 14 and 15 (Wynberg), lower CN counts were seen at the altitude of 170 m in comparison to altitudes greater than 170 m. This data correlates to the readings obtained for the gas analyses.

The size range of particles produced by vehicles and domestic burning are located between 0.1 to 1 µm. The total PCASP count profiles show low number concentrations of particulate matter at altitudes lower than 200 m in comparison to the higher altitudes. Two flight profiles, flight 13 (Robben Island) (figure 21) and flight 13 (Strand) (figure 20), do indicate some influence from a ground source. This observation is shown in both figures 20 and 21. When comparing the number concentrations from a non-haze day to a haze day it is apparent that the number concentrations are higher during a haze event.

This ground source could be an influence of domestic burning, as many people burn wood during the cold nights. Further knowledge can be gained from the PCASP volume analysis. The PCASP data (0.1 to 3 µm) reveal two volume fractions, the fine particles (0.1 to 0.9 µm) and the coarse particles (0.9 to 3 µm). The particles of interest lie within the fine fraction. When analysing the profiles that compare the coarse fraction to the fine fraction, a general trend indicates fine particles to be closely associated with the background levels below the altitude of 200 m. An exception to this trend can be seen in flight 13 (Robben Island). The profile of Robben Island in flight 13 shows values much greater than any other day. Robben Island has very scarce vehicle access and little, if any, domestic burning. Therefore, the PM levels for that afternoon must have been transported from another location (An indication of this can be seen in the normalised size distribution curves, the diameter mode for the low level altitude is between 1 and

2 μm). The morning wind (figure 14), which was a north easterly with an approximate wind speed of 24 m/s, could explain the high fine PM concentrations. These concentrations were therefore either blown from the Cape Town region during the morning or blown from the Table Bay area, hence, an influence of sea salt particles (coarse particle diameter ~2 μm). The source for the fine PM levels is unclear and could only be directly attributed to a specific source by means of elemental composition analysis.

The profile data gives a clear and representative picture as to what is contributing to the Brown Haze. Another method, elemental analysis of particles with the aid of the SEM, can be used to support these statements.

Elemental composition

From the Brown Haze phase one study, the major elemental contributions of particular sources was as follows: road dust – Al, Si, Ca, Fe; wood burning – K, Cl, C; tyre burning – Al, Si, Fe; diesel – S; petrol fuelled vehicles – Pb, Br; and oil fired boilers – Al, Ni, V, Si, Al. From this data, a contribution to the elemental analysis of the particle can be acquired. As previously discussed, the vehicle and domestic burning particles are between 0.1 and 1 μm in diameter.

For the analysis of the SEM data obtained for particles between 0.1 to 1 μm, evidence shows that common salt and soil particles were traced. Examples of these salt particles are in samples, 26-02a, 26-02c, 06-03a, 06-04a, 06-04c and 06-05a and examples of the general soil particle were seen in samples, 06-01b, 06-01c and 06-05b. Some other samples on the ABS filters showed signs of industrial activities (traces of Ni and Zn), agricultural activities (trace of K, P) and vehicle emissions (Pb and Br).

A significant particle was obtained on flight 17, it shows evidence that petrol fuelled emissions are present within the Brown Haze. The SEM analysis, 26-01b (which was taken above populated areas, as well as airport landing strips) shows the elemental composition to be primarily Br and Pb. This points directly to petrol fuelled vehicle emissions. Diesel emissions are also seen to be evident within the second SEM filter sample for the same flight as traces of sulphur are apparent.

Conclusion

From the gases discussed above, it can be stated that emissions from the sources of the Brown Haze are either being accumulated below an inversion layer over night or are

emitted into the atmosphere during the early morning. Early morning traffic and/or domestic burning during the evenings or early morning are possible sources. High levels of CO, SO_2 and PM are usually associated with domestic burning, and high levels of NO_x, CO_2 and CO are usually attributed to the transport sector. By distinguishing if the PM concentration was at high levels at low altitudes, a conclusion can be derived to differentiate between the primary and partial contributors - traffic or domestic burning.

When differentiating between the contributions of vehicle emissions and domestic burning, the occurrence of the high levels of fine PM at Robben Island and some traces of SO_2 in the profiles, stipulated above, are not convincing enough to state that the primary source of the Brown Haze is domestic burning. It does, however, give some indication that domestic burning does contribute to the Brown Haze.

Due to an abundance of NO_x, CO_2 and CO concentrations at low altitudes and evidence stated in the SEM analysis, it can be concluded that vehicle emissions are the primary source of the Brown Haze and this supports the evidence given in the Brown Haze Phase One study.

5.2.3 Characterisation

As both NO_2 and airborne particles influence the visibility to varying degrees, discovery of the relationship between the two is beneficial. From figures 17 and 30, obtained for the same vertical profile at Robben Island, it is clear that a relationship does exist. Figure 17 indicates particle peaks at approximate altitudes of 100, 700, 800, 1 100 and 1 250 m. Figure 30 shows NO_2 peaks at approximate altitudes of 70, 700 and 800 m. This shows that a relationship does exist for low altitudes (approximately less then 1 000 m).

It is therefore important when determining the vertical extent of the haze, to consider both the NO_2 and the particle concentrations. Observations of figures 20, 21 and 30, indicated that the Brown Haze never exceeded 1 400 m. The horizontal extent of the Brown Haze was in accordance to the wind conditions for that particular day. Strong winds brought about a flushing of pollutants, whereas calm and mild winds encouraged a high concentration of pollutants in one area. An example of pollutant accumulation was on flight 13, where the greatest values of contaminant's was observed over Strand. The westerly wind, which transports the pollution from the Cape flats region, as well as the trapping effect of the surrounding topography resulted in Strand having excessively high concentrations.

The horizontal extent of the Brown Haze is not only confined to the local areas of the Cape and Strand regions. The Brown Haze can extend several hundred kilometres off the coast of South Africa (figure 32), depending on the wind speed and consistent wind directions. The wind speeds and directions (Appendix CD-ROM) for the 14th July 2001 are consistent for both the Robben Island weather station and the Cape Point weather station. The meteorological data indicates a steady wind direction from the easterly direction, which conforms to the satellite image (figure 32), obtained from the SeaWIFS project from NASA.

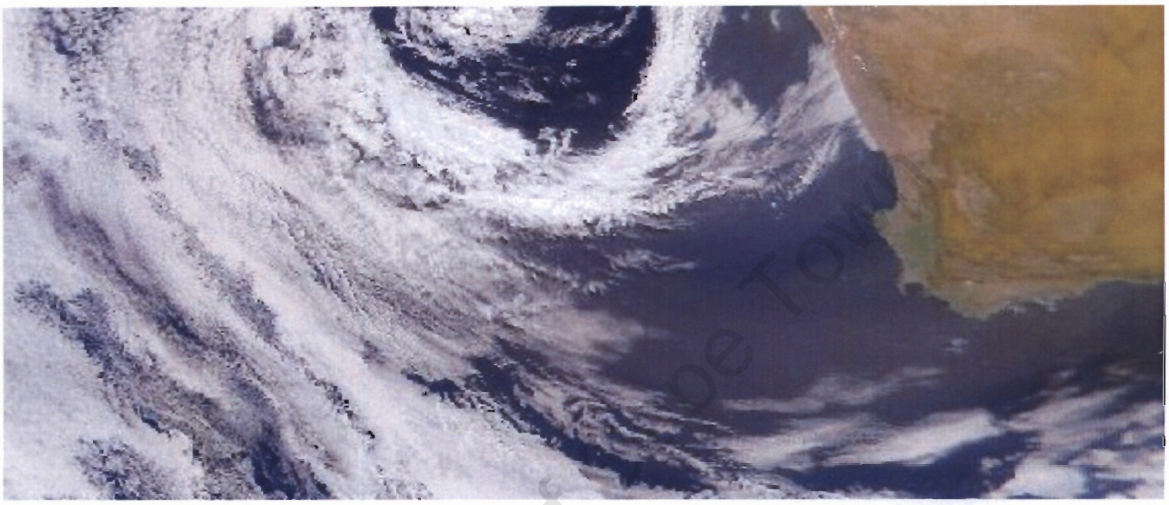

Figure 32: Satellite image (14th July 2001) of the South Western Coast of Southern Africa, with a brown coloured plume streaming off the Cape region. The plume is known as the Brown Haze. (Source: NASA – www.earthlink.nasa.gov).

When examining the particle concentrations with the potential temperature analysis (figure 16), a similar trend occurs for the fine particle concentrations. From the morning and afternoon vertical profiles obtained for the inversion layer comparison, the particle concentrations showed a similar concentration rise. (When the haze rises over the day, the concentrations at the lower levels also tend to decrease.)

Midday comparisons of haze and non-haze days were performed over Strand and Robben Island at altitudes from ground level to 600 m (figures 17 and 18). These comparisons show aerosol concentrations for a non-haze day of approximately 500 cm^{-3}, whereas the haze days show significantly higher concentrations (Some altitudes indicated 10 times greater concentrations of particles).

When analysing the sizes of the particles at various altitudes, trends were observed for the time of day. The afternoon normalised volume size distributions curves showed a

similar pattern for the fine mode at the various altitudes (figure 23), whereas the morning normalised volume size distribution curves indicated a change in the fine concentration of particles with altitude. The changes in the fine mode concentrations were also found to be higher than the background values found in figure 24. This shows, that an input from elsewhere was placed into the atmosphere at that altitude. Figure 24 also illustrates a decrease in fine particle concentrations and an increase in coarse particle concentrations with altitude.

Conclusion

The composition of the haze was predominantly particulate matter and NO_x (especially NO_2). This confirms that PM is a major contributor to the reduced visibility in the atmosphere. An insignificant contribution to light extinction is due to the NO_2 concentrations present, however enhanced NOx concentrations are indicators of traffic emissions. The fine particulate matter was comprised of various organic, salt, soil and composite particles. The composite particles showed signs of industrial activities (traces of Ni and Zn), agricultural activities (trace of K, P) and vehicle emissions (Pb, Br and S).

The nature of fine particulate matter, between 0.1 to 3 μm was such that it possessed a coarse mode between 1 and 3 μm. It was also observed that when comparing the time of day, the fine mode concentrations decreased from the morning levels to the afternoon levels. The finer particles between 0.1 to 0.4 μm were also found to have higher concentrations at the lower altitudes in comparison to the upper atmosphere.

From the photo's presented (figures 7 and 8) it can clearly be seen that the Brown Haze is rising during the course of the day. In addition, it can be stated that the Brown Haze is not a photochemical smog, as it starts off with high values at low altitudes in the morning and these values dissipate over the course of the day. (A photochemical smog tends to peak at midday, due to the ozone reactions). It is further evident that the finer particles are directly related to the rising effect. The fine mode particles, as stated previously, are from gas and particle processes or from condensation, which are attributed to vehicles or other combustion sources. It is therefore apparent that the source of the Brown Haze is predominantly from vehicle emissions and partially due to domestic burning.

The lateral extent of the haze was determined by the landscape of the surrounding region, the wind conditions and the time of day. Further studies in prediction modelling and monitoring of satellite images could bring about detailed descriptions of the lateral extent. The vertical extent, which never exceeded 1 400 m in this study was determined

by the inversion layer and the time of day (the haze was dense at low altitudes only during the morning).

From the numerous observations made, both through scientific evidence, as well as visualisation; a better understanding of the Brown Haze characteristics has been acquired. Together with fellow students, whom are also interpreting various aspects of the Brown Haze Two campaign, an overall understanding of the Brown Haze phenomenon will be achieved.

References

ATSDR - Agency for Toxic Substances and Disease Registry, 2003, *Benzene patient information*, www.atsdr.cdc.gov/MHMI/mmg5.html, U.S. Department of Health and Human Services.

Annegarn H.J., 1997, *A bird's eye view of air pollution issues in South Africa*. National Association for Clean Air, 28th Annual Conference, Iscor Club, Vanderbijlpark, 20 November 1997.

Annegarn H.J., Terblanche A.P.S., Sithole J.S., Rorich R.P. AND Turner C.R., 1996, *Residential air pollution*. In: Held G., Gore B.J., Surridge A.D., Tosen G.R., Turner C.R. and Walmsley R.D. (Eds), *Air pollution and its impacts on the South African Highveld*. Environmental Scientific Association, Cleveland, Chapter 8, pp 47-57.

Boubel R.W., Fox D.L., Turner D.B. and Stern A.C., 1994, *Fundamentals of Air Pollution*, third edition, Academic Press, San Diego CA, USA.

CMC – Cape Metropolitan council, 2003, *CMC Policy makes inroads on local air pollution*, www.capetown.gov.za (Health section). Press release, Friday, September 22, 2000.

Department of Environmental Affairs and Tourism, 2003, *Air Quality Bill*, www.environment.gov.za, Environmental Management, Pretoria, South Africa.

US EPA, 2003, *IRIS - Integrated Risk Information System*, www.epa.gov/iris/index.html

Hoskins J.A., 1995, *Environmental VOCs - The Hazard and the Risk*, Proceedings of the Second International Conference on Volatile Organic Compounds in the Environment, Indoor Air International. London. November 1995.

Keen C.S., 1994, *Meteorological Aspects of Pollution Transport over the South Western Cape*, Department of Geography, University of Cape Town.

Kinney P.L., 1999, *The Pulmonary Effects of Ozone and Particle Air Pollution*, Columbia School of Public Health, Division of Environmental Health Sciences, New York, Seminar in Respiratory and Critical Care Medicine **20**, 601-607, Thieme Medical Publishers, New York, NY.

McGrath J.J. and Barnes C.D., 1982, *Air pollution – physiological effects*. Academic Press, New York, NY.

Particle Measuring Systems Inc., *Passive Cavity Aerosol Spectrometer Probe Operating Manual*, Boulder, Colorado.

Ramanathan V. and Crutzen P.J., 2003. *New Directions: Atmospheric Brown "Clouds"*, *Atmospheric Environment*, **37**, 4033-4035.
URL: www.elsevier.com/locate/atmosenv. . doi:10.1016/S1352-2310(03)00536-3.

Scholes R.J. and van der Merwe M.R., 1996. *Chapter 2: South Africa and the global atmosphere – South Africa's greenhouse gas emissions*. In: Shackleton L.Y., Lennon S.J. and Tosen G.R. (Eds). Global climate change and South Africa. Environmental Scientific Association, Cleveland, Johannesburg.

Seinfield J. H., 1986, *Atmospheric Chemistry and Physics of Air Pollution*, John Wiley and Sons, New York, NY.

South African Legislation - *National Environmental Management Act (NEMA)*, *Act 107 of 1998*, www.environment.gov.za.

Swap R.J., Annegarn H.J., Otter L., 2002, Southern African Regional Science Initiative (SAFARI 2000): Summary of Science Plan. *South African Journal of Science* **98**, 119-124.

Swap R.J., Annegarn H.J., Suttles J.T., Haywood J., Helmlinger M.C., Hely C., Hobbs P.V., Holben B.N., Ji J., King M.J., Landmann T., Maenhaut W., Otter L., Pak B., Piketh S.J., Platnick S., Privette J., Roy D., Thompson A.M., Ward D., Yokelson R., 2002, The Southern African Regional Science Initiative (SAFARI 2000): overview of the dry season field campaign. *South African Journal of Science* **98**, 125-130.

The World Bank, 2003, *Urban Air Pollution - The Science of Health Impacts of Particulate Matter*, http://www.worldbank.org/sarurbanair.

Thermo Environmental Instruments Inc. Instruction Manual 2000a, Model 41C High Level, Gas Filter Correlation CO2 Analyzer, Franklin, Massachusetts.

Thermo Environmental Instruments Inc. Instruction Manual 2000b, Model 42C, Chemiluminescence NO-NO2-NOx Analyzer, Franklin, Massachusetts.

Thermo Environmental Instruments Inc. Instruction Manual 2000c, Model 43C, Pulsed Fluorescence SO2 Analyzer, Franklin, Massachusetts.

Thermo Environmental Instruments Inc. Instruction Manual 2000d, Model 48C, Gas Filter Correlation CO Analyzer, Franklin, Massachusetts.

Thermo Environmental Instruments Inc. Instruction Manual 2000e, Model 49C, UV photometric O3 Analyzer, Franklin, Massachusetts.

Tyson P.D., 1987, *Atmospheric circulation over Southern Africa*, Chapter 5 in Climatic change and variability in Southern Africa, Oxford University Press, Cape Town, South Africa.

US EPA (United States Environmental Protection Agency), 1998, *Guidance for using continuous monitors in PM Monitoring 2.5 networks*, Office of Air Quality, EPA-454/R-98-012.

Watson J.G., Chow J.C., Richards L.W., Neff W., Anderson S., Dietrich D., Houck J. and Olmez I., 1988, *The 1987-88 Metro Denver Brown Cloud Study,* Volume III - Data Interpretation, Desert Research Institute, Reno, Nevada.

Wicking-Baird M.C., De Villiers M.G., Dutkiewicz R.K., 1997. *Cape Town Brown Haze Study*, Energy Research Institute, University of Cape Town. 80 pp.

World Health Organisation, 2003, URL: www.who.int.

World Health Organisation, 2001, *WHO Strategy on Air Quality and Health*, Revised final draft, Geneva, Italy. 12pp.

Appendices

Appendix A – Meteorological Data

Strand - 6 August 2003

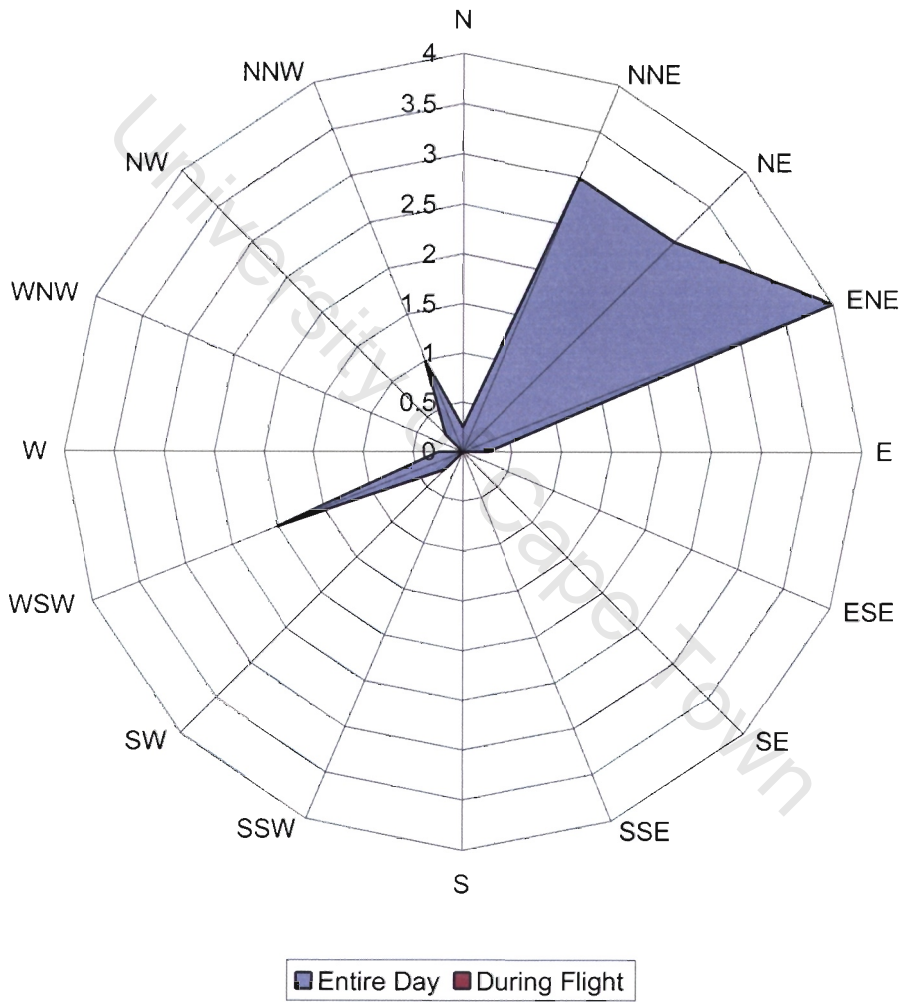

Cape Town - 6 August 2003

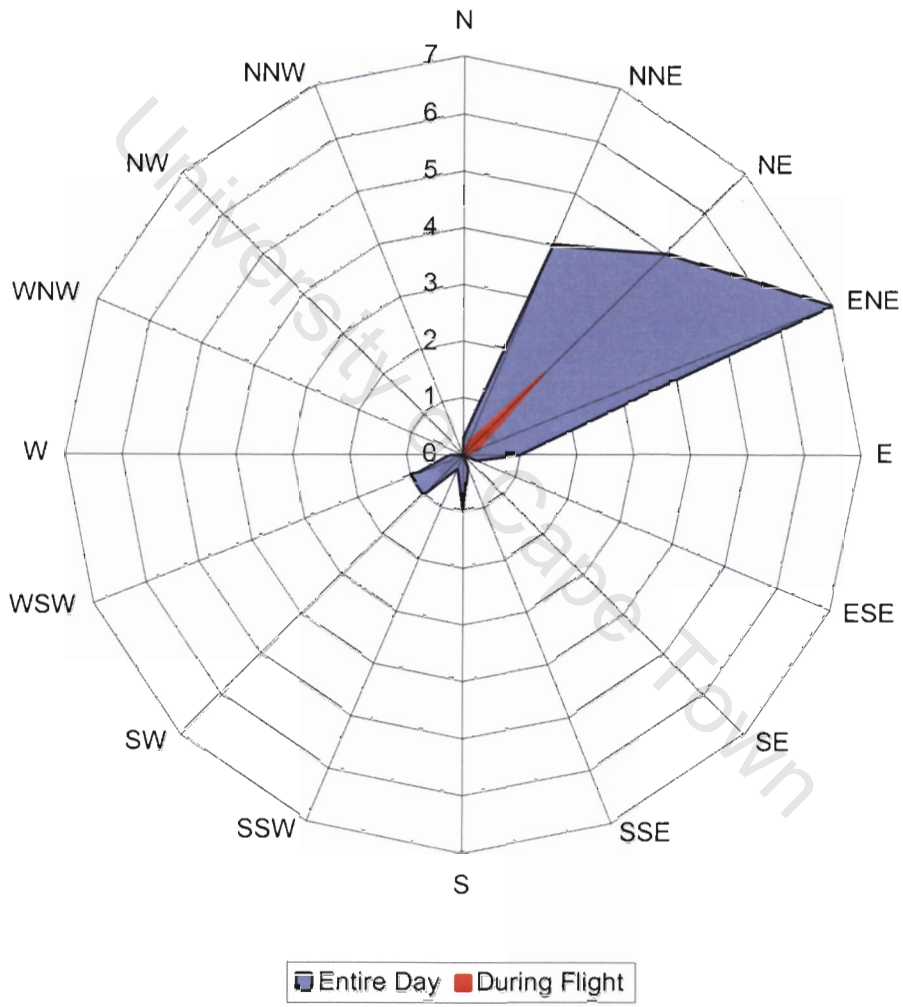

Strand - 13 August 2003

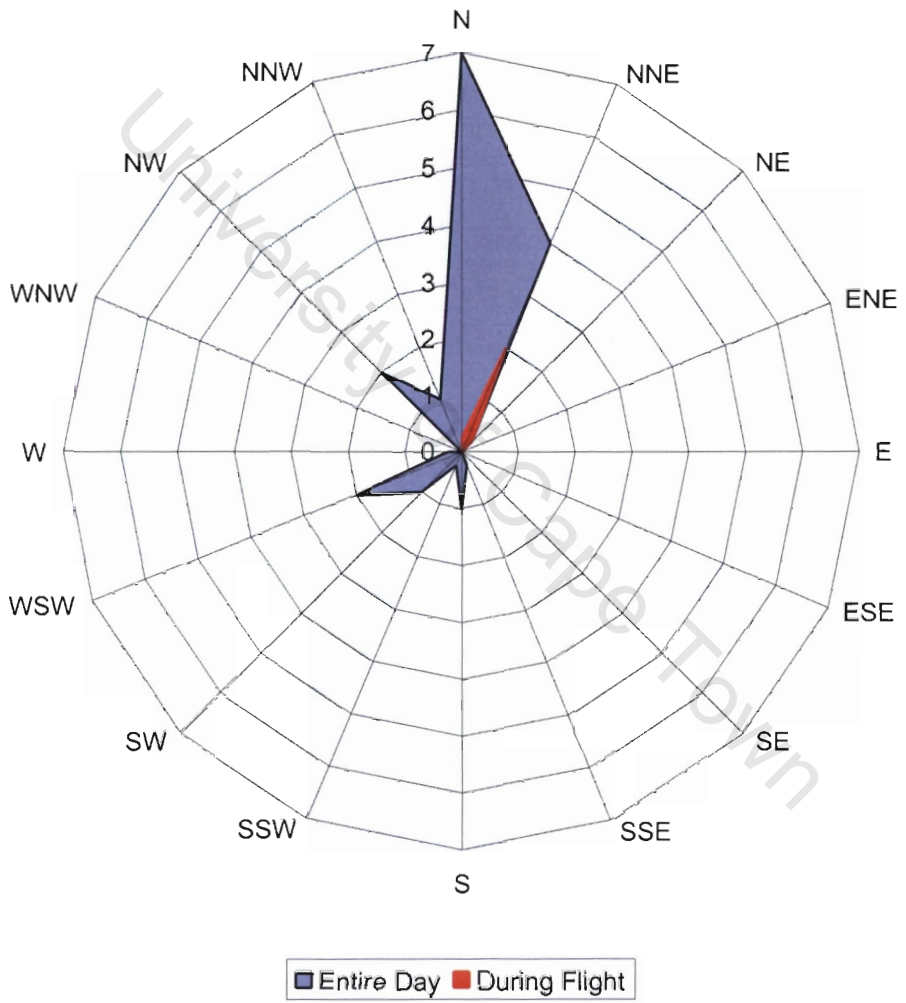

Cape Town - 13 August 2003

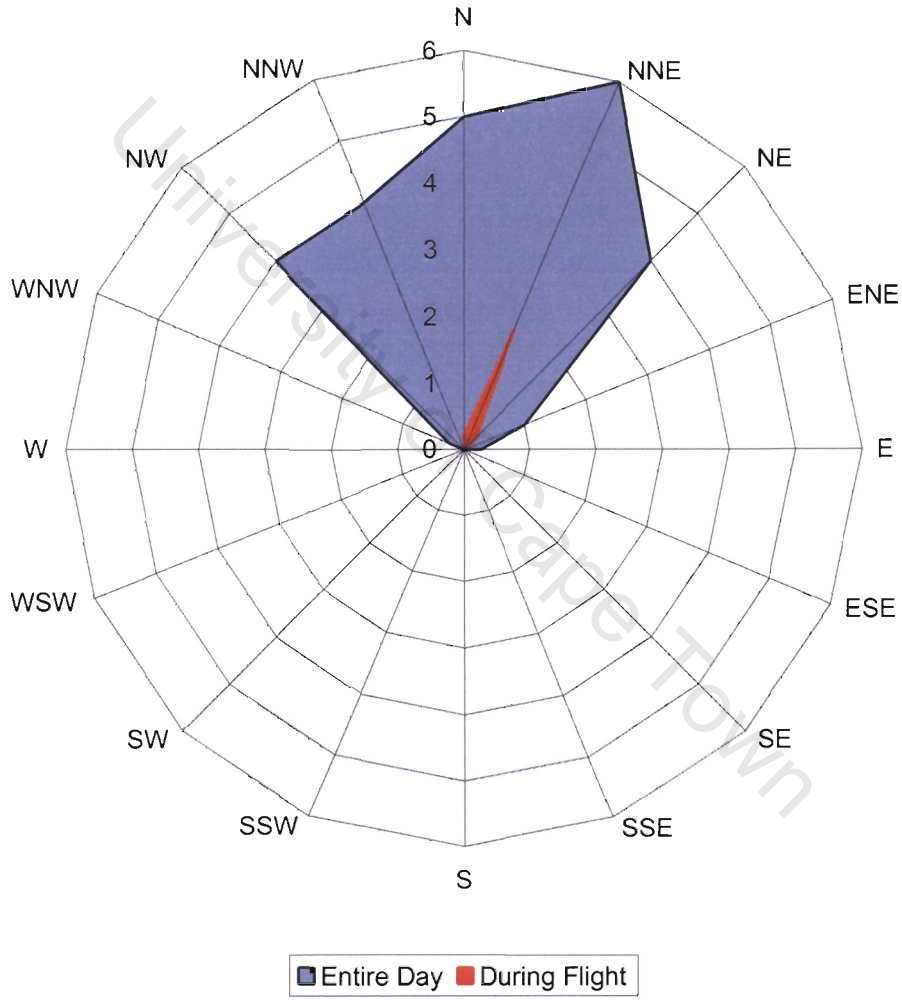

Strand - 15 August 2003

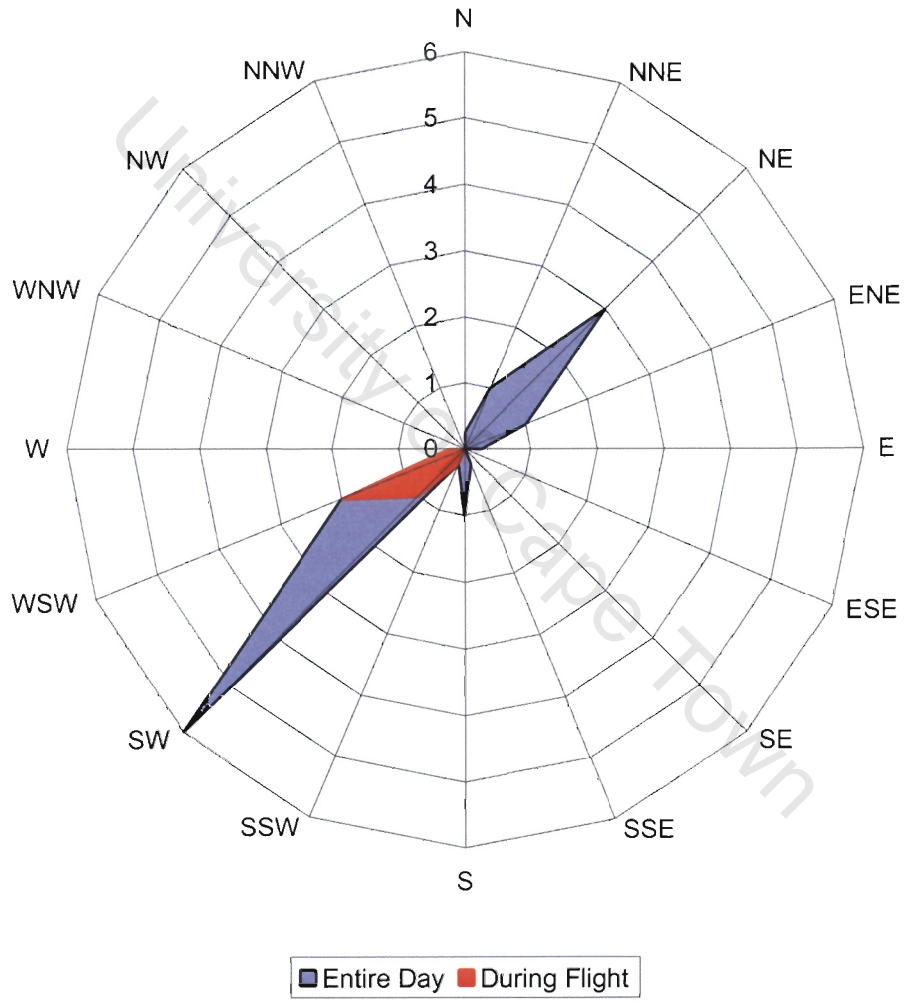

Cape Town - 15 August 2003

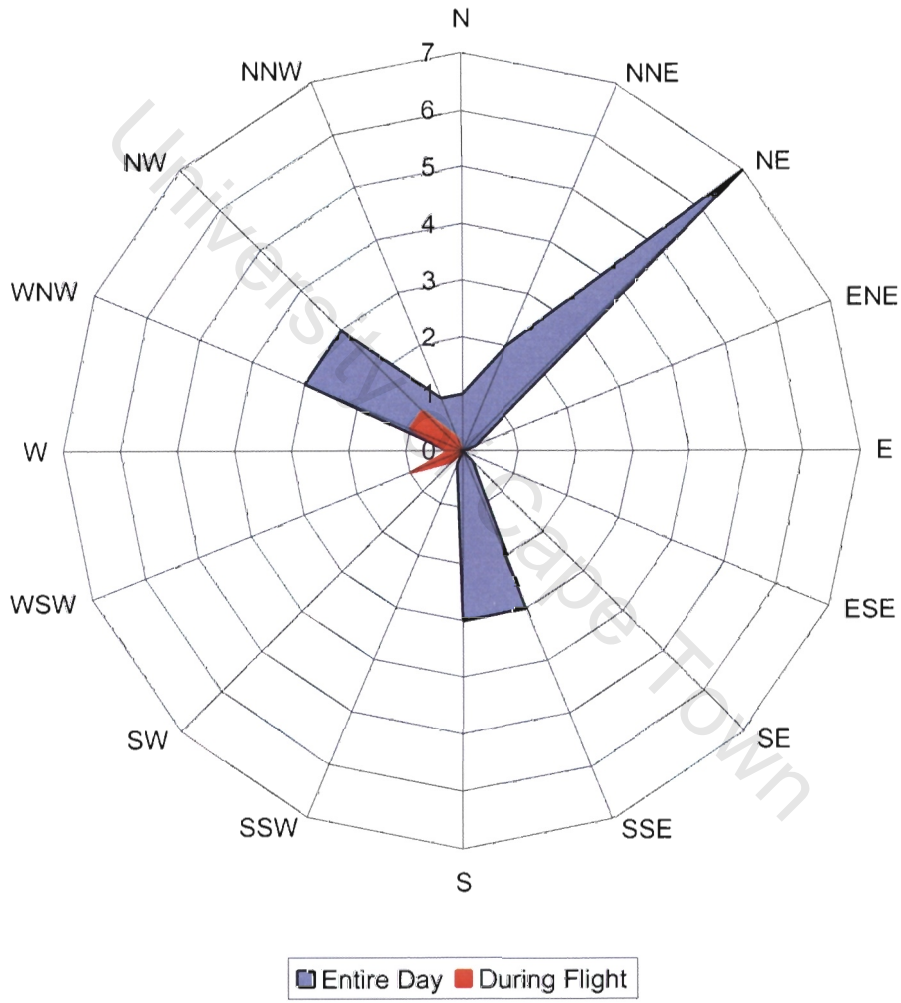

Strand - 22 August 2003

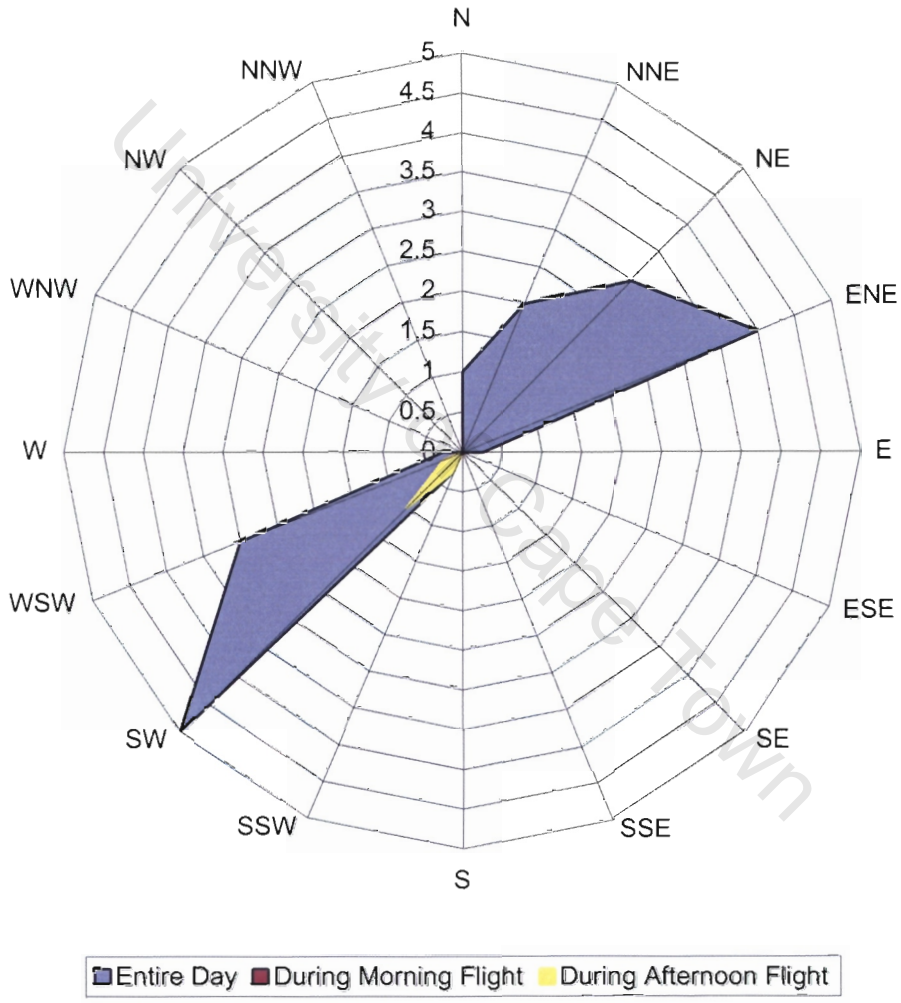

Cape Town - 22 August 2003

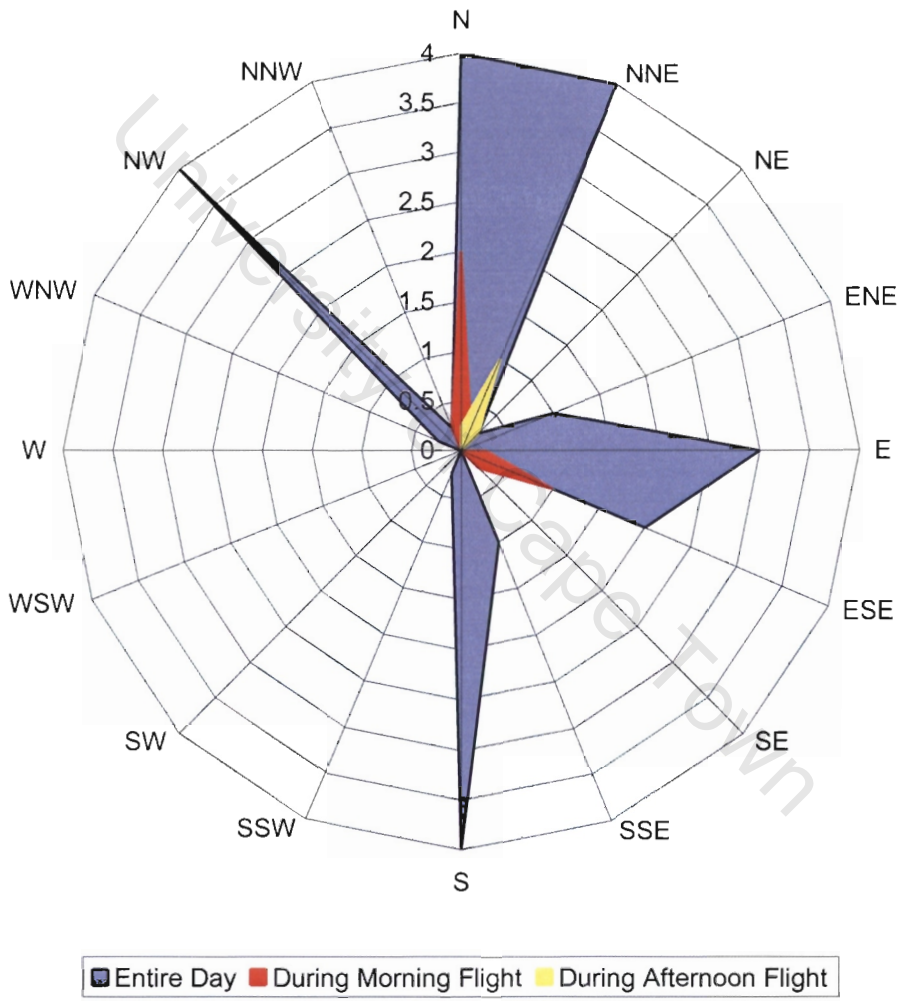

Strand - 26 August 2003

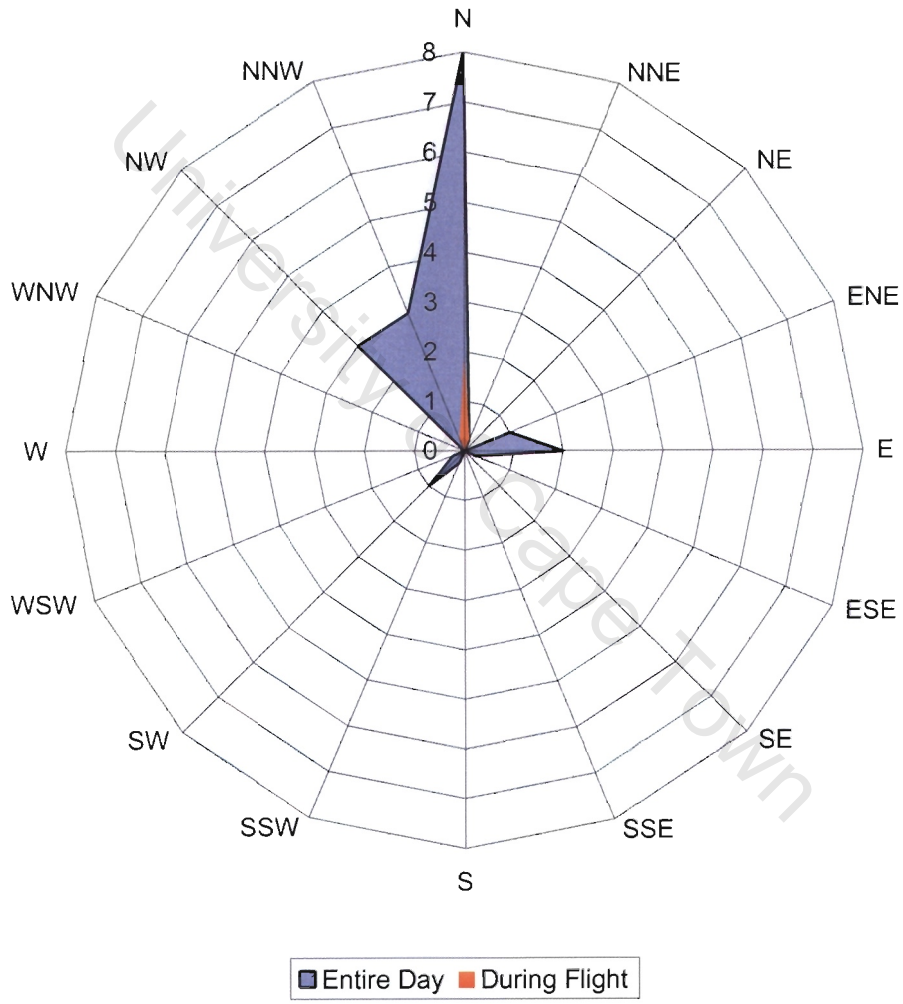

Cape Town - 26 August 2003

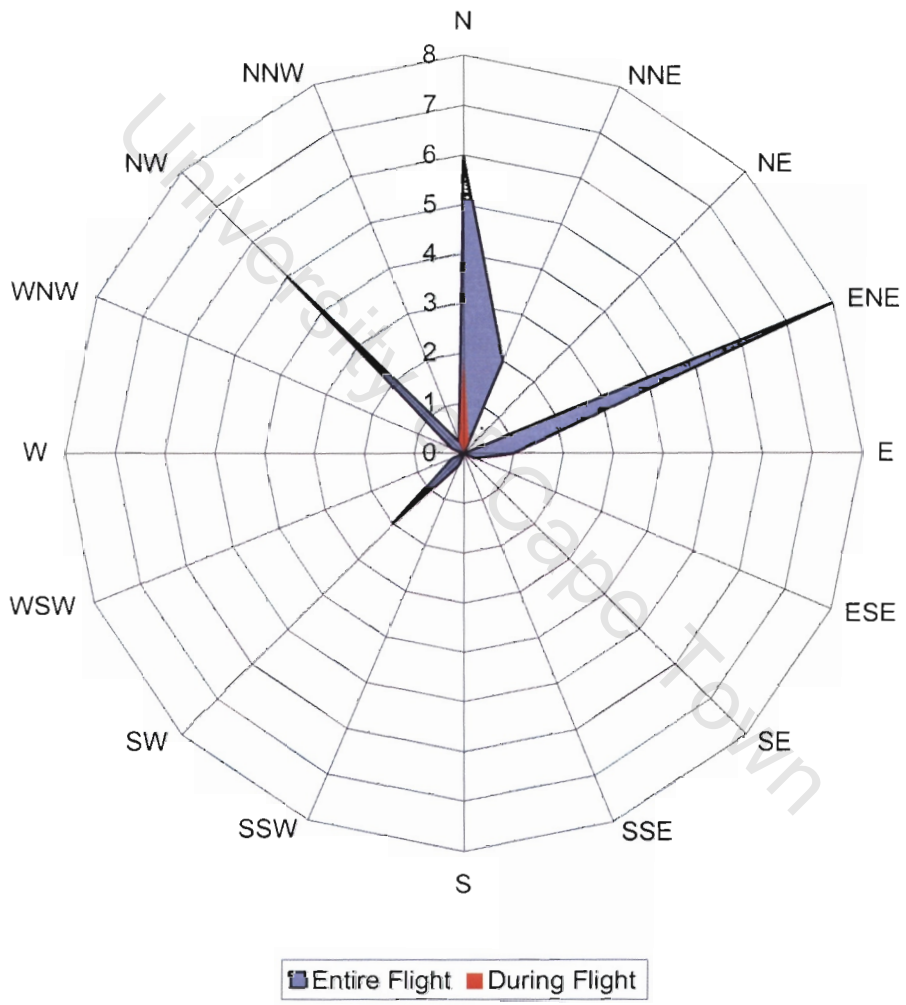

Appendix B – SEM analysis

[A N A L Y S I S R E P O R T]

GENERAL CONDITIONS

Result File	: STEVE26-01B
File Version	: 1
Background Method	: Fit
Decon Method	: Gaussian
Decon ChiSquared	: 1.71
Analysis Date	: 1-DEC-2003
Microscope	: SEM
Comments	:

ANALYSIS CONDITIONS

Quant. Method	: ZAF/ASAP
Acquire Time	: 60 secs
Normalization Factor	: 100.00

SAMPLE CONDITIONS

kV	: 20.0
Beam Current	: 100.0 picoAmps
Working Distance	: 25.0 mm
Tilt Angle	: 0.0 Degrees
TakeOff Angle	: 35.0 Degrees
Solid Angle*BeamCurrent	: 0.6

Element	Line	Weight%	Error	K-Ratio	Atomic%
O	Ka	8.79	0.369	0.0249	46.09
Al	Ka	0.00	0.000	0.0000	0.00
Si	Ka	1.87	0.056	0.0131	5.59
S	Ka	0.00	0.000	0.0000	0.00
Cl	Ka	2.42	0.074	0.0135	5.72
Cu	Ka	1.71	0.085	0.0193	2.26
Br	Ka	9.04	0.405	0.0985	9.49
Pb	La	76.18	1.832	0.6835	30.85
Total		100.01			

[A N A L Y S I S R E P O R T]

GENERAL CONDITIONS

Result File	: STEVE26-02A
File Version	: 1
Background Method	: Fit
Decon Method	: Gaussian
Decon ChiSquared	: 9.21
Analysis Date	: 1-DEC-2003
Microscope	: SEM
Comments	:

ANALYSIS CONDITIONS

Quant. Method	: ZAF/ASAP
Acquire Time	: 60 secs
Normalization Factor	: 100.00

SAMPLE CONDITIONS

kV	: 20.0
Beam Current	: 100.0 picoAmps
Working Distance	: 25.0 mm
Tilt Angle	: 0.0 Degrees
TakeOff Angle	: 35.0 Degrees
Solid Angle*BeamCurrent	: 0.6

Element	Line	Weight%	Error	K-Ratio	Atomic%
O	Ka	30.49	1.686	0.0670	47.06
Na	Ka	13.14	0.487	0.0515	14.11
Mg	Ka	1.13	0.126	0.0050	1.14
Si	Ka	5.31	0.205	0.0368	4.67
P	Ka	0.64	0.071	0.0047	0.51
S	Ka	3.24	0.150	0.0271	2.49
Cl	Ka	37.41	0.523	0.3041	26.06
Ca	Ka	2.55	0.150	0.0208	1.57
Cu	Ka	6.10	0.392	0.0531	2.37
Total		100.01			

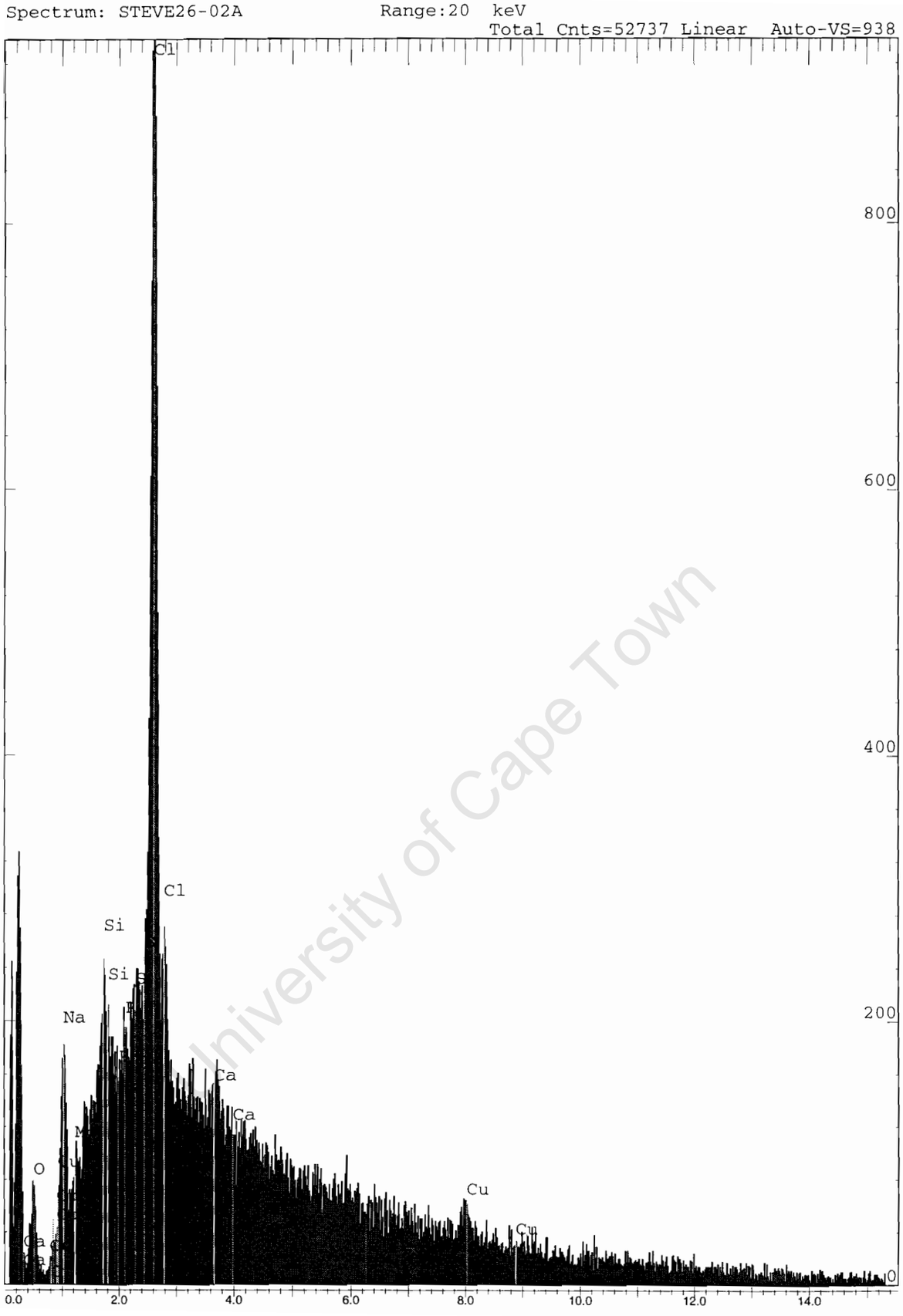

[A N A L Y S I S R E P O R T]

GENERAL CONDITIONS

Result File	: STEVE6-1C
File Version	: 1
Background Method	: Fit
Decon Method	: Gaussian
Decon ChiSquared	: 1.81
Analysis Date	: 1-DEC-2003
Microscope	: SEM
Comments	:

ANALYSIS CONDITIONS

Quant. Method	: ZAF/ASAP
Acquire Time	: 60 secs
Normalization Factor	: 100.00

SAMPLE CONDITIONS

kV	: 20.0
Beam Current	: 100.0 picoAmps
Working Distance	: 25.0 mm
Tilt Angle	: 0.0 Degrees
TakeOff Angle	: 35.0 Degrees
Solid Angle*BeamCurrent	: 0.6

Element	Line	Weight%	Error	K-Ratio	Atomic%
O	Ka	27.70	1.214	0.1050	45.44
Al	Ka	14.98	0.387	0.0833	14.57
Si	Ka	28.73	0.519	0.1662	26.85
Fe	Ka	23.33	0.586	0.2136	10.96
Cu	Ka	5.27	0.364	0.0453	2.18
Total		100.01			

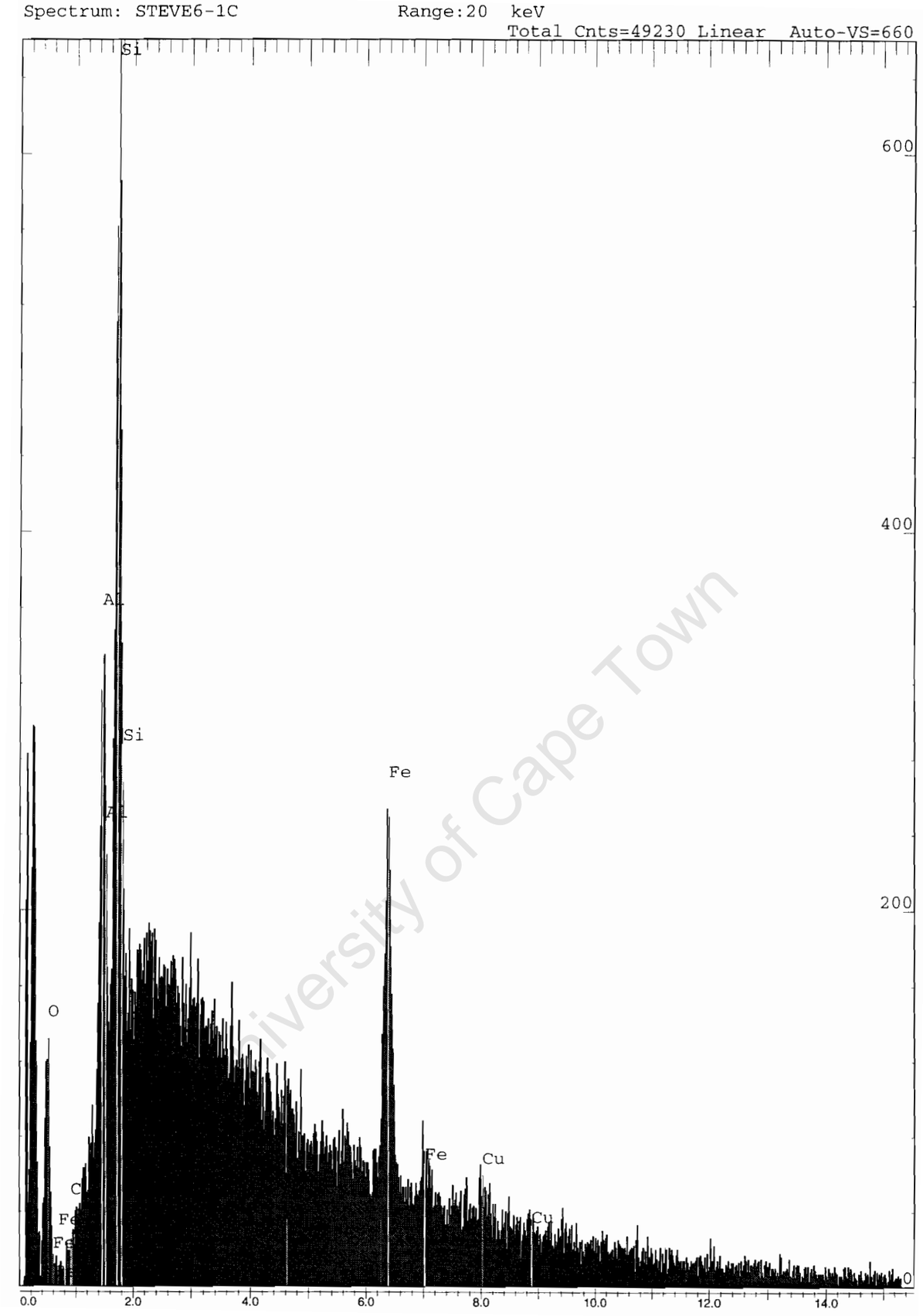

[A N A L Y S I S R E P O R T]

GENERAL CONDITIONS

Result File	: STEVE6-3C
File Version	: 1
Background Method	: Fit
Decon Method	: Gaussian
Decon ChiSquared	: 1.71
Analysis Date	: 1-DEC-2003
Microscope	: SEM
Comments	:

ANALYSIS CONDITIONS

Quant. Method	: ZAF/ASAP
Acquire Time	: 60 secs
Normalization Factor	: 100.00

SAMPLE CONDITIONS

kV	: 20.0
Beam Current	: 100.0 picoAmps
Working Distance	: 25.0 mm
Tilt Angle	: 0.0 Degrees
TakeOff Angle	: 35.0 Degrees
Solid Angle*BeamCurrent	: 0.6

Element	Line	Weight%	Error	K-Ratio	Atomic%
O	Ka	25.03	2.468	0.0847	47.54
Si	Ka	12.16	0.681	0.0707	13.16
S	Ka	9.83	0.569	0.0697	9.31
Cl	Ka	8.30	0.534	0.0579	7.11
Fe	Ka	15.89	0.945	0.1554	8.65
Ni	Ka	11.60	0.966	0.1074	6.00
Cu	Ka	17.19	1.311	0.1518	8.22
Total		100.00			

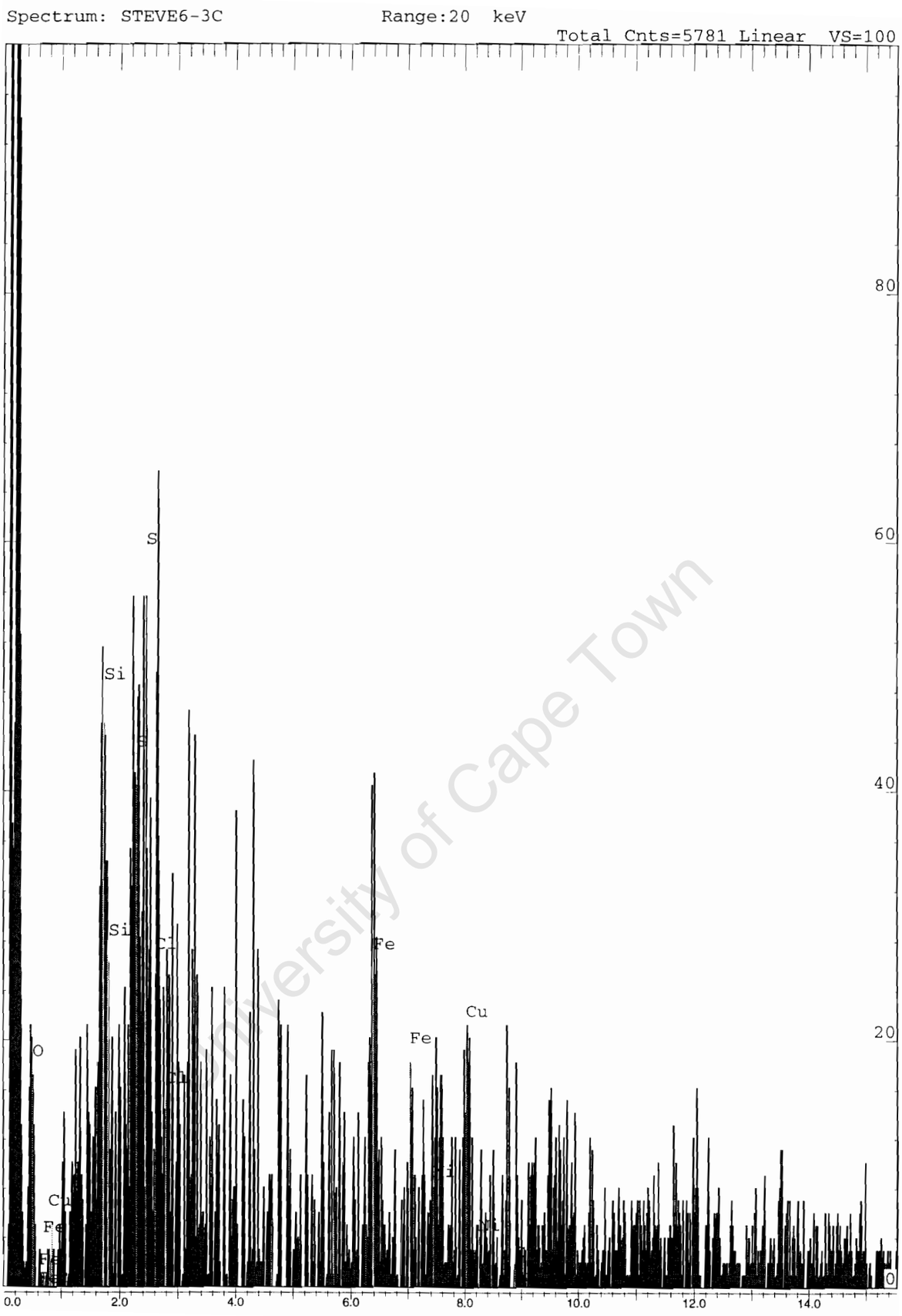

[A N A L Y S I S R E P O R T]

GENERAL CONDITIONS

Result File	: STEVE6-5C
File Version	: 1
Background Method	: Fit
Decon Method	: Gaussian
Decon ChiSquared	: 6.66
Analysis Date	: 1-DEC-2003
Microscope	: SEM
Comments	:

ANALYSIS CONDITIONS

Quant. Method	: ZAF/ASAP
Acquire Time	: 60 secs
Normalization Factor	: 100.00

SAMPLE CONDITIONS

kV	: 20.0
Beam Current	: 100.0 picoAmps
Working Distance	: 25.0 mm
Tilt Angle	: 0.0 Degrees
TakeOff Angle	: 35.0 Degrees
Solid Angle*BeamCurrent	: 0.6

Element	Line	Weight%	Error	K-Ratio	Atomic%
O	Ka	33.67	2.149	0.1132	54.91
Al	Ka	12.50	0.572	0.0607	12.09
Si	Ka	12.81	0.542	0.0695	11.90
P	Ka	1.90	0.211	0.0105	1.60
S	Ka	3.93	0.279	0.0260	3.20
Cl	Ka	3.64	0.266	0.0251	2.68
Ca	Ka	2.23	0.203	0.0197	1.45
Fe	Ka	3.69	0.343	0.0356	1.72
Cu	Ka	18.85	1.027	0.1667	7.74
Zn	Ka	6.77	0.678	0.0599	2.70
Total		99.99			

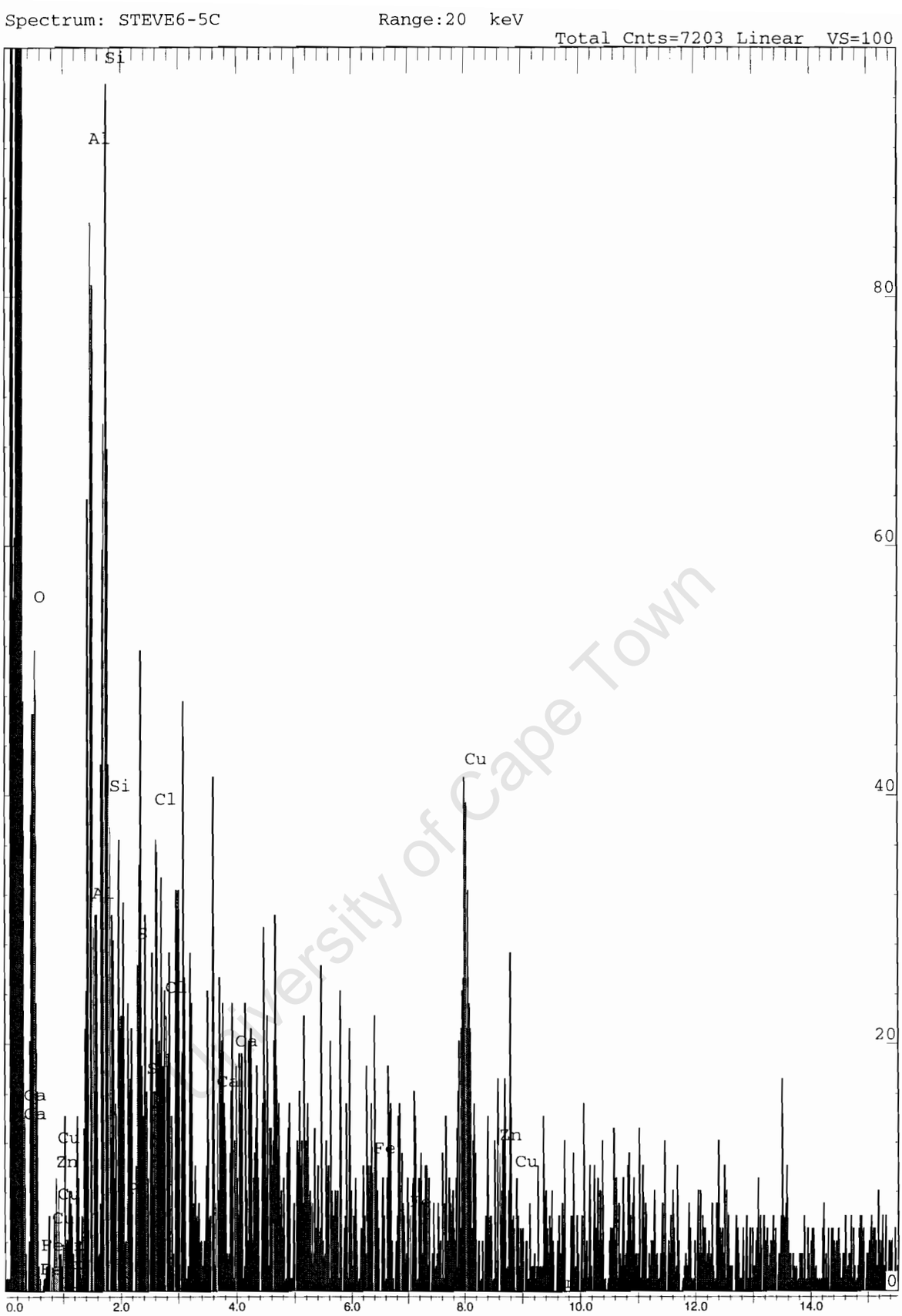

Appendix CD-ROM